GEOLOGY OF THE SAND CREEK PORPHYRY MOLYBDENUM PROSPECT

A Thesis submitted in partial fulfillment
of a
Master of Science

To

The Department of Geological Sciences
Brock University
St. Catharines, Ontario

By

David Lloyd Dillon

Dedicated to the memory of Donald A. Dillon

Acknowledgements

The author would like to express thanks to the following people for their advice and assistance: supervisors - Prof. S.J. Haynes and Prof. H.R. Williams, as well as Prof. P.A. Peach and Prof. W.T. Jolly who gave advice on mineral identification. Thin sections were produced by the author and Mr. J. McCarthy, with the assistance of Mr. B. Janser, Miss M.P. Blasko, Miss G.M. Wilson and Mr. J. Barnsley. Miss Wilson, Miss Blasko and Mr. S. Dougherty assisted with drafting the final maps.

Finally I would like to thank the people of Canadian Nickel Company for the opportunity to map this area, Dr. P. Peto for supervision in the field and Mr. J.S. Vincent for encouragement.

ABSTRACT

The Sand Creek Prospect is located within the eastern exposed margin of the Coast Plutonic Complex. The occurrence is a plug and dyke porphyry molybdenum deposit. The rock types, listed in decreasing age: 1) metamorphic schists and gneisses; 2) diorite suite rocks - diorite, quartz diorite, tonalite; 3) rocks of andesitic composition; 4) granodiorites, coarse porphyritic granodiorite, quartz-feldspar porphyry, feldspar porphyry; and 5) lamprophyre.

Hydrothermal alteration is known to have resulted from emplacement of the hornblende-feldspar porphyry through to the quartz-feldspar porphyry. Molybdenum mineralization is chiefly associated with the quartz-feldspar porphyry.

Ore mineralogy is dominated by pyrite with subordinate molybdenite, chalcopyrite, covelline, sphalerite, galena, scheelite, cassiterite and wolframite. Molybdenite exhibits a textural gradation outward from the quartz-feldspar porphyry. That is, disseminated rosettes and rosettes in quartz veins to fine-grained molybdenite in quartz veins and potassic altered fractures to fine-grained molybdenite paint or smears in the peripheral zones.

The quartz-feldspar porphyry dykes were emplaced in an inhomogeneous stress field. The trend of dykes, faults and shear zones is 041° to 063° and dips between 58° NW and 86° SE. Joint Pole distribution reflects this fault orientation. These late deformation maxima are probably superimposed

upon annuli representing diapiric emplacement of the plutons.

A model of emplacement involving two magmatic pulses is given in the following sequence: Diorite pulse (i) diorite-quartz diorite, (ii) tonalites; granodiorite pulse (iii) hornblende-fildspar microporphyry, hornblende/biotite porphyry, (iv) coarse grained granodiorite, (v) quartz-feldspar porphyry, (vi) feldspar porphyry, and (vii) lamprophyre.

The combination of plutonic and coarse porphyritic textures, extensive propylitic overprinting of potassic alteration assemblages suggests that the prospect represents the lower reaches of a porphyry system.

Table of Contents

Figures

Tables

Tables (continued)

Plates

Plates (continued)

Introduction

The Sand Creek Prospect is located at latitude 51° 38'N and longitude 125° 04'W within the eastern part of the Coast Mountain Range in the southern half of British Columbia. Sand Creek is a minor tributary of Mosley Creek and the Homathko River which empties into Bute Inlet and the Pacific Ocean. Figure 1 is a location map containing the Sand claims. these are presently held by the Esperanza Company and were under option to the Canadian Nickel Company while field work was done. Access may be made via White Saddle Ranch, south of Tatla Lake which is on the Williams Lake-Bella Coola highway.

This molybdenite occurrence has been previously mapped (and assessment file reports filed) by Pacific Petroleum Limited (1970) and Cities Services Mineral Corporation(1973 and1974). Previous work by the Geological Survey of Canada has not covered this area.

Figure 2 is a compilation of the previous mapping by Cowan and Linn for Pacific Petroleum Limited, Murton (1973) and Salazar and Murton (1974) for Cities Services Mineral Corporation. It should be noted that there is no unified nomenclature for the rock types in this compilation, therefore this will be addressed in a subsequent chapter.

General Geology

The Sand Creek Map Sheet is located in the eastern portion

FIGURE 1 : LOCATION MAP

of the Coast Range Batholith (Baadsgaard et al, 1961) which is also referred to as the Coast Plutonic Complex by Roddick and Hutchinson (1973) and Monger and Hutchinson (1970). According to Jackson (1976) and Carter (1974), these rocks are of late Cretaceous to early Tertiary age. The rocks of this prospect include some feldspar porphyries, and quartz-feldspar porphyries in association with molybdenite mineralization and a large gossan zone approximately four by five kilometres. It is therefore considered to be a porphyry molybdenum occurrence.

The area is underlain by two massive plutonic complexes which cut the metamorphic basement. This basement is found both in part overlying and as stoped blocks, within the plutons. One of the plutonic masses is termed the diorite suite. It ranges from diorites to tonalites in composition and displays a granitic texture. It has undergone considerable brittle deformation as evidenced by abundant faults, andesitic sills and dykes of grey microporphyry, hornblende/biotite feldspar porphyry, quartz-feldspar porphyry, feldspar porphyry and lamprophyres.

The other major body is a large mass of coarse grained porphyritic quartz-monzodiorite/granodiorite which cuts and is roofed by the diorite suite rocks and is cut by fewer dykes of quartz feldspar porphyry, feldspar porphyry and lamprophyre. The porphyritic nature is assumed to indicate a deep subvolcanic complex.

Figure 3 is a portion of the area immediately surrounding

Figure 3 Locations of Known Molybdemun Occurences in the vicinity of the Sand Creek Prospect

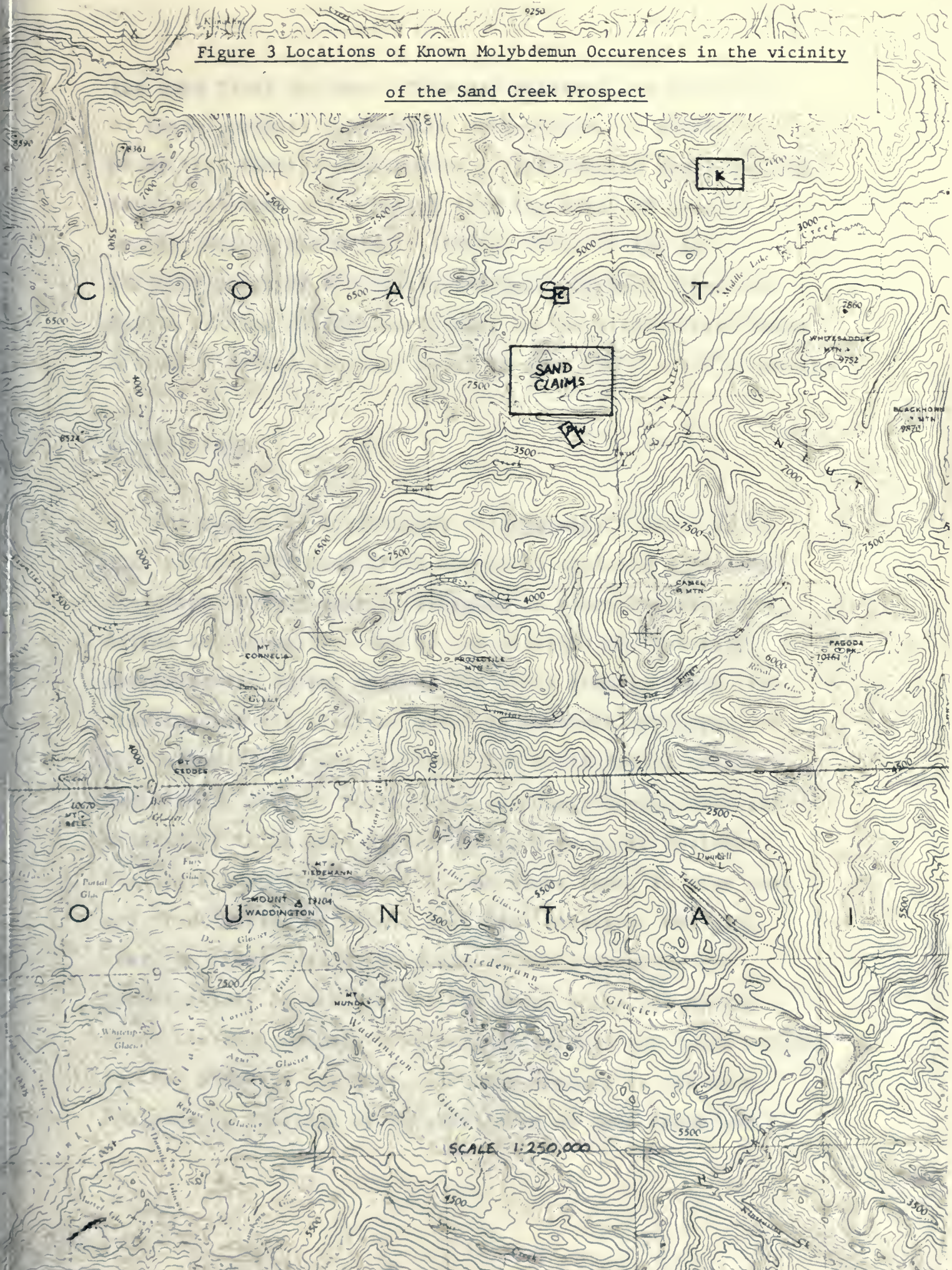

the Sand Creek prospect. This map contains the locations of known porphyry molybdenum occurrences. It should be noted that these deposits form a line running roughly north-east/south-west and parallel with the trend of a major valley. Murton and Salazar (1974b) refer to the set of feldspar porphyry and quartz-feldspar porphyry dykes and faults running roughly north-east as the Middle-Twist Lakes system. A second set they refer to as a N70°W - N30°W system.

Physiography

The region is mountainous with physical relief up to 1200 metres. The Sand Creek map sheet contains a maximum elevation of 2603 metres, dropping to approximately 1400 metres in one valley. Due to the altitude and latitude, approximately 80 per cent of the study area is above the treeline and six glaciers occur on northern exposures. The valley floors are littered with frost-heaved boulders and glacial debris. South, west and eastern exposures are covered by talus that grades upward from large boulders that have been transported to the slope base, to fine dust and frost-heaved materials that have undergone movement near the ridge crests and peaks. Outcrop accounts for approximately 25 per cent of the area, while ice covers about the same amount. Moraines, felsenmeer and talus account for the other 50 per cent. One tarn appears in the area. Drainage is provided by the two forks of Sand Creek and

and Hell Raving Creek.

Mapping Techniques

Mapping was done on an outcrop map prepared from a photomosaic at a scale of 1:5000 with the aid of aerial photos and a stereoscope. Areas of glacial debris, talus and felsenmere were also mapped by this method. The photomosaic, prepared by Pacific Survey Corporation, was also used in the field as a base for overlay sheets from which information was transferred to the outcrop map. Lineaments on the photomosaic were used to help interpret trends of dykes and faults.

Float composition was mapped in areas of extensive frost-heaving (ie. felsenmeer) as an indication of underlying bedrock composition, as well as at the bases of some ridges as an indication of rocks of those ridges.

Traverses were conducted on both ridge tops and sides. Only two days were spent mapping valley floors. These were to map frost-heaved material which was seen to be unmoved laterally by virtue of the close packing arrangement and homogenous composition of the cobbles and boulders.

The location of each rock sample was plotted on a second map and a third map was employed to plot the location of structural measurements.

The sample location map was then used in conjunction with petrographic studies of 342 thin sections to outline

the alteration zones. Types of molybdenite mineralization were also plotted on this map.

Details of the structural map were condensed and added to the petrography to form the geology map. Both maps are in the back sleeve.

The field party used Silva Ranger Compasses and a Brunton Pocket transit for structural measurements and triangulation of points.

A system of differentiating between rock types was developed for the field work by Dr. P. Peto, who supervised this work. This system was revised slightly as a result of succeeding petrographic studies.

Igneous-Metamorphic Sequence

These rocks may be broken down on the basis of field relations and petrographic characteristics into the intrusive system given in Table 1.

The metamorphic schists and gneisses (1), form blocks which were stoped and rafted into the diorite suite rocks (2). The diorites (2a) grade vertically into quartz diorites (2b). These are then cut by tonalite which also carries xenoliths of diorite. The tonalite aplite dykes (2c) cut both the metamorphic rocks and earlier diorites and quartz diorites. These dykes are of the order of a decimetre wide and are rare.

The diorite suite rocks are cut by andesitic rocks (3),

Table 1 Igneous - Metamorphic Sequence

	Unit Number	Rock Type
Youngest	5	lamprophyre dykes
	4d	feldspar porphyry dykes
	4c	quartz-feldspar porphyries
	4b	coarse grained porphyritic granodiorite
	4a	coarse grained granodiorite
	3b	grey hornblende/biotite-feldspar porphyry dykes (andesite)
	3a	grey hornblende-feldspar microporphry sheets and dykes (andesite)
	2c	coarse grained tonalite and tonalite aplite dykes
	2b	medium to coarse grained quartz diorite
	2a	fine to medium grained diorite
Oldest	1	metamorphic schists and gneisses

which are present as grey hornblende-feldspar microporphyry sheets and dykes (3a). These contain xenoliths of tonalite and are cut by grey hornblende/biotite-feldspar porphyry dykes (3b). These dykes and sheets may be apophyses to a larger underlying chamber. Stoping of quartz diorite into a large body of 3b occurred in the western-most extremity of the area. In one place on the eastern edge of the gossan zone, the apex of one of these dykes is exposed, where it intrudes and alters the host tonalite.

Coarse grained granodiorite (4a) is found in only a few places in the west and south portions of the map area. It overlies the coarse grained porphyritic granodiorite (3b) and may be rafted or near an extremity of the pluton.

The coarse grained porphyry is partially roofed by diorites and the intruded andesites. The quartz-feldspar porphyry dykes (4c) cut both plutonic complexes. They commonly bifurcate vertically in the dioritic rocks and apices may be found north of the north branch of Sand Creek. The feldspar porphyry (4d) is not seen to cut the quartz-feldspar porphyry (4c). However, it does cut both the earlier grey hornblende biotite-feldspar porphyry (3b) and the coarse grained porphyritic granodiorite (4b). Vertical bifurcation and dyke apices of 4d are exposed quite commonly.

Lamprophyre dykes (5) cut all other units.

Structural Geology

In analyzing the structural data, an attempt was made to demonstrate the nature of the emplacement and deformation of the plutons exposed in the map area. It was presumed that emplacement involved diapiric rise of crystal charged magma: 1) as crystal mush in the case of the plutonic rocks and, 2) that volcanism related to the gnessis of the deposits of molybdenite occurred within a field of stress which led to the oblong shape of the gossan.

The data collected concerning geological structures of the Sand Creek Prospect was compiled and put through rigorous analysis in the following manner. Lineament trends were taken from a photomosaic of the area and plotted on rose diagrams with the assumption that the dip of such lineaments is vertical (this will be seen later to be unjustified in some cases). Orientation of dykes, faults andshears were plotted on stereograms and subjected to statistical analysis using the method of Kamb (1959). Joints were treated in the same manner.

It is necessary to qualify the value of this study due to a number of limiting factors. These are namely sampling bias, sampling of unloading features, and problems of lineament orientation.

Sampling bias by the author involved collecting data primarily from ridge tops and some slope outcrops due to the abundance of talus, glacial debris and frost-heaved

material on lower slopes and valley floors. In some areas dyke orientations reflect joint orientation which is due to late regional stress. Such dykes were of prior interest to the author during the collection of data and therefore were not incorporated into the joint stereograms. The bias involved in the lineament study is one of ice cover on northern exposures leaving mainly south facing slopes for sampling.

In addition, it is possible that at least some of the joints are unloading joints. These are exfoliation features rather than major tectonic features. Their degree and significance is unknown.

Given these qualifications, the following analysis postulated.

The Sand Creek map area is covered by sets of lineaments dominantely trending northeast, as can be seen in the rose diagram, Figure 4. These lineaments are mainly faults and dykes with a trend maximum occurring between 050° and 060° with a slightly broader envelope appearing between 020° and 070°. These data were taken from a 1:5000 photomosaic using a protractor. The edges of the orthophoto were assumed to be exactly north-south and east-west lines. This was roughly verified in the field although small errors in triangulation were noticed.

Analysis of stereograms of joint pole and fault, dyke and shear pole distribution was done in accordance with the method outlined by Kamb (1959). This method involves

FIGURE 4

Rose diagram for lineaments in the map area. Maxima occur between 020° and 070° and 120° and 130°. The absolute maximum is between 050° and 060°. A total of 295 trends were used.

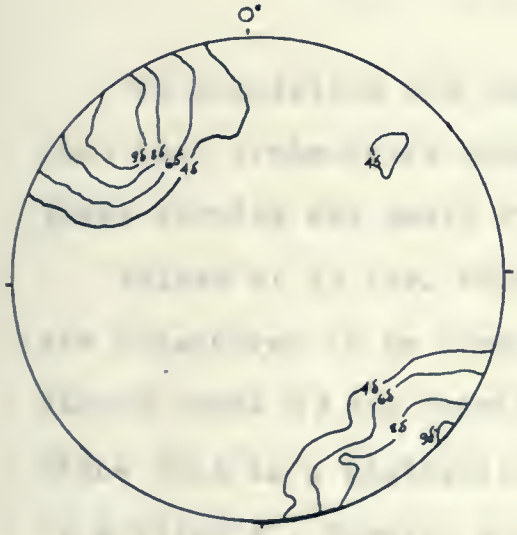

FIGURE 5

Pole distribution for faults, dykes and shears. The maximum is centered on 322°/14°. Trend and plunge variations are ± 011 and ± 18° respectively. Corresponding planes trend between 041° and 063° and dip 58°NW to 96°SE. The pole population is 45.

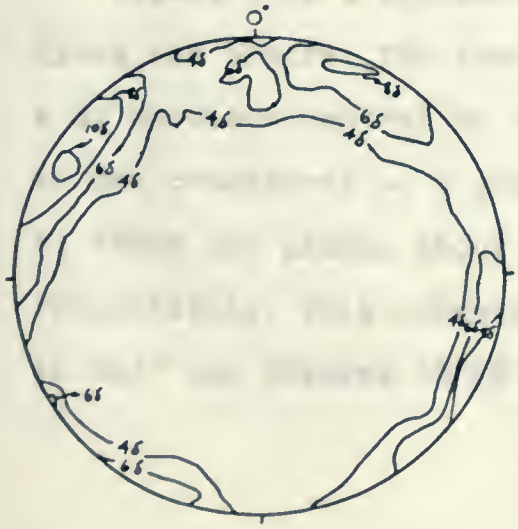

FIGURE 6

Joint pole distribution for the map area. Pole maxima are centered on 316°/11° and 025°/08°. Trend and plunge variations for these maxima are: ±004° and ± 05°; and ± 007° and + 02° respectively.

contouring population densities as multiples of the standard deviation, δ. The following formulae were used to calculate δ:

$$\delta/E = (1-A)/NA$$

$E = NA$ - number of points expected to fall within the area, A of a counting circle.

N - total number of points in the stereogram.

A - area of the counting circle expressed as a percentage or fraction of the area of the stereogram.

δ/E - is set at 1/3.

The population was counted by moving the counting circle such that cross-hairs intersected at joins of the major great circles and small circles where numbers were plotted.

Values at 3δ (ie. three times the standard deviation) are considered to be comparable with random distribution. Values above 6δ are considered to be very significant. Since this is a statistical method no 'ideal' orientation is arrived at, however an envelope of values is defined.

Figure 5 is a stereogram of pole distribution for faults, dykes and shears. The limited variation is contained within a 9δ envelope centred on the point 322°/14°. (This point is not considered as a general orientation). The variations of trend and plunge about this point are $\pm$ 011° and $\pm$ 18° respectively. This corresponds with planes trending 041° to 063° and dipping 58°NW to 86°SE.

The distribution of joint pole maxima treated in the same way yield areas centred on 316°/11° and 025°/08° in figure 6. Variations about these centre points in trend and plunge are ± 004° and ± 05° respectively and ± 007° and ± 02° respectively. These centres are given as only significant with respect to the highest encircling contour. To account for possible spatial variation, the map sheet was broken down into three subareas on the basis of dominant rock types and readily apparent alteration. The south half of the sheet (A) dominated by coarse porphyritic granodiorite, while the north half is dominated by coarse to fine-grained phaneritic diorite suite rocks. The northwest quadrant of dioritic rocks (B) is relatively unaltered whereas the southeast quarter (C) has a strong gossan zone and abundant monzogranite dykes (see figure 7).

Rose diagrams of the lineaments do show spatial variation and to a lesser degree, so do the joint pole distributions. Fault and dyke data were considered to be too few to give statistically valuable results.

Figures 8a, b and c exhibit the spatial variation of the maxima of the lineaments. Subarea 'A' contains an absolute maximum between 050° and 060° with relative maxima between 100° and 110°, and 000° and 010°. Subarea 'B' exhibits an absolute maximum between 020° and 030°. Relative maxima also appear between 120° and 130° and 060° and 170°. Region 'C' is the most complex diagram having an absolute maximum between 020° and 030°, secondary maxima between 040° and

Figure 7 Breakdown of the Sand Creek Map Area into subareas.

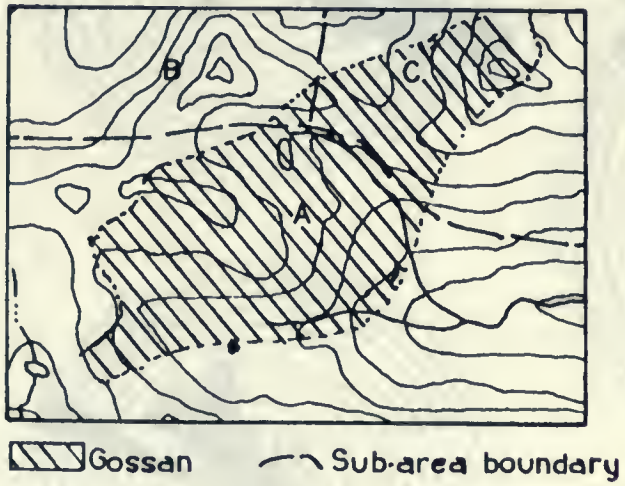

Fig. 8a Lineament Trends for Subarea A

This diagram is generated from 136 trends diagram exhibits preferred orientation of lineaments in the younger of two plutons, the 50° difference between the two sets represented conjugate shear directions.

Fig. 8b Lineament Trends for Subarea B
This diagram is generated from 71 trends and represents preferred orientation of lineaments in the older of two plutons. Maxima are held to represent conjugate shear directions. Angular displacement of these lineament trends is 80°.

Fig. 8c Lineament Trends for Subarea C

This diagram was generated from 88 trends. The distribution of maxima coincide with maxima of figures five a, b with on notable exception. This is between 070° and 080° in which molybdenite mineralization is present. The complex distribution of maxima in the five a, b. Maximum B represents lineaments in the oldest rocks. A similarily represents lineaments in the younger of the two major plutons. 'Mo' represents lineaments containing abundant molybdenite. Since this reflects magmatic differentiation as well it may be said that the stresses involved rotate through time.

060° and 070° and 080°, and tertiary maxima between 100° and 110°, 120° and 130°, and 140° and 150°. These values are tabulated for comparison in table 2. For most of the maxima of 'C' there are corresponding maxima in one or the other of subareas 'A' and 'B'. This is considered to be due to the fact that 'C' represents an area of overlap of processes which have affected 'A' and 'B'. It should be expected that the formation of lineaments in 'B' should be accompanied by the same in 'C' since they are dominated by rocks of the same intrusion. The lineaments in 'A' run mainly in a northeast-southwest direction which is sympathetic with the trend of the gossan zone and distribution of the monzo-granite dykes (see Petrography map). The area of gossan overlaps and the lineaments of this zone are also expressed in area 'C'. Notably, one deviation occurs from this scheme. That is, a secondary maximum between 070° and 080°. This trend coincides with the trend of some subtle lineaments noted by the author in which molybdenite mineralization was found in abundance. The search for such lineaments in subarea 'A' was not conducted, and because the known lineaments were visible from the base camp, a bias was produced. However, it is suggested that the lineaments of figure 8c exhibit a trend from 020° - 030° to 070° - 080° in accordance with the relative age of the rocks involved. The primary maximum at 020° - 030° in 'C' coincides with that in the older rocks (in 'B') while the secondary maximum at 040° - 060° includes the absolute maximum associated

Table 2 Maxima Envelopes and Relative Size Values

Subarea A		Subarea B		Subarea C	
Size Value	Trend	Size Value	Trend	Size Value	Trend
		I	020° -030°	I	020° -030°
I	050° -060°			II	040° -060°
				II	070° -080°
II	100° -110°			III	100° -110°
		II	120° -130°	III	120° -130°
II	140° -150°			III	140° -150°
		II	160° -170°		
II	000° -010°				

with younger rocks in 'A'. To complete this argument it is considered that these rocks represent successive products of magmatic differentiation which have later included the emplacement of molybdenite mineralization for which trends between 070° and 080° have found. The stresses responsible for the lineaments would have rotated from 020° - 030° to 070° - 080° from oldest to youngest.

Joint sets in these areas also show some variability Pole maxima, shown in Figures 9a, b and c, and are derived in accordance with Kamb (1959). Table 3 gives the attitudes of joint pole maxima, standard deviation (δ) factor and associated plane orientation.

Similarities in pole distribution may be seen immediately in regions 'A' and 'C' in that two maxima are well defined and the more significant maxima (8δ) are essentially identical. Beyond this little may be said except in speculation about the reasons for maxima destribution in 9b. The distribution appears to be in an annulus mainly between 10° and 20° from the primitive circle. It may be taken as representing biased sampling of a body affected by radial and concentric jointing due some diapirism either in the emplacement of the body itself or as a result of emplacement of the coarse porphyritic granodiorite. However, a number of factors leave this suggestion untenable. Sampling of joint orientations initially perceived by the author to be a random sample did not consider the influence of unloading in joint creation. Coupled with the low number of joint poles used (44 points),

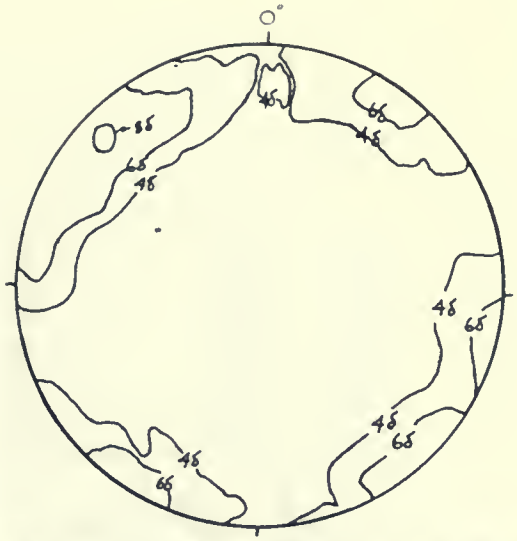

Fig. 9a Joint Pole Maxima for Subarea A

Joint pole maxima occur at 311° ±004° /15° ±05° and 036° ±007° /03° ±15°. These correspond with sets of planes trending between 037° and 045°, dipping between 70° SE and 80° SE and trending between 119° and 133° and dipping between 72° SW and 78° NE. The diagram was generated from 83 points.

Fig. 9b Joint Pole Distribution for Subarea B

This diagram was generated by 44 points and therefore represents a study of limited significance. Joint pole maxima appear at 024° ±014° /26° ±10°, 101° ±006° /20° ±03°, 120° ±008° /05° ±25° and 280° ±007/10° ±13°.

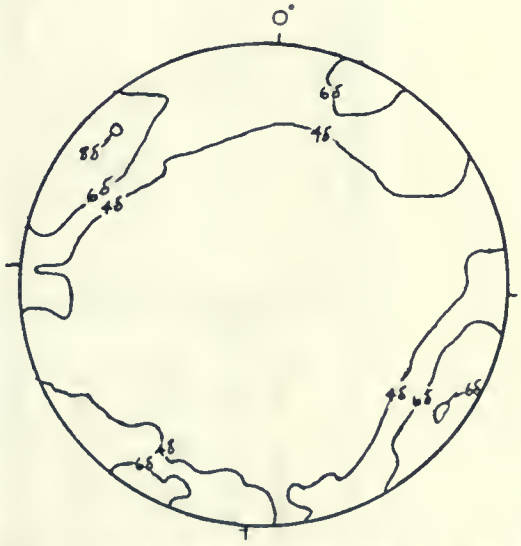

Fig. 9c Joint Pole Distribution for Subarea C

Joint pole maxima occur at 024° ±010° /06° ±20° and 312° ±002° /15 ±02°. These correspond with planes trending between 040° and 044°, dipping at 73° to 77° and trending 104° to 124 and dipping 64° SW to 76° NE. This diagram was generated from 64 points.

Table 3 Attitudes of Joint Pole Maxima Planes and 6 Factors

Poles (6 Factor)			Planes		
Sub area A	B	C	Sub area A	B	C
	024/26 (56)			011/70 /W (56)	
036 /003 (66)		024 /06 ±20 (66)		021 /80 /SE (56)	
	101 /20 (56)			030/85 /NW (56) (±25 SE)	
	120 /05 ±25 (56)		41 /75 /SE (86)		042 /75 /SE (86)
	280 /10 (56)			114 /64 /SW (56)	
311 /15 (86)		312 /15 (86)	126 /37 /SW (66)		114 /84 /SW (66)

this leads the author to abandon such speculation.

Evidence of sampling bias is readily seen in figure 9c. While the area is underlain by the same host rock, joints were sampled adjacent to dykes. Therefore, the annulus is cut by a girdle of values below 3δ (ie. below random orientation).

The planes associated with the joint pole maxima are presented again in table 4 for comparison with lineament orientations.

A number of conclusions may be drawn from this comparison notably, that there is a correlation between joint planes and the lineaments. However the correlation is such that the assumption of the lineaments being vertical, is not supported by the data. An example of this non-vertical attitude is found in the western-most ridge of the property. The plane was measured in the field as having the attitude 080°/70°/S wheras the corresponding lineament trend was 057°.

Further, it may be seen that two joint planes, 125°/90° and 011°/70°/W do not correspond with lineaments in their own areas (subareas 'A' and 'B' respectively). However in these cases, lineaments do appear in other subareas and are probably related to the same process.

The evidence presented here leads the author to conclude that while there is support for the notion of emplacement in an inhomogeneous stress field, these data do not demonstrate that they are the result of local diapirism.

Table 4: Joint Planes Compared With Lineament Trends

Sub area A		Sub area B		Sub area C		Total Area
Joints	Lineaments	Joints (5S)	Lineaments	Joints	Lineaments	Fault
	000 -010 (II)	011 /70 /W			020 -030 (I)	
		021 /80 /SE	020 -050 (I)	042 /75 /SE (8S)	040 -060 (II)	
		030 /85 +25 /NW			070 -080 (II)	
041 /75 /SE (8S)	050 -060 (I)				100 -110 (III)	046 /64 /SE
	100 -110 (II)			114 /84 /SW (6S)	120 -130 (III)	
126 /87 /SW (6S)		114 /64 /SW	120 -130 (II)		140 -150 (III)	
	140 -150 (II)					
			160 -170 (II)			

The structural analysis involved in this study was based upon rose diagrams of lineaments, and stereograms of joint pole population using the method of Kamb (1959). The results of which show that the map area has undergone a complex tectonic history. It may be said that the area has undergone emplacement of quartz-feldspar porphyry in a regime of inhomogeneous stress.

The association of a sequence of rock types with lineament trends leads to the suggestion that the stress field varied in time resulting in a rotation of preferred lineament direction.

Petrography

Introduction

The rocks studied range from unaltered to highly altered rocks. The facies of alteration used here are adapted from the work of Schwartz (1936), Burnham (1962), Creasey (1966), Henley (1968), Bray (1969), Lowell and Guilbert (1970), Sillitoe (1973), Ghorashi-Zadeh (1979) and Mutschler et al (1981). The assemblages of alteration observed are listed here in order of implied increasing temperature and generally increasing K^+/H^+ ratio.

Propylitic - chlorite - epidote(clinozoisite, pistacite) pyrite ± carbonate ± sphene ± rutile

Argillic - quartz - kaolin - smectite ± chorite

Phyllic - quartz - sericite - muscovite - pyrite

Potassic a) quartz - orthoclase - biotite ± sericite

b) quartz - biotite ± sericite

Silicic - quartz - orthoclase - sericite - cassiterite - scheelite - wolframite

Petrographic reports appear in the appendix.

Unaltered Rocks

A summary of modal percentages of the minerals in the following rock types appears in Table 5. The igneous rocks are plotted in Figure 10.

Table 5 Mineralogy Modal Percentages and Textures of Unaltered Rocks

Spec. no.	DW 66	DT 188	DT 184	DT 311	DT 180	DT 286	DT 213
Mineral	schist	diorite suite rocks			hornblende - feldspar porph.		granodiorite
Plagioclase	50	60	48	66	4* 86	10* 44	48
Species	An_{48}	An_{44-28}	An_{43}	An_{37-30}	An_{39}* An_{35}*	An_{31}* An_{29}*	An_{37-18}
Orthoclase				trace			20
Quartz			2	22		trace	17
Hornblende	30	30	44	trace	6	4 35	3
Biotite	15	6	4	10	3	trace	8
Opaques	5	2	1	0.5	trace	6	2
Apatite	1	trace	trace	trace	trace	trace	1
Sphene		trace	trace	trace		trace	trace
Zircon			rare	trace			
Chlorite			rare	trace	trace		trace
Epidote			rare	trace		trace	trace
Clays				trace			trace
Hematite	trace		trace		trace		trace
Texture	phyllitic	equigranular massive			aphanitic porphyritic exhibiting fluxion		coarse porphyritic

* denotes figures associated with phenocrysts and microphenocrysts.

Figure 10 : QKP Diagram Plot of Unaltered Igneous Rocks

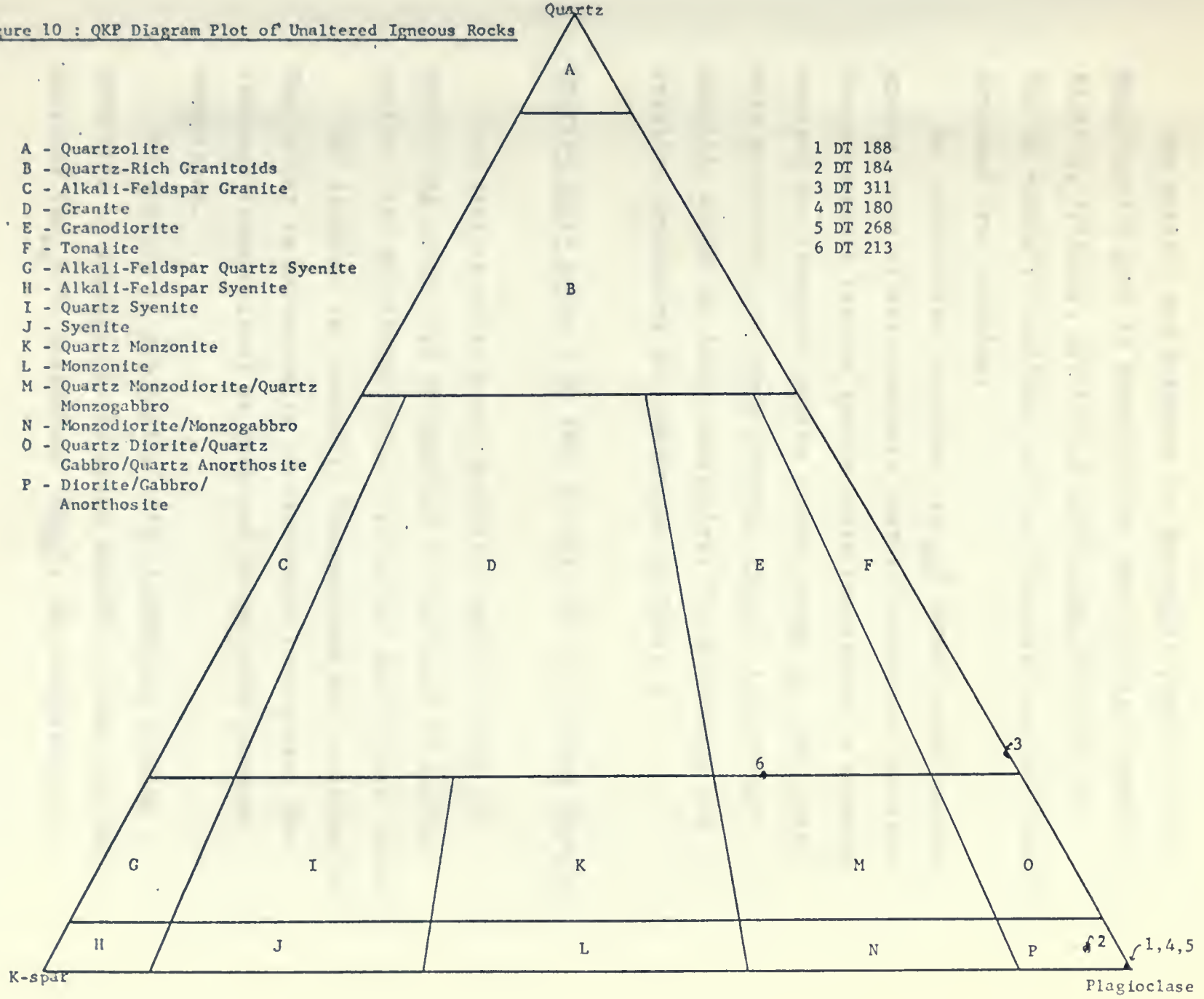

A - Quartzolite
B - Quartz-Rich Granitoids
C - Alkali-Feldspar Granite
D - Granite
E - Granodiorite
F - Tonalite
G - Alkali-Feldspar Quartz Syenite
H - Alkali-Feldspar Syenite
I - Quartz Syenite
J - Syenite
K - Quartz Monzonite
L - Monzonite
M - Quartz Monzodiorite/Quartz Monzogabbro
N - Monzodiorite/Monzogabbro
O - Quartz Diorite/Quartz Gabbro/Quartz Anorthosite
P - Diorite/Gabbro/ Anorthosite

1 DT 188
2 DT 184
3 DT 311
4 DT 180
5 DT 268
6 DT 213

Schists and Gneisses - DW 66 (Plate 1)

The schists and gneisses are generally phyllitic and melanocratic grey in handspecimen. They contain identifiable biotite, feldspar, pyrite and hornblende. The rock has low to moderate competence and the weathered surface exhibits abundant iron staining.

In thin-section, andesine (An_{48}) forms equant anhedral grains, some of which contain apatite inclusions. Biotite forms anhedral tabular grains while hornblende is anhedral embayed and elongate. Pyrite occurs mainly in association with hornblende and forms anhedral grains. Apatite and hematite appear in trace quantities. The mineralogy and relative abundances are summarized in Table 5.

Diorite Suite Rocks - DT 188, DT 184, DT 311 (Plates 2a,b,c)

The diorite suite rocks exhibit a general trend of increasing grain size accompanied by increases in quartz content, the biotite/hornblende ratio and leucocratic colour.

The diorites are generally fine-grained and equigranular. The colour is melanocratic to mesocratic grey-green. The feldspar (plagioclase) is grey and occurs with abundant hornblende.

The texture is subophitic with plagioclase forming subhedral to euhedral laths which exhibit strong zonation - andesine (An_{44}) to oligoclase (An_{20}). The hornblende is

Plate 1 DW66 Metamorphic Schist - exhibiting pronounced foliation of biotite and hornblende grains. Top: cross polarized light; bottom plane polarized light.

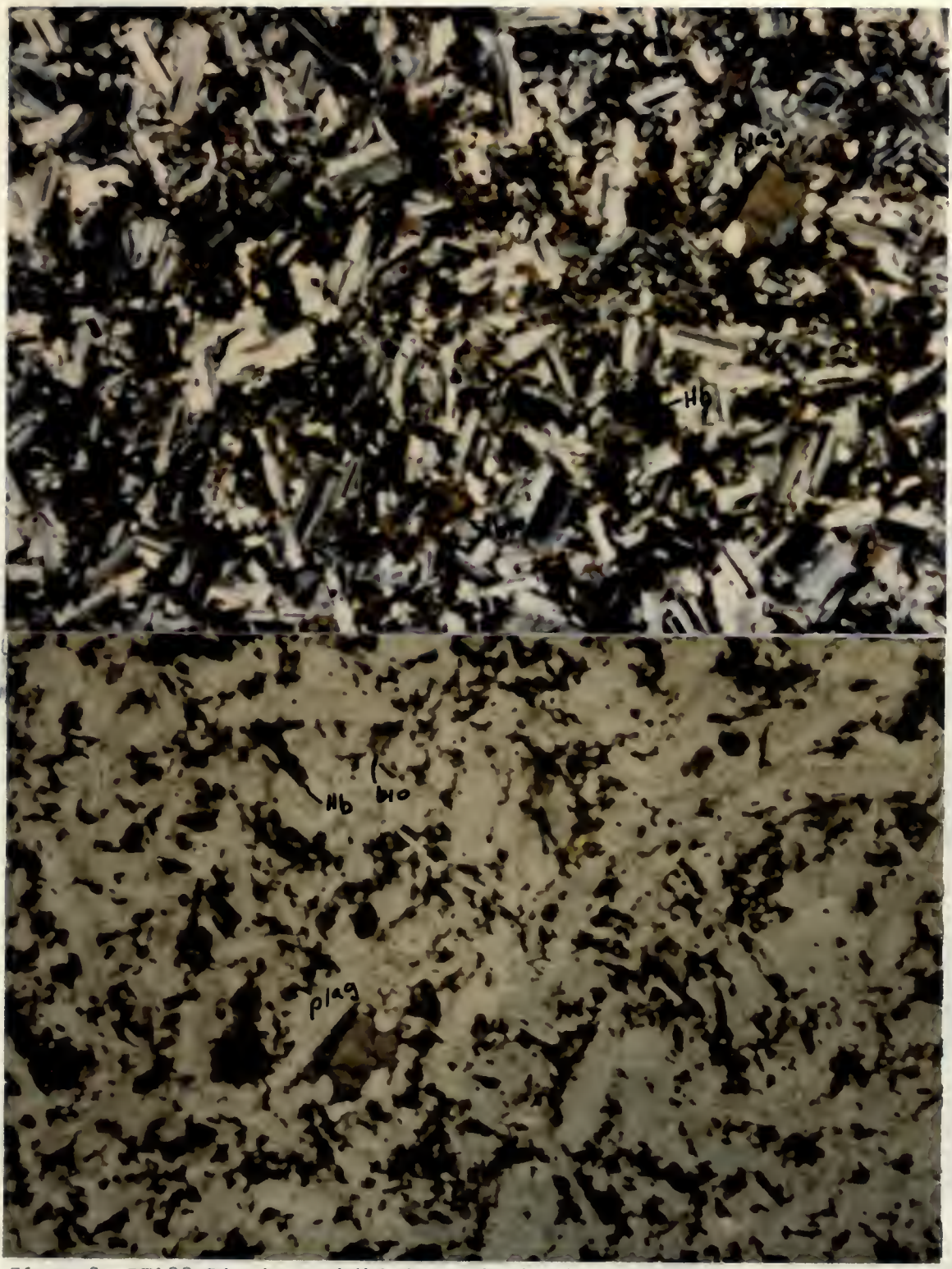

Plate 2a DT188 Diorite exhibiting subophitic texture. Top: crossed polars; bottom: plane polarized light. Plagioclase (Plag), Hornblende (Hb), Biotite (Bio).

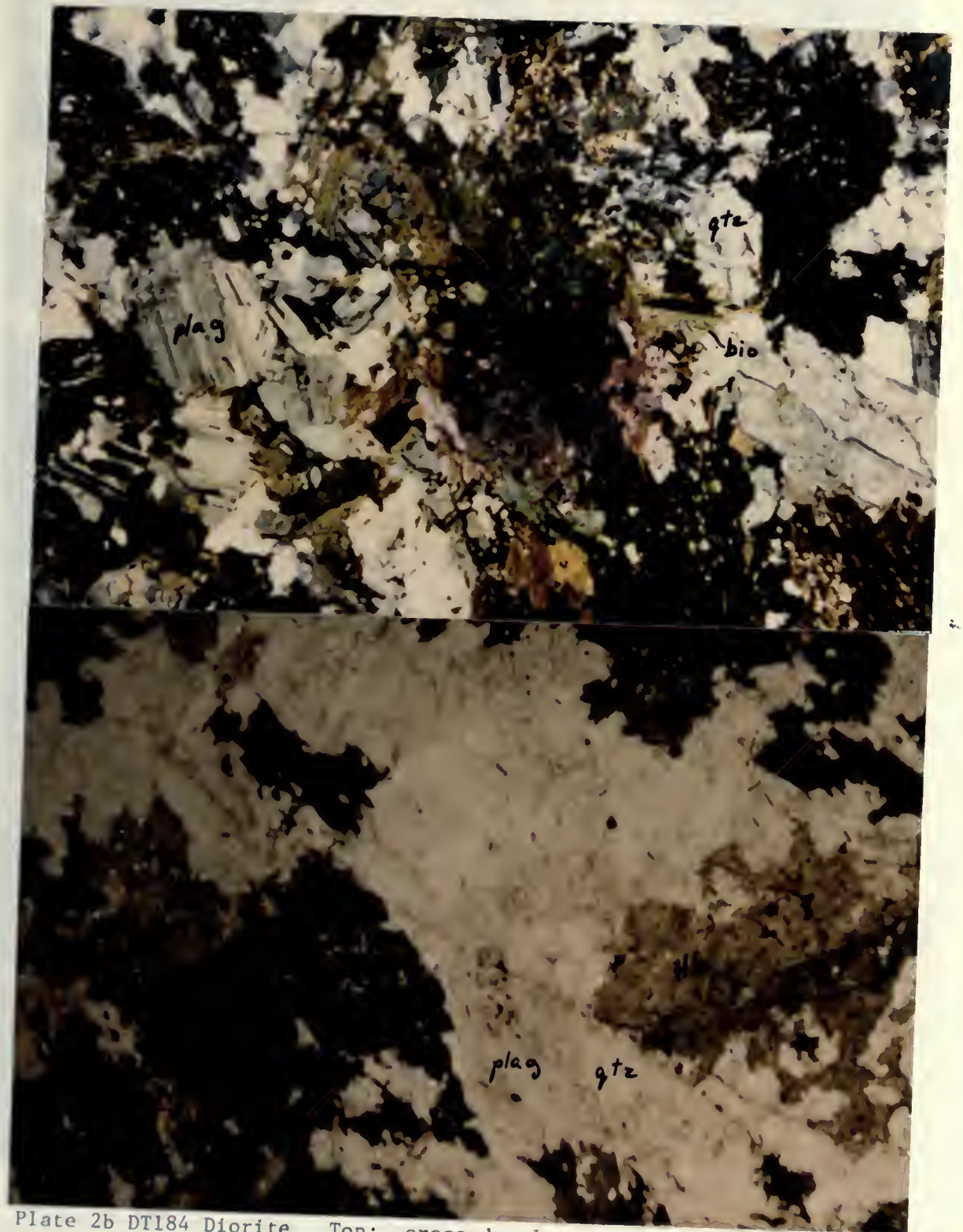

Plate 2b DT184 Diorite Top: crossed polars; bottom: plane polarized light. Plagioclase (Plag), Hornblende (HB), Biotite (Bio), Quartz (qtz).

0 1mm

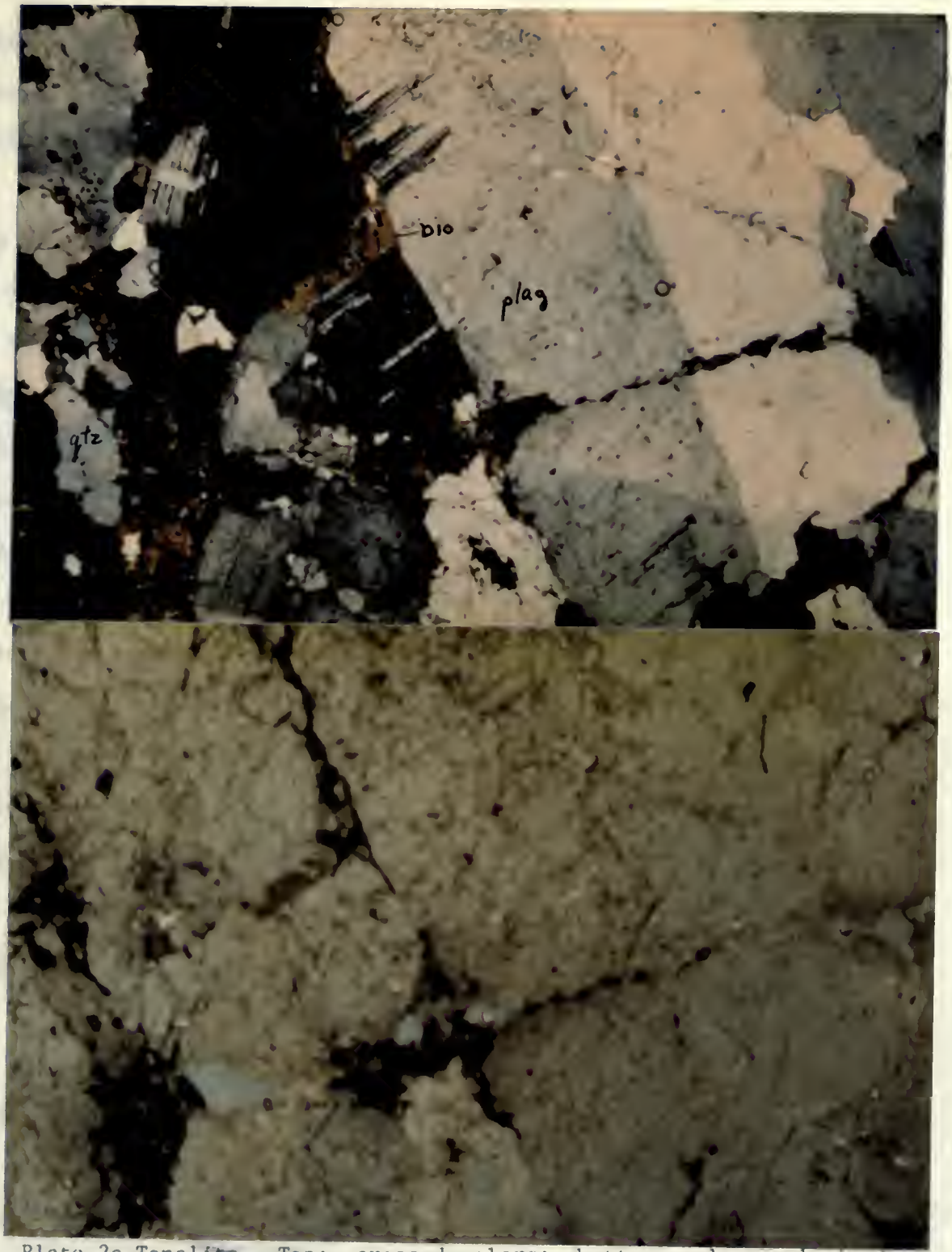

Plate 2c Tonalite Top: crossed polars; bottom: plane polarized light. Plagioclase (Plag), Biotite (Bio), Quartz (qtz).

anhedral and forms ragged laths. Biotite partially replaces hornblende. The accessory minerals are opaques (presumably pyrite), apatite and sphene.

The tonalites are generally coarse-grained, equigranular and leucocratic grey. The plagioclase is light grey. Biotite is the only observable mafic mineral. Quartz is abundant in handspecimens. The plagioclase grains are subhedral to anhedral with warped lamellae and overgrown breaks. Other quartz-bearing members of this suite (some diorites and quartz diorites) also exhibit these characteristics. Biotite, the dominant mafic, makes up approximately ten percent of the rock. Hornblende occurs in traces. Accessories include opaques (pyrite), apatite, sphene and zircon. Andesine zonation is from An_{37} to An_{30}.

The diorite suite mineralogy is summarized in Table 5 and these rocks are plotted on the Streckeisen diagram, Figure 10.

Hornblende-Feldspar Microporphyry - DT 180, DT 268 (Plate 3a,b)

These fine-grained to aphanitic dykes and intrusive sheets are slightly porphyritic. They contain phenocrysts of andesine and microphenocrysts of andesine and hornblende. The andesine phenocrysts exhibit little zonation. The composition of plagioclase microlites varies from specimen to specimen: in DT 180, they are andesine (An_{35}) and in DT 268, oligoclase (An_{29}). Such variation may be related to spatial variation

Plate 3A DT180 Hornblende-Feldspar Microporphyry - exhibiting fluxion (flow structure). Top: cross polarized light; bottom: plane polarized light. The groundmass consists of plagioclase, hornblende and biotite microlites. Microphenocrysts are hornblende.

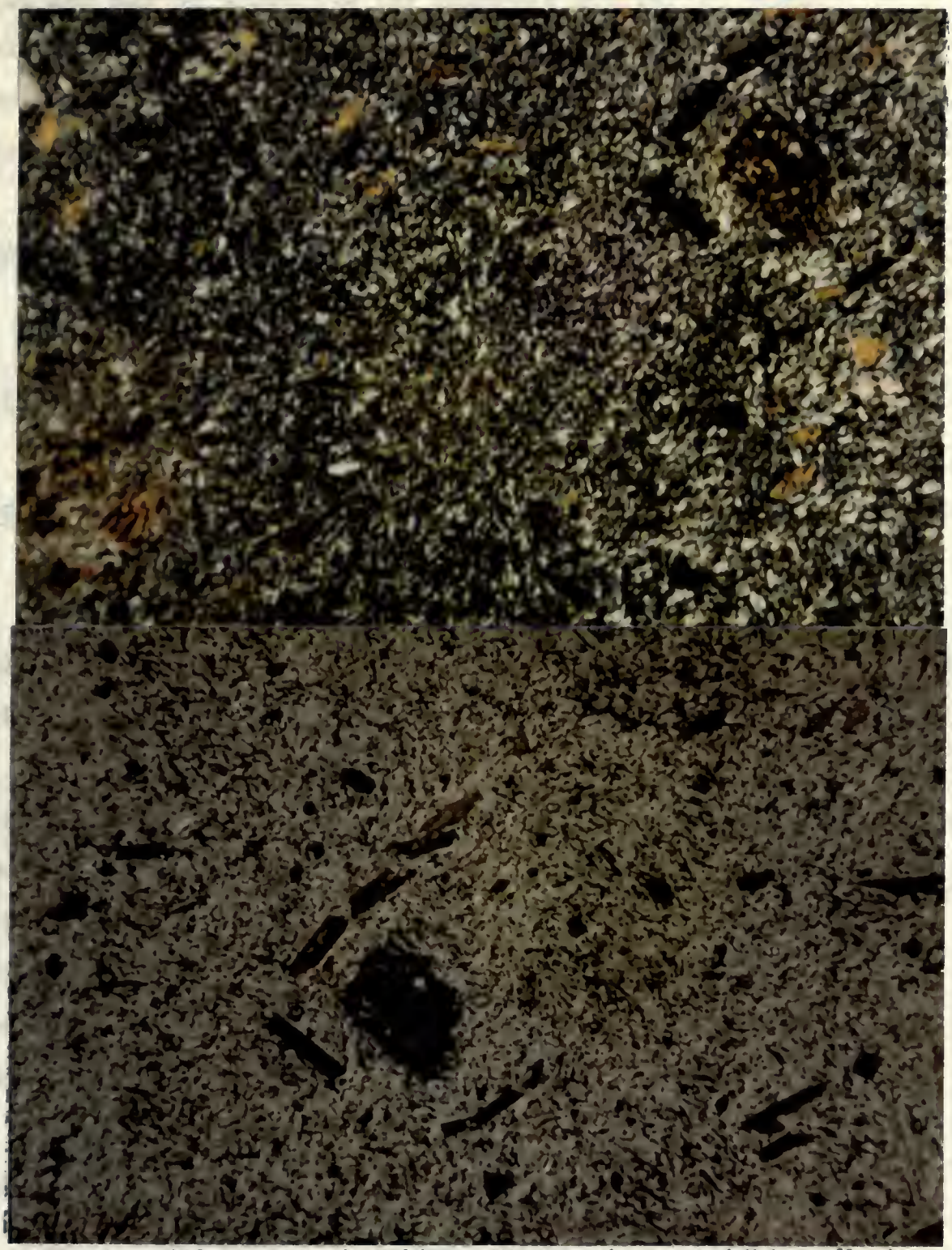

Plate 3b DT268 Hornblende-Feldspar Microporphyry - exhibitng fluxion (flow structure). Top: crossed polars; bottom: plane polarized light. Microlites are dominantly plagioclase and hornblende phenocrysts seen here are hornblende.

(DT 268 may be closer to the magmatic source) or slight alteration could account for the disparity since DT 268 contains traces of sphene and epidote. These rocks are summarized and plotted in Table 5 and Figure 10 respectively.

Hornblende/Biotite-Feldspar Porphyry

No unaltered specimens of this rock were found. Therefore its description will appear in 'Altered Rocks'.

Coarse-Grained Porphyritic Granodiorite DT 213 (Plate 4)

In handspecimen this rock is mesocratic to leucocratic and slightly pinkish. It is a coarse-grained porphyry containing pinkish-white and white feldspars, quartz and biotite.

The megacrysts are orthoclase. The mineralogy is dominated by zoned plagioclase (An_{37} to An_{18}) with subordinate orthoclase, quartz and biotite. Accessory minerals include hornblende, apatite, sphene and opaques (pyrite). On the Streckeisen diagram, Figure 10, this rock plots along the boundary between granodiorite and quartz-monzodiorite. Table 5 contains modal percentages of the mineralogy.

Later Dyke Rocks

The quartz-feldspar porphyry, feldspar porphyry and lamprophyre have undergone alteration and descriptions

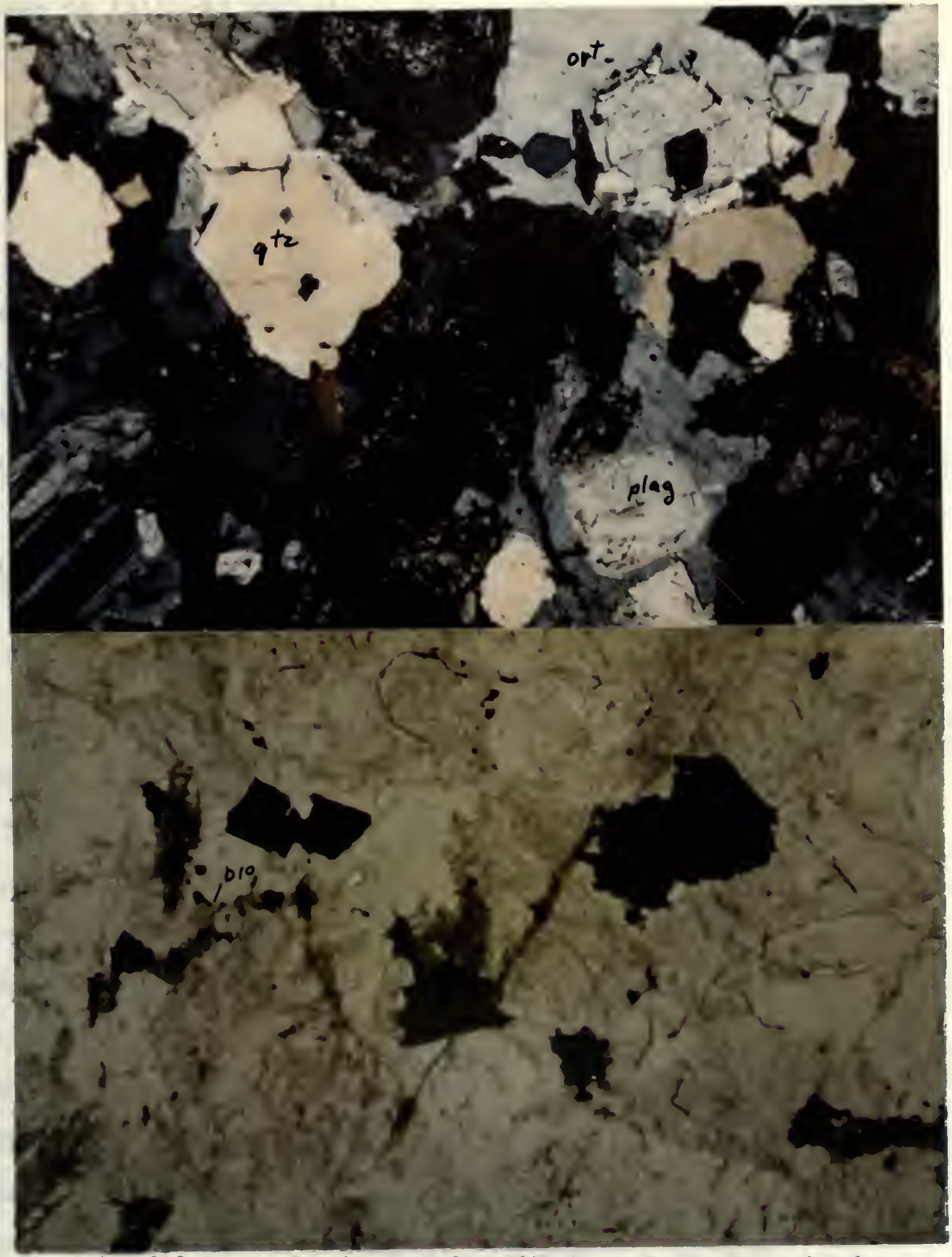

Plate 4 DT213 Coarse Porphyritic Granodiorite. Top: crossed polars; bottom: plane polarized light. Plagioclase (Plag), Orthoclase (ort), Quartz (qtz), Biotite (Bio), Opaques are pyrite.

appear in 'Altered Rocks'.

Altered Rocks

Modal abundances of minerals are summarized in Tables 6 to 10 inclusive. The quartz-plagioclase-orthoclase data were plotted on a mineral histogram and a ternary diagram, Figures 11 and 12, to uncover trends. Most of the rocks exhibit retrograde overprinting. The 'Alteration Zone Map of the Sand Creek Prospect' appears in the back sleeve.

Schists and Gneisses DT 101 (Plate 5)

The progressive alteration of the schists and gneisses involves a slight lightening of the rock in hand-specimen although the rocks remain essentially melanocratic.

The rocks are silicified (quartz) and propylitized (epidote-chlorite). The alteration is accompanied by an increase in grain size in both the mafic and sialic silicate.

Sphene is also present in trace quantities. The plagioclase species could not be determined optically because crystal grains were not large enough to do optical determination of sign and lack of albite twinning made the Michel-Levy Method inapplicable. Other accessories are hematite, apatite, opaques (pyrite ?). The relative abundances of biotite and hornblende are reversed with respect to the fresh rock. This may be due to modal difference within the original

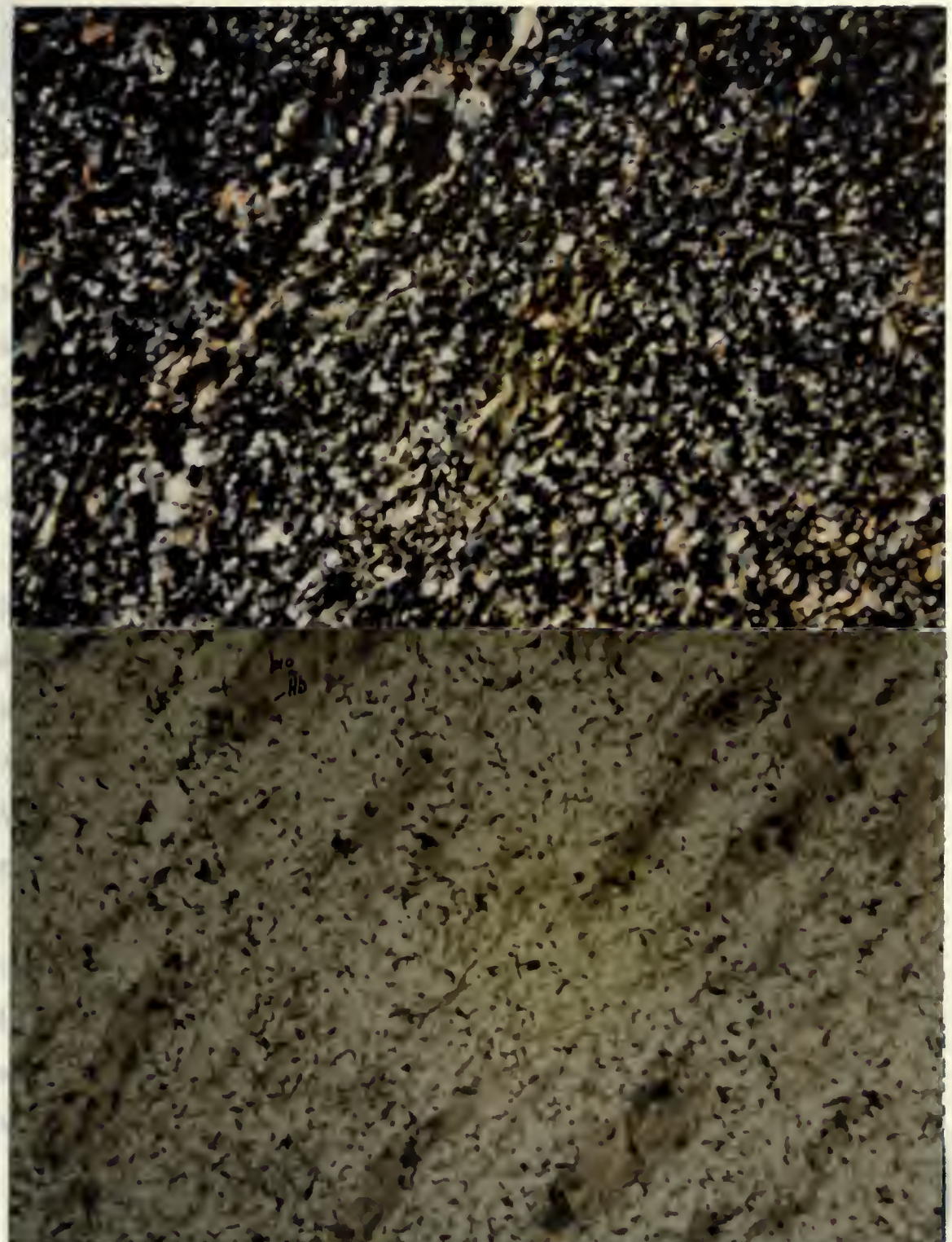

Plate 5 D1101 Altered Metamorphic Schist - containing biotite - hornblende augen. Top: crossed polars; bottom: plane polarized light. Biotite (Bio), Hornblende (Hb), the sialic matrix consists of plagioclase and quartz.

0 1mm

rocks rather than alteration.

Diorite Suite Rocks DT 177, DT 203, DT 324, DT 328 (Plate 6)

The diorite suite rocks have undergone hydrothermal alteration to potassic facies grade . The tonalitic aplite dykes are only known from altered samples therefore they will be described here. Sample DT 177 has undergone weak propylitic alteration. It is a leucocratic cream colour and contains quartz, white feldspar and chlorite.

Thin-section DT 177 is dominated by anhedral plagioclase exhibiting warped lamellae and partial alteration to kaolinite. The plagioclase species is An_{27}, oligoclase. Quartz is the other major silicate. Microcline is minor. Biotite and apatite appear to be the only primary accessories. Chlorite, epidote, limonite and sericite appear in trace quantities.

Successive alteration of the diorite suite members involves an increase in quartz content, obliteration of primary zonation in plagioclase grains, and growth of sphene grains in the propylitic zone. In the higher grade facies sphene disappears.

In DT 203, propylitic alteration is weak. The plagioclase is zoned from An_{41} labradorite to An_{32} andesine. DT 324 has undergone phyllic alteration with argillic overprinting, while DT 328 has undergone potassic alteration with phyllic and propylitic overprinting. These latter specimens contain

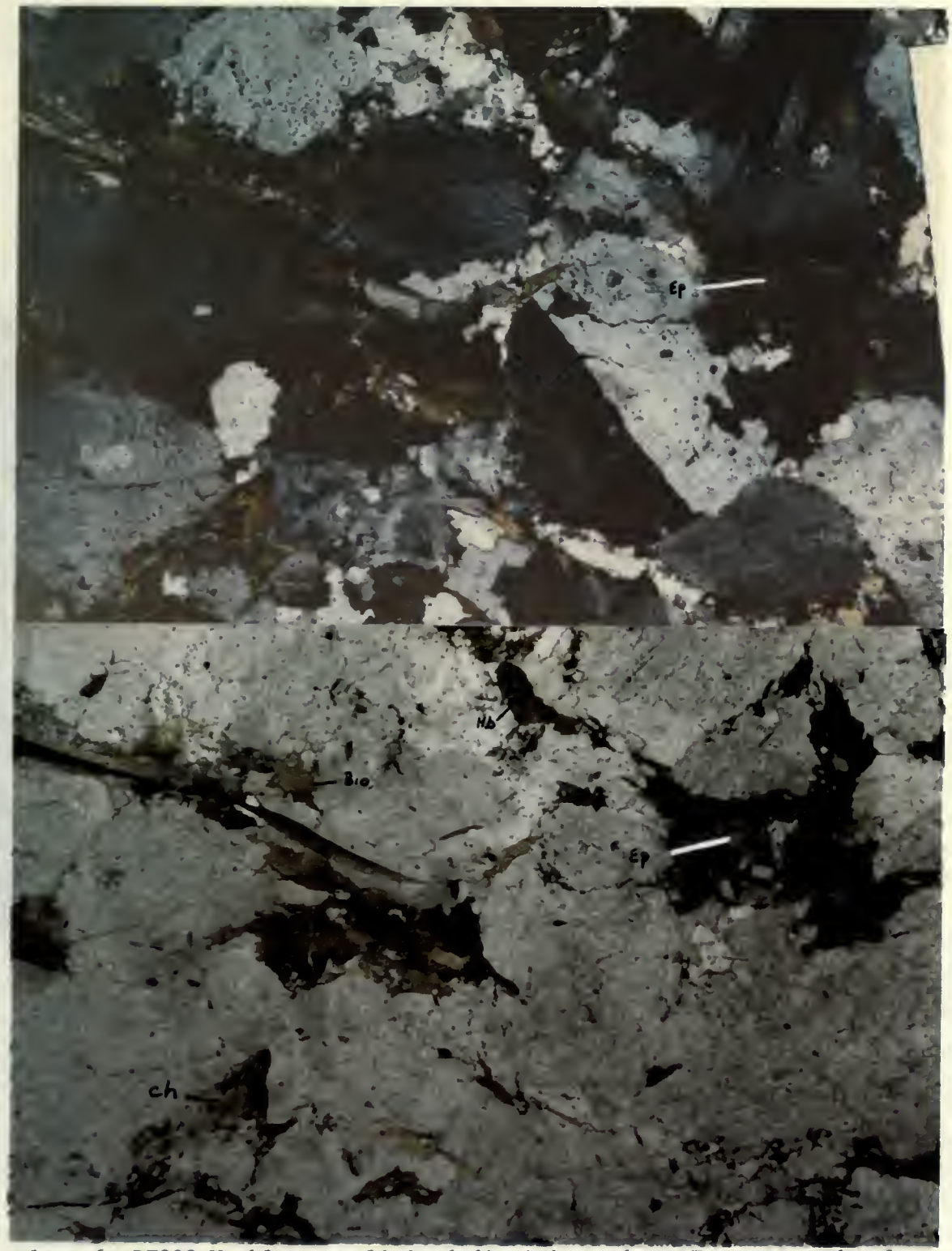

Plate 6a DT203 Weakly propylitized dioritic rocks. Top: crossed polars, Bottom: plane polarized light. Epidote (Ep), chlorite (ch), biotite (bio), hornblende (Hb). Note partial replacement of biotite by chlorite.

Plate 6b DT324 Argillic alteration of dioritic rock. Note lack of mafic silicates. Kaolin (kao), quartz (qtz). In plane polarized light.

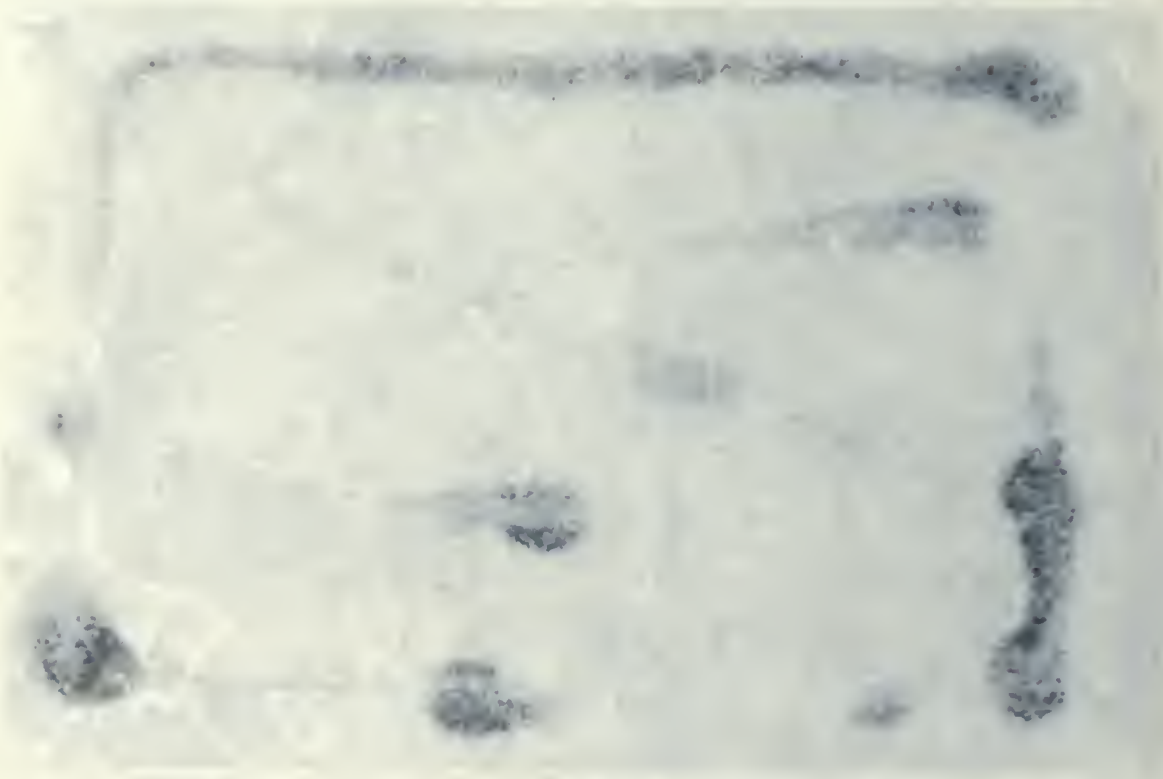

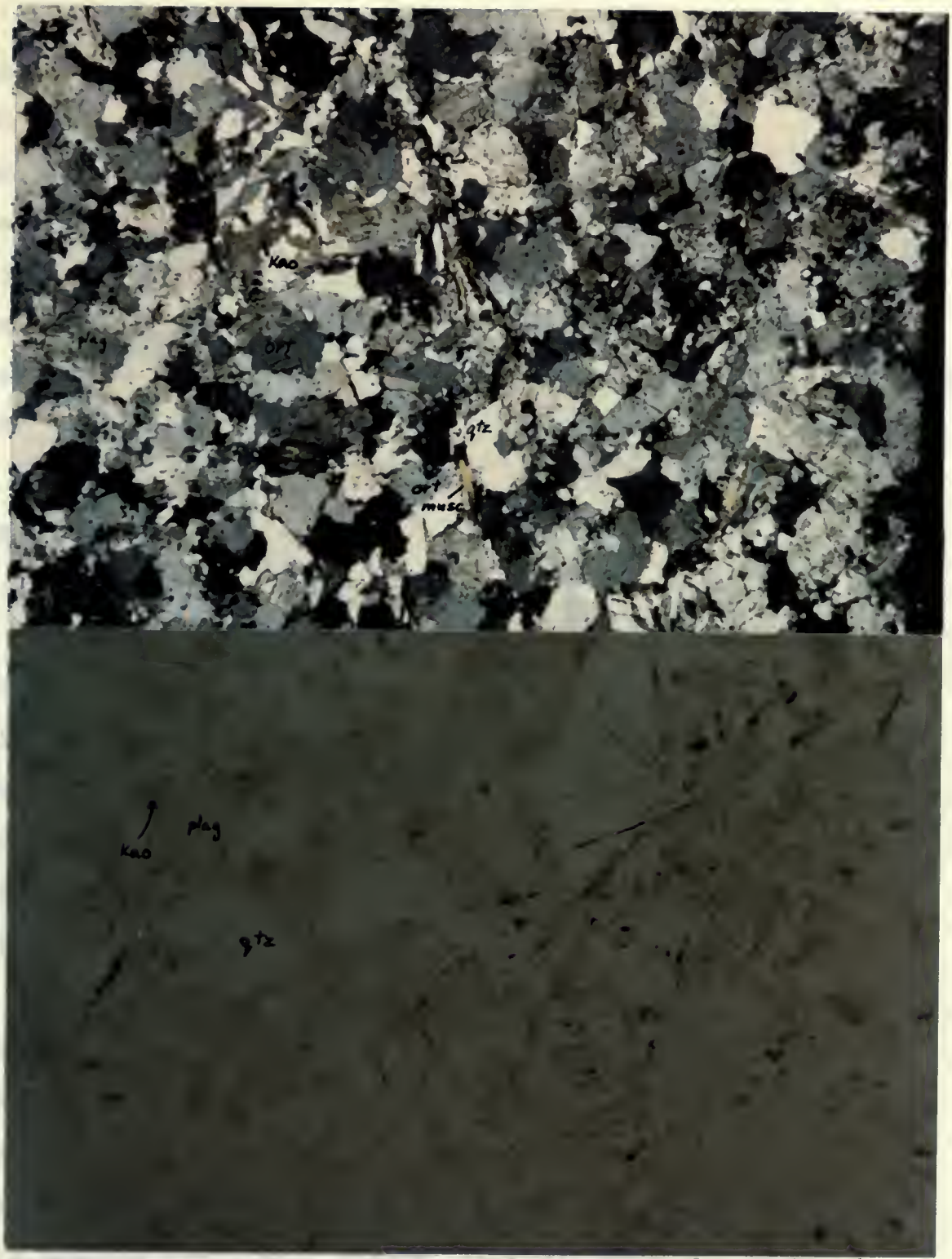

Plate 6c DR328 Dioritic rock altered from potassic facies through phyllic, argillic to propylitic facies by retrograde processes. Later overprinting is weak. Top: crossed polars, Bottom: plane polarized light. Quartz (qtz), orthoclase (ort), plagioclase (plag), muscovite (musc), kaolin (kao).

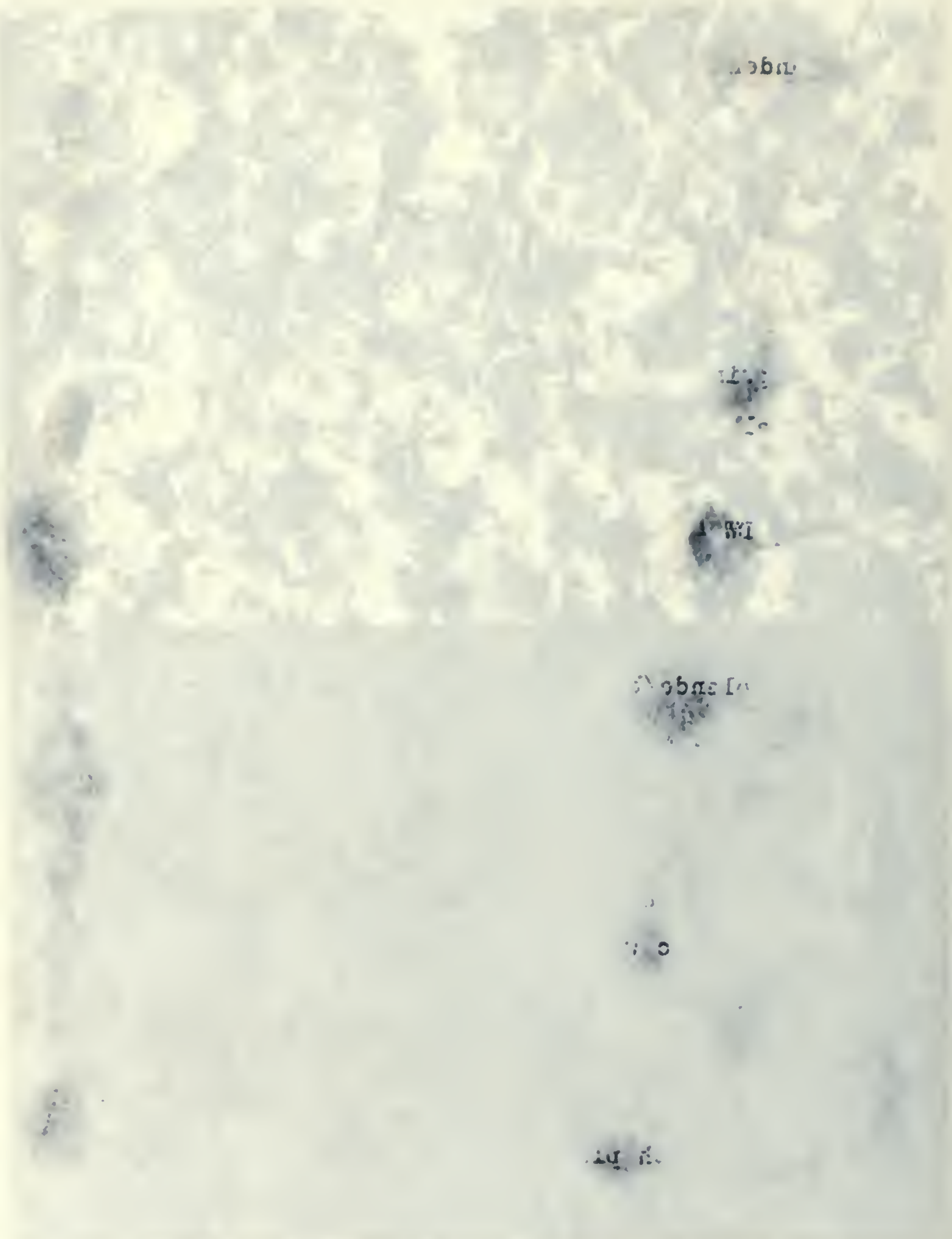

unzoned An_{32} andesine. Mineral assemblages change from hornblende-biotite-sphene-epidote-chlorite in the propylitic zone to orthoclase-muscovite-smectite-kaolinite-limonite in the rock of the phyllic facies with argillic overprinting to ort-secondary biotite (bi II)-musc-kaol-ep-rutile (rt) in the rocks of potassic facies with phyllic, argillic and propylitic overprinting. Table 6 and Figures 11 to 13 summarizes the mineralogical variation of the alteration zones.

Andesitic Rocks DW 40, DT 139, DT175 (Plate 7)

This section will deal primarily with the alteration of the grey hornblende/biotite-feldspar porphyry dykes (3b) since few samples of altered grey hornblende-feldspar microporphyry were collected. Hydrothermal alteration assemblages observed are prophlitic (DW 40), and potassic with strong phyllic-argillic and weak prophlitic overprinting (DT 139), and potassic with weak propylitic overprinting.

The least altered of these rocks, DW 40, is dominated by plagioclase phenocrysts and microlites. The phenocrysts exhibit slight zonation. Quartz appears as very fine (2-4u) wormy intergrowths with plagioclase. Biotite partially or completely replaces larger hornblende grains. Accessories are opaques (pyrite?), sphene, apatite, monazite, with traces of chlorite and epidote.

With increasing grade of alteration, the assemblages change from quartz, hornblende, biotite, apatite, sphene,

Table 6. Modal Percentages of Minerals in Altered Dioritic Rocks

Spec. no.	DT 177	DT 203	DT 324	DT 328
Mineralogy Facies (overprinting)	Propylitic	Propylitic	Argillic	Potassic (phyllic argillic propylitic)
Quartz	37	9	50	33
Plagioclase (species)	58 (An_{27})	75 (An_{41-32})	25 (An_{32})	38 (An_{32})
Orthoclase (microcline)	(2)		trace	24
Hornblende		4		
Biotite	trace	7		trace
Sphene		2		
Apatite	trace	trace	trace	trace
Opaques		1	3	trace
Rutile				rare
Epidote	trace	2		rare
Chlorite	trace	trace		
Kaolinite	1		17	3
Smectite			2	
Sericite/muscovite	trace		trace	1

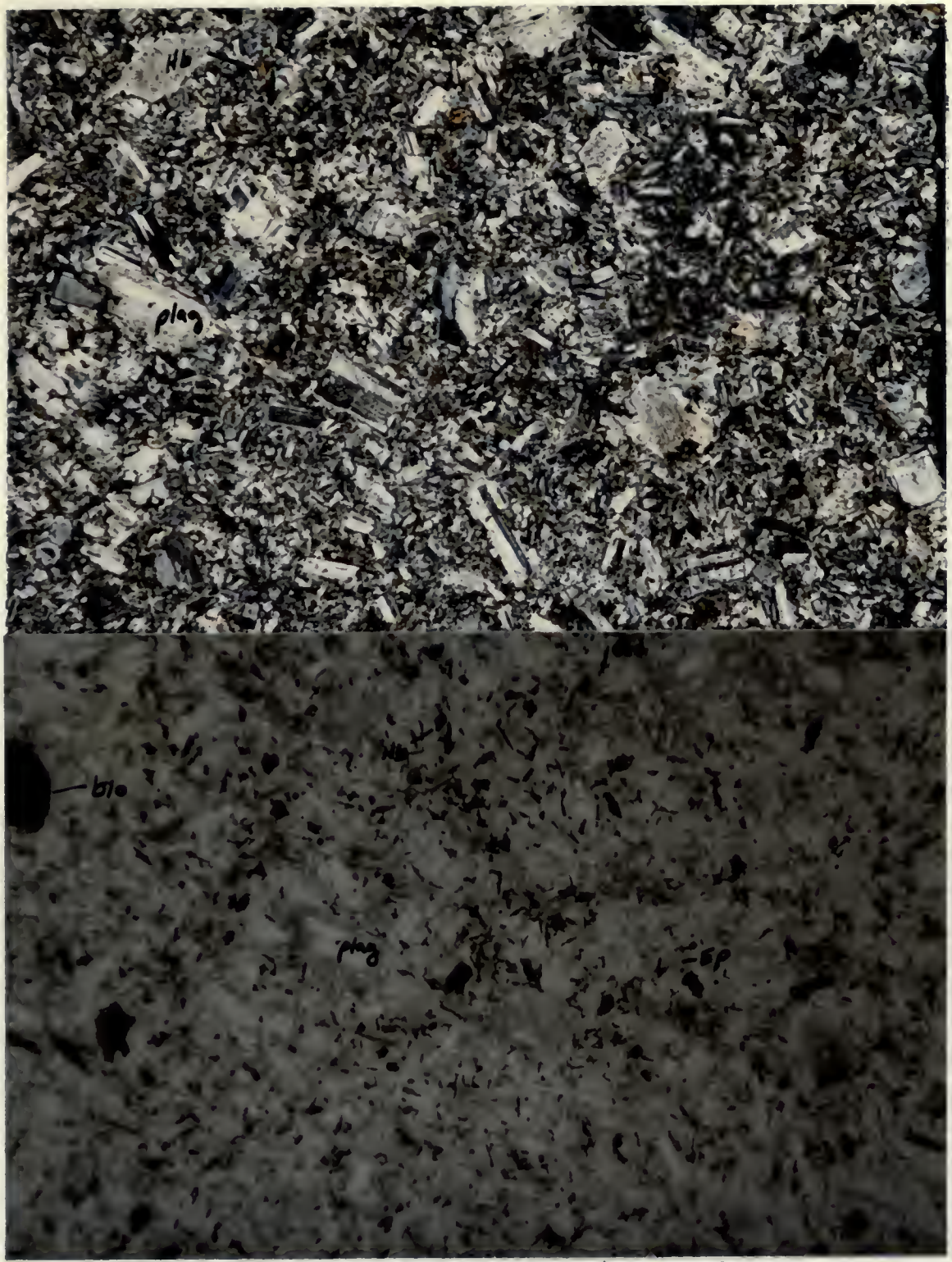

Plate 7a DW40 Weakly propylitized hornblende/biotite feldspar porphyry. Top: crossed polars, Bottom: plane polarized light. Plagioclase (plag), Biotite (bio), hornblende (Hb), epidote (ep).

0 1 2mm

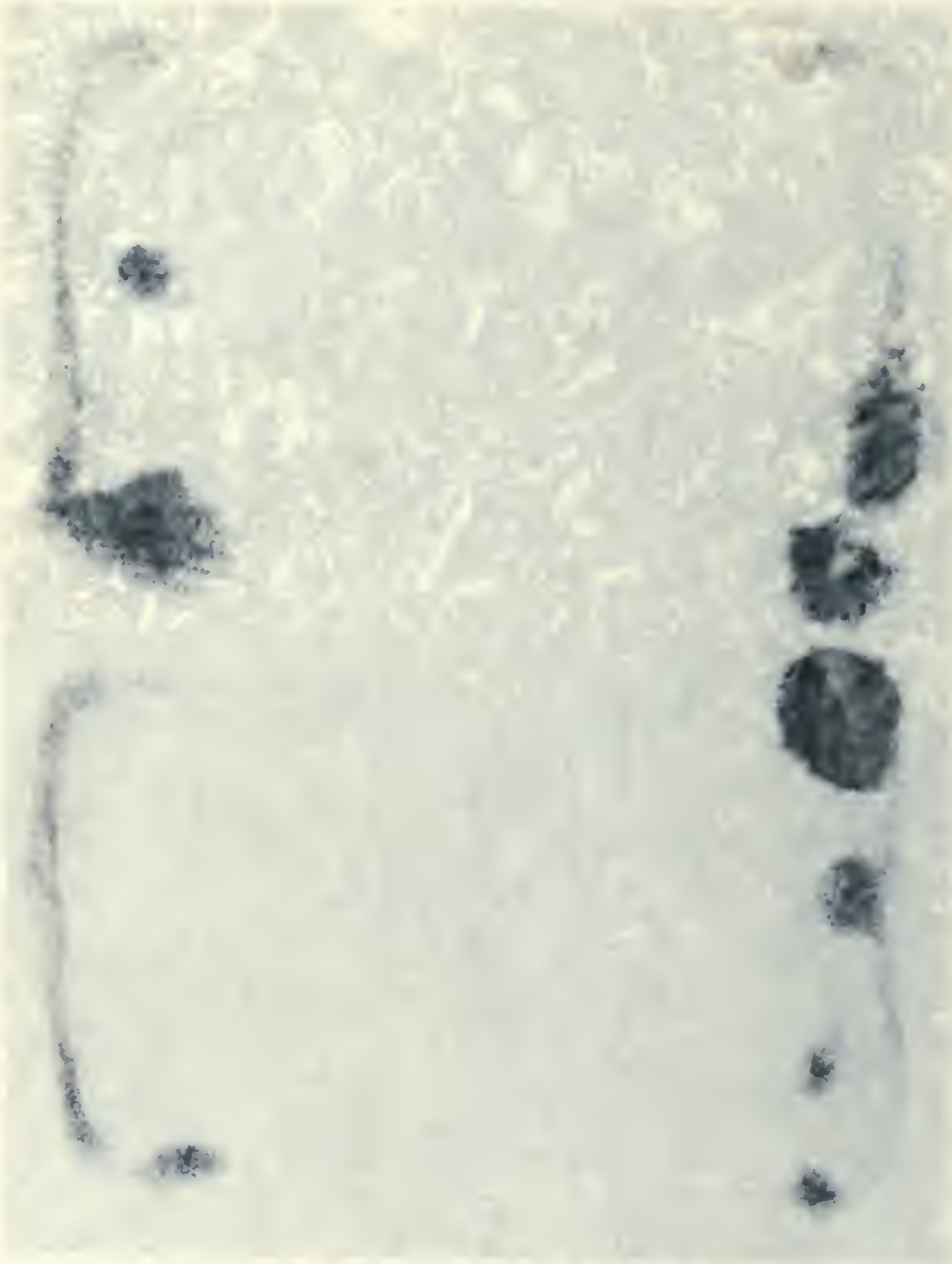

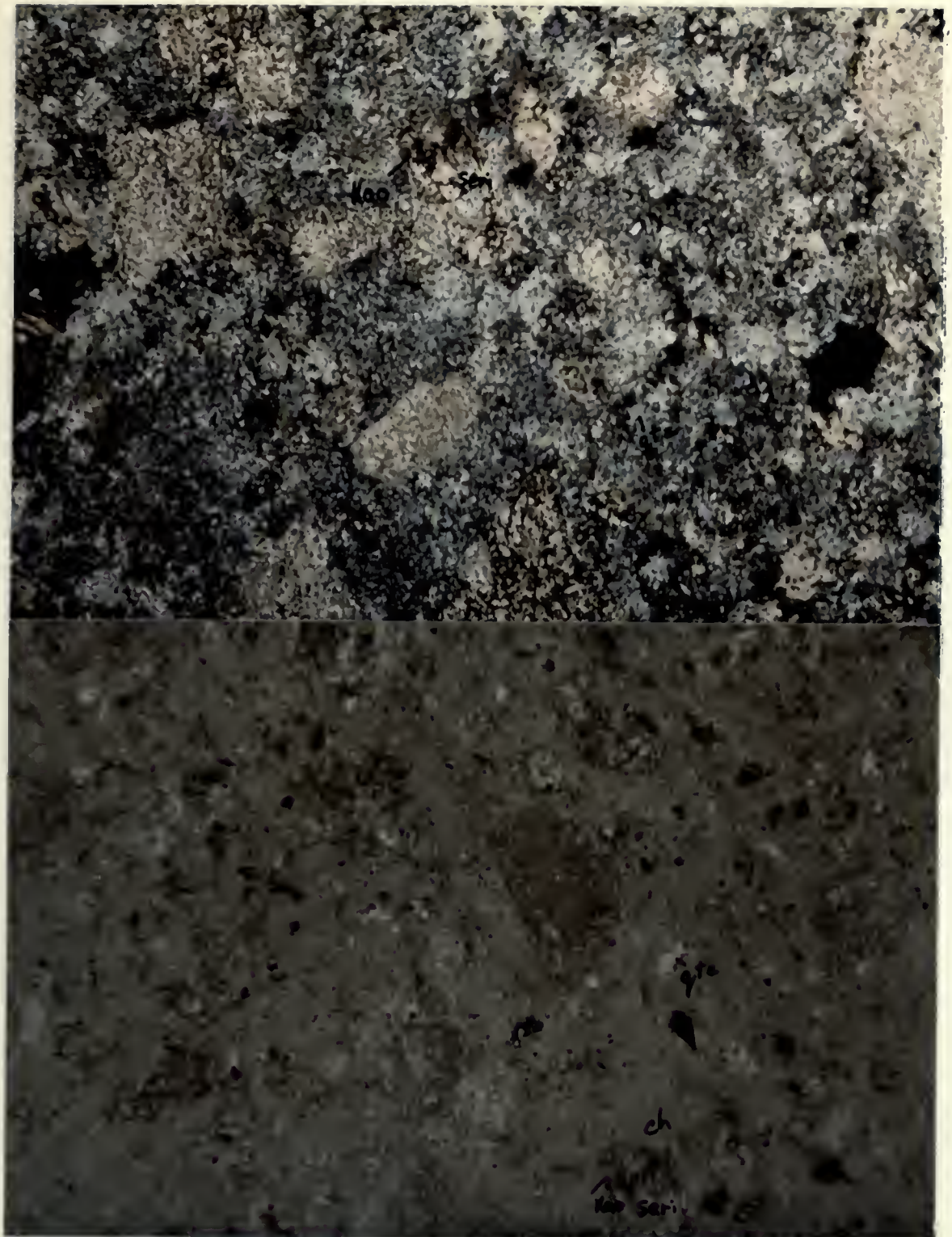

Plate 7b DT139 Hornblende/biotite feldspar porphyry altered to potassic facies with strong phyllic-argillic and weak propylitic alteration. Plagioclase is replaced by sericite (seri) and kaolin (kao). Quartz (qtz), and Chlorite (ch) appear. Top: crossed polars, Bottom: plane polarized light.

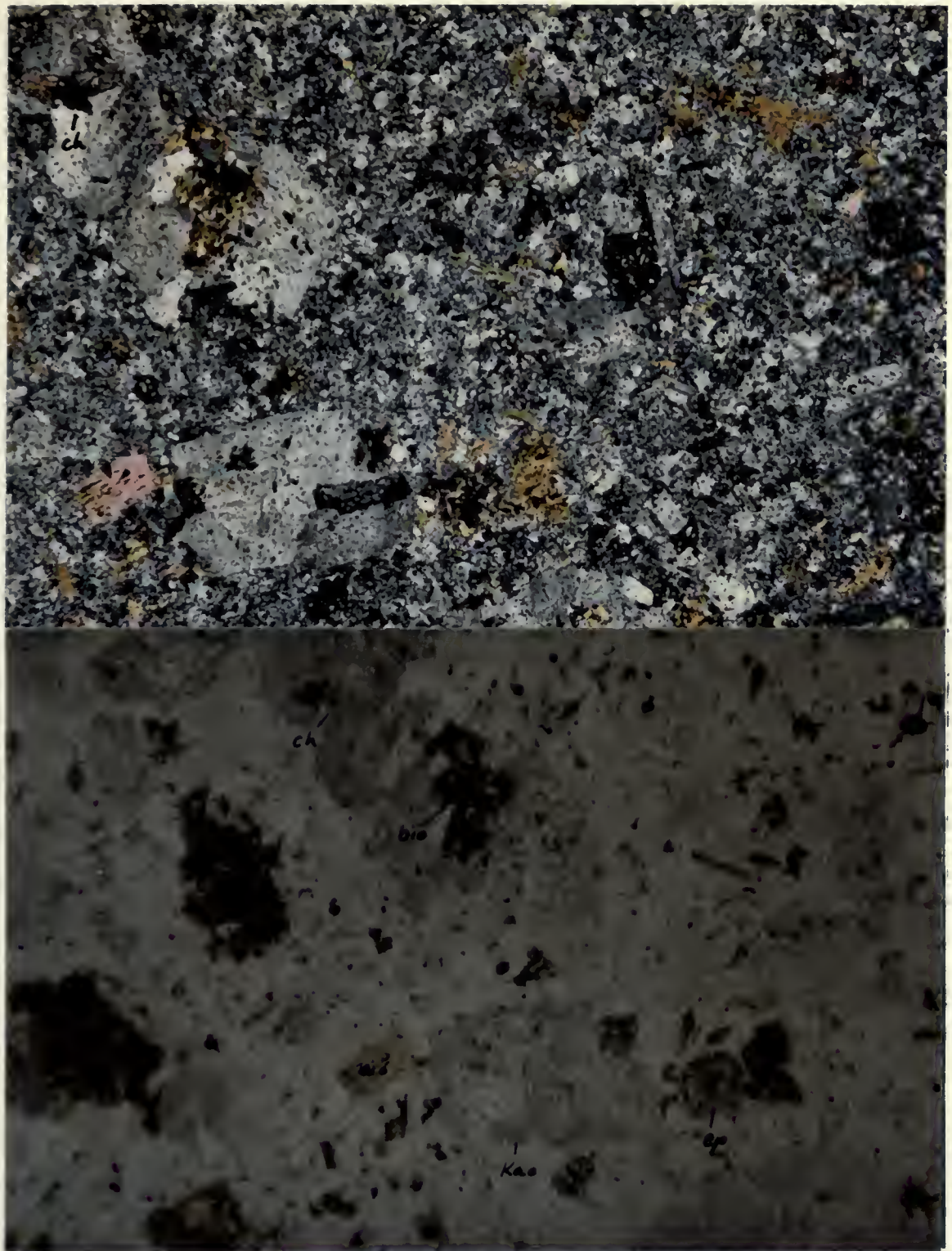

Plate 7c DT175 Hornblende/biotite feldspar porphyry altered to potassic facies with weak propylitic overprinting. Plagioclase partially replaced by sericite and kaolin (kao), biotite is of both primary (bio) and secondary (II) origin. Chlorite (ch) and epidote (ep) appear.
Top: crossed polars, Bottom: plane polarized light.

Table 7 Modal Percentages of Minerals in the Altered Andesitic Rocks

Mineralogy | Spec. no.	DW 40	DT 139	DT 175
	Propylitic	Potassic (Phyllic-Propylitic)	Potassic
Quartz	8	16	27
Plagioclase (species)	78 (An_{44})	16 (An_{34})	48 (An_{36-20})
Orthoclase		26	8
Hornblende	7		
Biotite	5		15
Sphene	0.5		
Apatite	trace	trace	2
Monazite	trace		trace
Opaques	1	4	1
Zircon			trace
Epidote	trace	1	
Chlorite	trace	7	trace
Rutile		rare	
Carbonate		7	
Kaolinite		11	
Muscovite		11	

monazite, chlorite, epidote (DW 40) to quartz, orthoclase, muscovite, kaolin, carbonate, chlorite, epidote (DT 139) to quartz, orthoclase, biotite, secondary biotite, zircon, apatite, monazite, chlorite (DT 175). Table 7 provides a summary of mineral percentages of the altered grey-hornblende/ biotite-feldspar porphyry rocks. The hand specimens become slightly lighter in colour with increasing grade. Argillic alteration is marked by substantially lighter colour. The plagioclase phenocrysts are opaque rather than transluscent, as in the other alteration facies, because of clays.

Granodioritic Rocks

Coarse Porphyritic Granodiorite DT 258, DT 239, DT 306, DT 303 (Plate 8)

In hand specimen, the coarse porphyritic granodiorite undergoes only slight changes in colour with increasingly alteration facies. The propylitic rock is brown to grey depending upon the depth of weathering of pyrite. The argillic rocks are buff to tan and crumble readily. Potassic and silicic rocks are orange-grey and light grey respectively.

The alteration assemblages and overprinting present here are: very weak argillic, weak propylitic (DT 258); phyllic with weak propylitic alteration (DT 239); potassic with weak phyllic-argillic, propylitic alterations (DT 306); and silicic-potassic alteration (DT 303).

As in the previous assemblages, plagioclase decreases

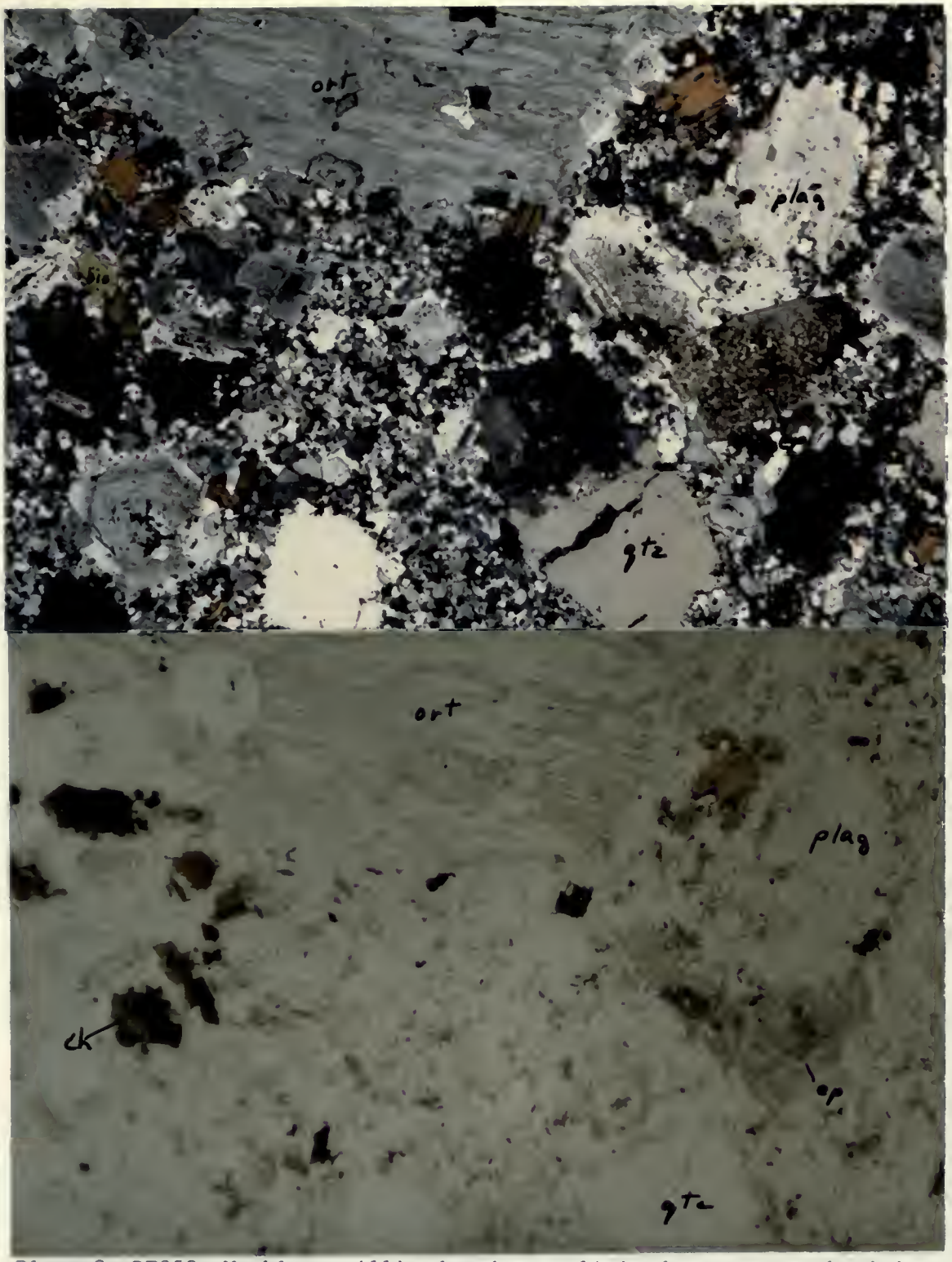

Plate 8a DT258 Weakly argillized and propylitized coarse porphyritic granodiorite. Top: crossed polars, Bottom: plane polarized light. Orthoclase (ort), quartz (qtz), plagioclase (plag), biotite (bio), kaolin (kao) plus smectite, chlorite and epidote (ep) appear.

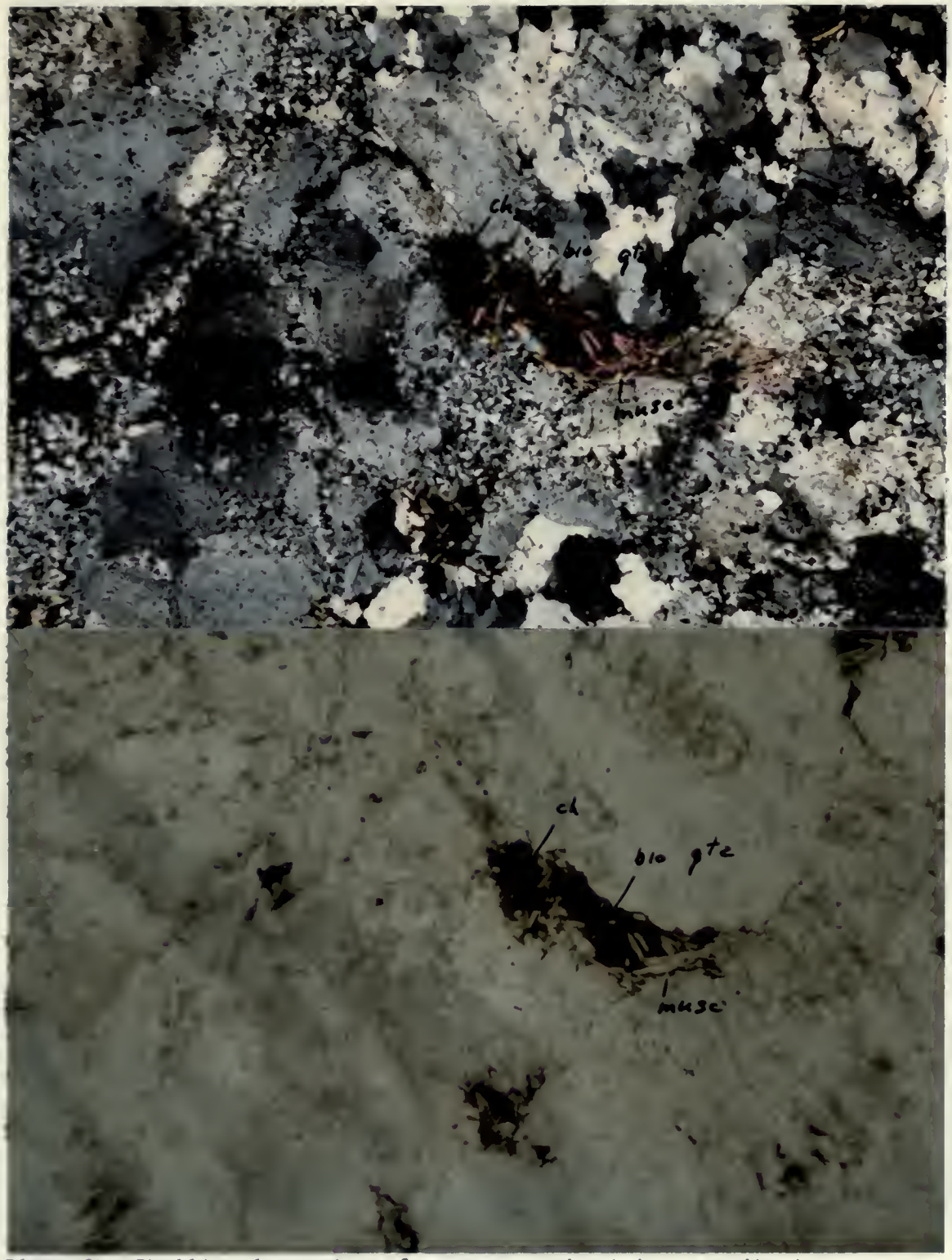

Plate 8b Phyllic alteration of coarse porphyritic granodiorite. Quartz (qtz), muscovite (musc), biotite (bio) and chlorite may be readily seen. Top: cross polarized light, Bottom: plane polarized light.

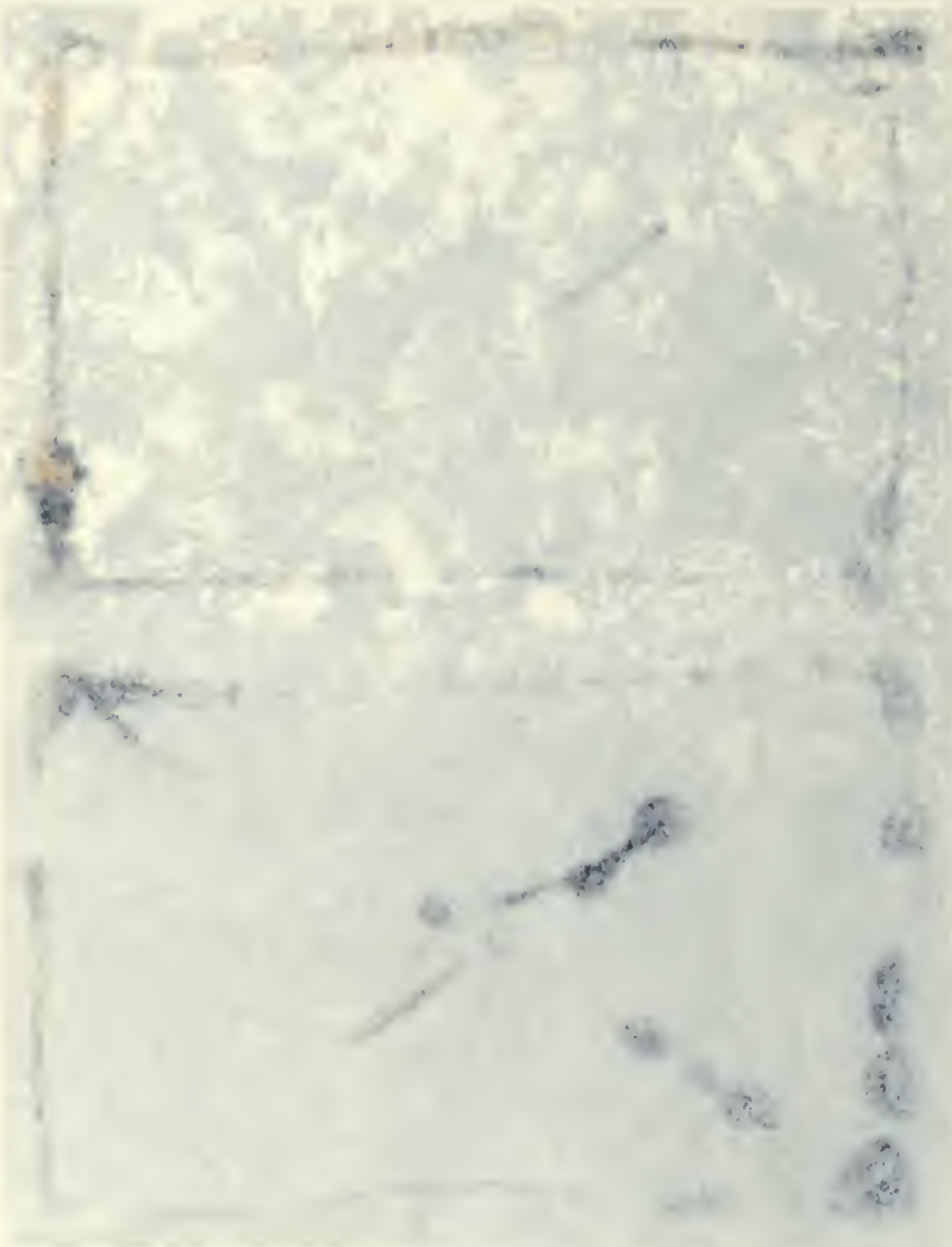

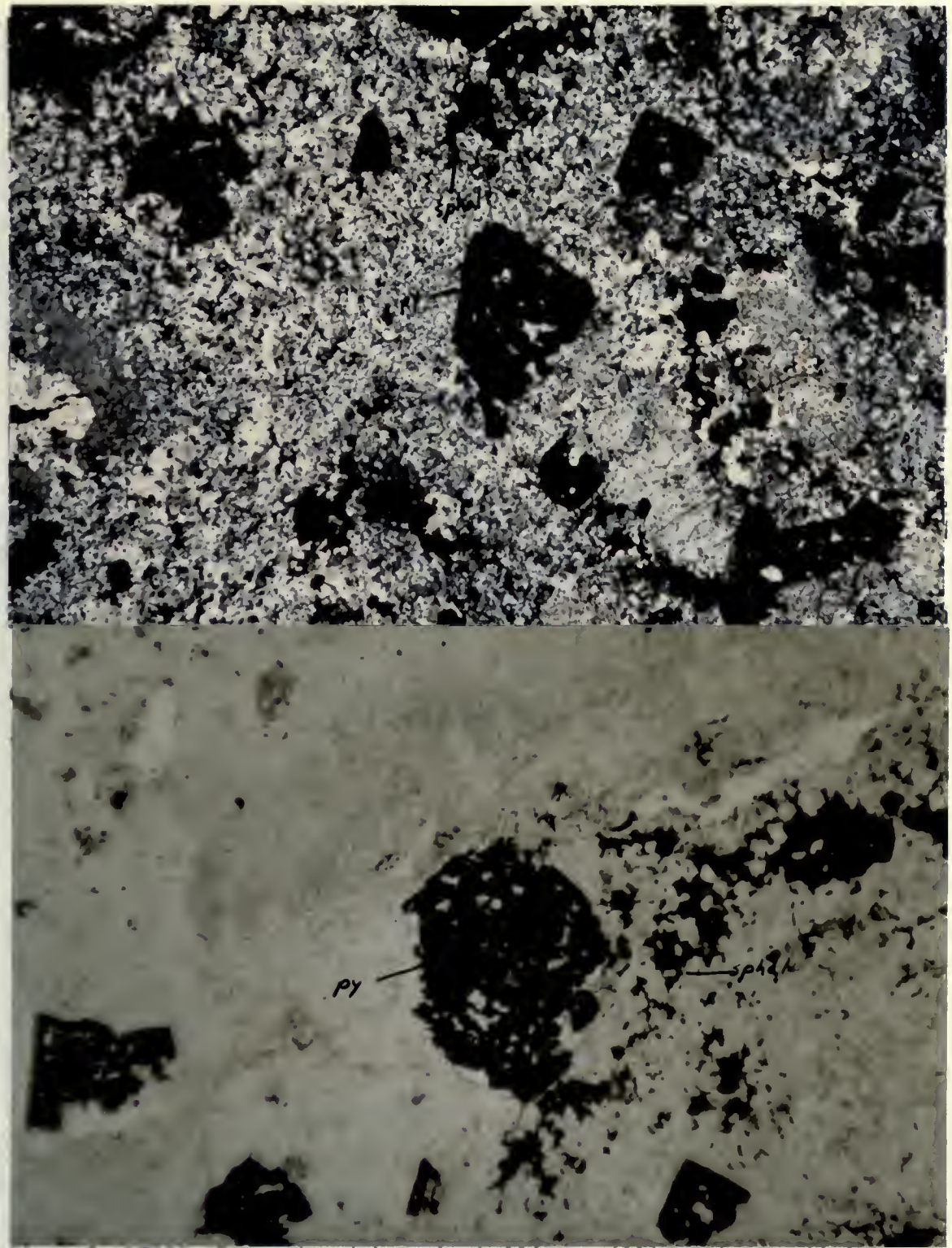

Plate 8c DT306 Potassic with weak phyllic-argillic and propylitic alteration of coarse porphyritic granodiorite. Top: crossed polarized light, Bottom: plane polarized light. Opaques are pyrite (py) and sphalerite (sphal) among others.

0 1 2

Plate 8d DT303 Silicic - potassic alteration of coarse porphyritic granodiorite. Top: crossed polars, Bottom: plane polarized light.

0 1 2mm

Table 8 Modal Percentages of Minerals of Porphyritic Granodiorites

Spec. no. / Mineralogy / Alteration (overprinting)	DT 258	DT 239	DT 306	DT 303
	Propylitic	Phyllic (propylitic)	Potassic (Phyllic-Argillic Propylitic)	Silicic-Potassic
Quartz	19	47	60	62
Plagioclase (species)	49 (An_{38-6})	28 (An_{12})	5 (An_{33})	
Orthoclase	26	22	25	22
Hornblende	trace			
Biotite (phlog)	3	1		(11)
Sphene	trace		rare	
Apatite	trace	rare	1	
Monazite?		rare		
Opaques	1	trace	*	*
Zircon			trace	
Epidote	trace	trace	trace	
Chlorite	trace	trace	rare	
Kaolinite			1	
Sericite/muscovite	trace	1	trace	
* Sphalerite			2	rare
* Pyrite			6	5
* Covelline			trace	
* Chalcopyrite			0.2	trace
* Molybdenite			trace	0.1
* Wolframite				rare
Scheelite				trace
Cassiterite				trace

both in abundance and anorthite content; whereas quartz and orthoclase generally increase. The remaining portion of each assemblage changes from biotite, hornblende, apatite, smectite, sphene, epidote, chlorite (DT 258) to biotite, monazite, apatite, muscovite, chlorite, epidote, garnet (DT 239) to zircon, apatite, muscovite, kaolin, sphene, epidote, chlorite, molybdenite, chalcopyrite, covelline, pyrite and sphalerite (DT 306) to phlogopite, cassiterite, scheelite, wolframite, molybdenite, chalcopyrite, pyrite, sphalerite (DT 303).

Quartz-Feldspar Porphyry DT 8, DT 37, DT 69A, DT 310 DT 333 (Plate 9)

The quartz-feldspar porphyry is considered to be the magmatic phase associated with the formation of the large gossan zone and the porphyry ore system. Outcrops of this porphyry are mainly dykes, although Cowan (1970) considered a large set of outcrops in the northeast portion of the map area to represent a stock.

The quartz-feldspar porphyry has undergone varying degrees of alteration. It is fine-grained to aphanitic and contains quartz-plagioclase and orthoclase phenocrysts. Both biotite and hornblende are observable in the least altered handspecimen.

In thin-section the plagioclase phenocrysts are seen to change from An_{37-25} zoned grains (DT 8) to An_{14} unzoned

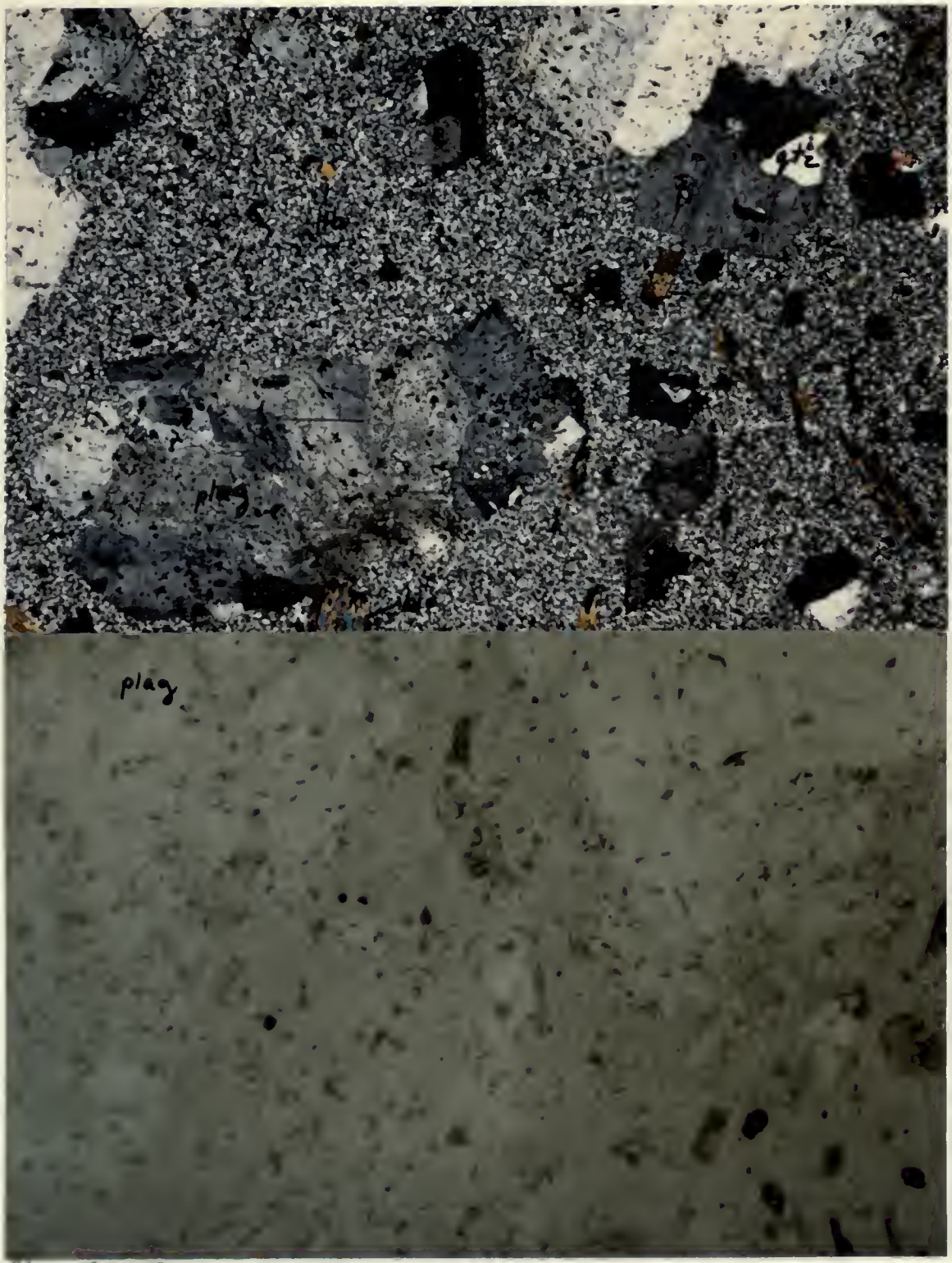

Plate 9a DT8 Propylitized quartz-feldspar porphyry. Top: crossed polars, Bottom: plane polarized light. Plagioclase (plag), quartz (qtz), biotite (bio), chlorite (ch) epidote (ep), hornblende (hb).

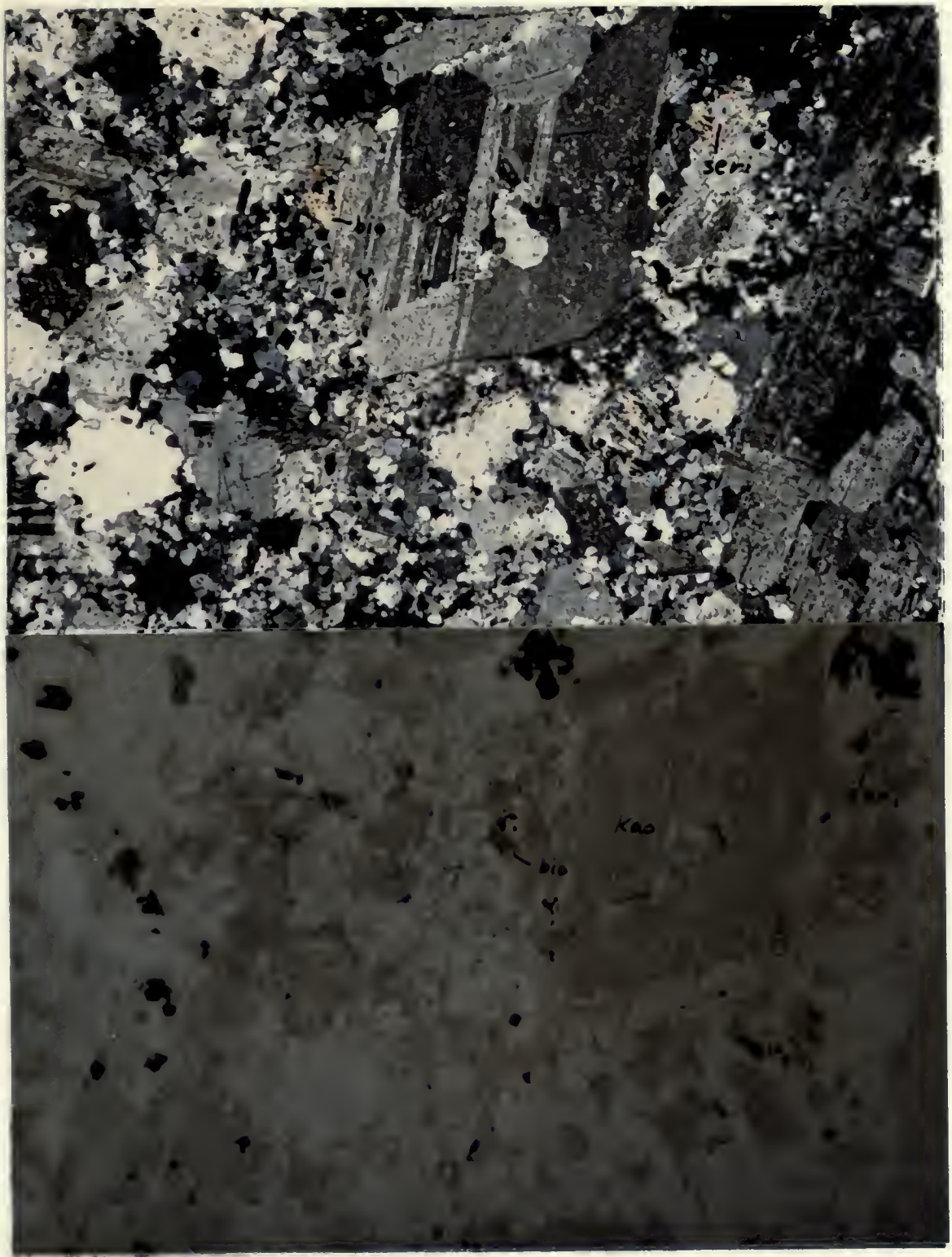

Plate 9b NDT69A Phyllic-argillic altered quartz-feldspar porphyry Top: crossed polars, Bottom: plane polarized light. Kaolin (kao), sericite (seri), biotite relicts (bio).

0 1 2mm

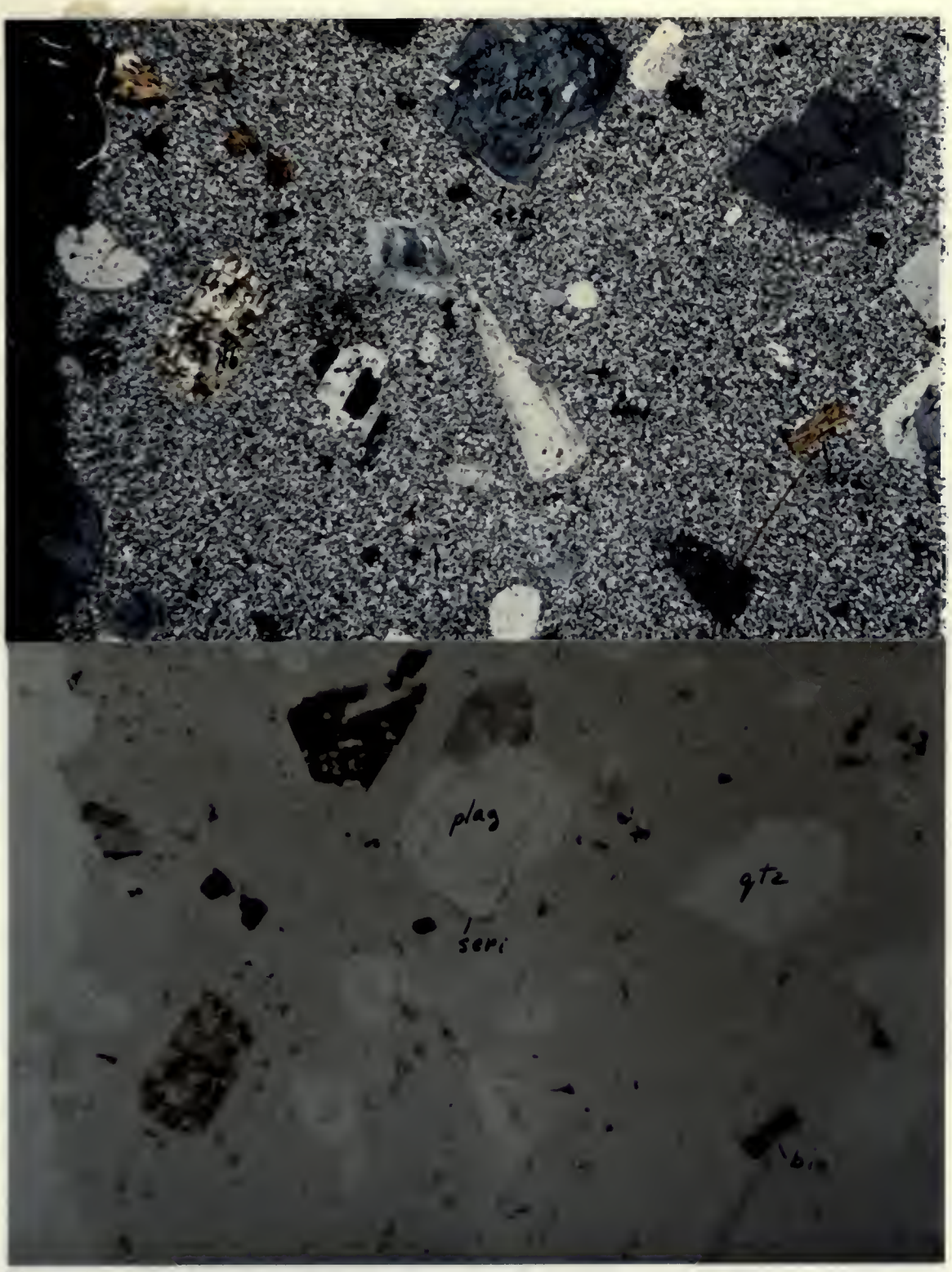

Plate 9c DT310 Quartz-feldspar porphyry-potassic with weak argillic overprinting. The groundmass is dominated by potash feldspar grains. Top: crossed polars, Bottom: plane polarized light. Plagioclase (plag), quartz (qtz), biotite (bio), hornblende (Hb), sericite (seri), kaolin (kao).

Plate 9d Quartz-feldspar porphyry highly altered 1) potassic alteration gave rise to formation of a mosaic of felted orthoclase mats 2) over-printing of phyllic-argillic and propylitic facies followed. An alteration rim occurs on the quartz grain. Top: crossed polars, Bottom: plane polarized light. Quartz (qtz), sericite (seri), kaolin (kao), epidote (ep).

(DT 37), to An_6 (NDT 69A) to An_{31-22} (DT 310).

The mineral assemblages suggest successive overprinting by weak retrograde alteration. These assemblages change from: quartz, orthoclase, hornblende, sphene, monazite, epidote, chlorite (propylitic) (DT 8); to quartz, orthoclase, biotite, hornblende, apatite, monazite, rutile, chlorite (propylitic) (DT 37); to quartz, orthoclase, biotite, muscovite, smectite, kaolin, rutile, epidote (phyllic-argillic with weak propylitic alteration) (NDT 69A); to biotite, hornblende, smectite, sphene, monazite, chlorite (potassic with weak argillic and very weak propylitic) (DT 310); to biotite, apatite, muscovite, kaolin, carbonate, chlorite (strong potassic alteration with weak phyllic, argillic and propylitic alteration) (DT 333). The sample DT 333 is especially interesting in that the original plagioclase of the groundmass has been replaced by orthoclase which forms felted mats containing crystal grains of the same or closely similar orientation. Similar replacement, albeit weaker, is also present in sample DT 310. The abundance of hydrous minerals in DT 333 suggests that high H_2O fugacity may be responsible for the degree to which this replacement and growth occurs. Samples DT 8, NDT69A, DT 310 and DT 333 in Plates 9a to 9d. The mineral abundances for these rocks are summarized in Table 9 and Figures 11, 12 and 13.

Feldspar Porphyry DT 205 (Plate 10)

The feldspar porphyry is a post-ore mineral dyke rock

Table 9 Modal Percentages of Minerals in Altered Quartz-Feldspar Porphyry

Spec. no.	DT 8	DT 37	NDT 69A	DT 310	DT 333
Mineralogy Alteration (overprinting)	Propylitic	Propylitic	Phyllic (Propylitic)	Potassic	Potassic (Phyllic-Argillic)
Quartz	33	32	40	17	3
Plagioclase (species)	38(An_{37-25})	42(An_{14})	47(An_{6})	17(An_{31-22})	8(An_{32})
Orthoclase	18	21	2	64	57
Biotite		2	trace	1	trace
Hornblende	3	1		trace	
Apatite			trace		rare
Sphene	trace			rare	
Monazite	trace	rare		rare	
Chlorite	5	trace		1	2
Epidote	1		trace		
Rutile		rare	trace		
Opaques	1	1	1	trace	2
Kaolinite			1		4
Smectite			6	trace	
Sericite/musc			1		23

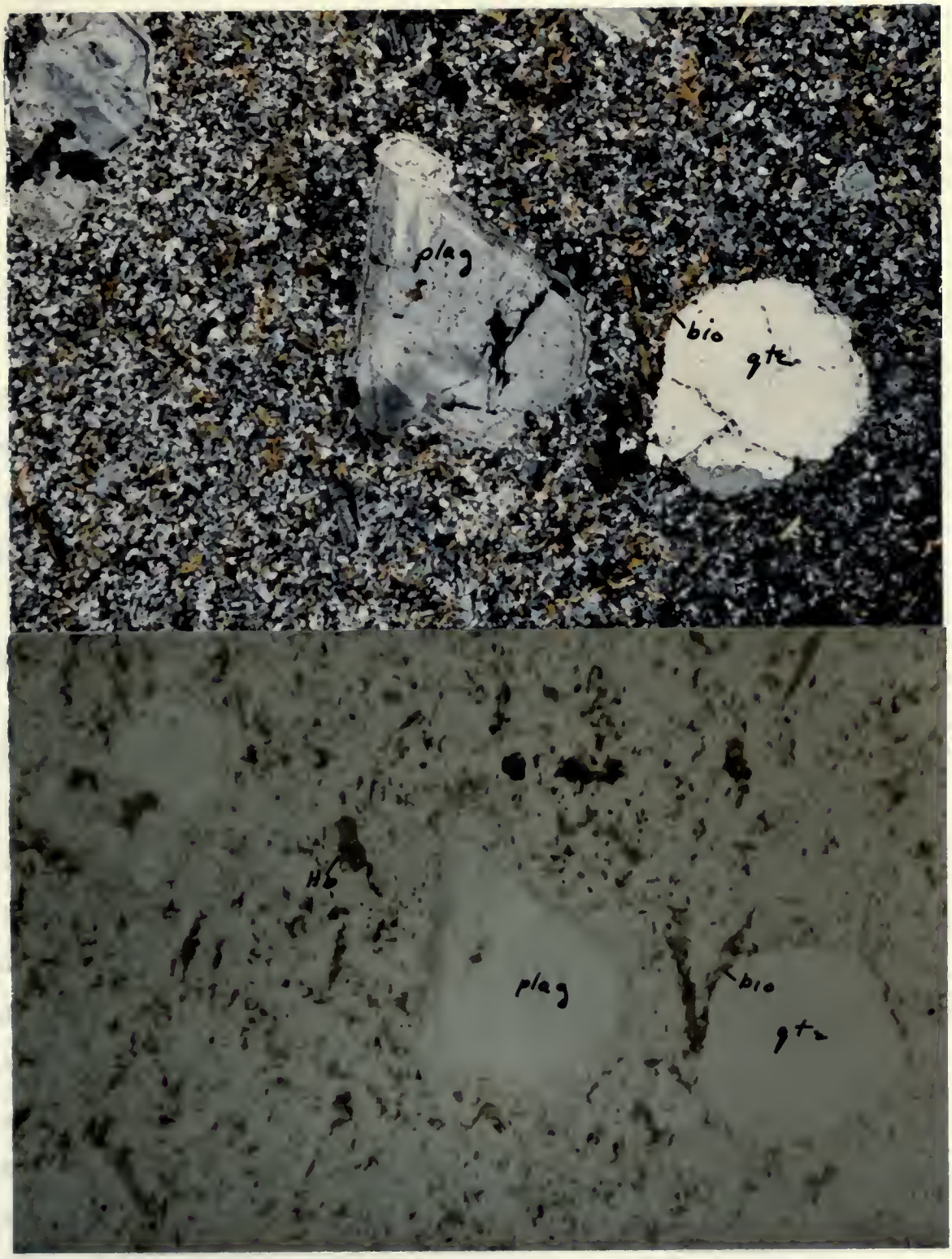

Plate 10 DT205 Feldspar porphyry containing a partially rimmed xenocryst of quartz (qtz), groundmass consists of plagioclase, orthoclase, biotite (bio) and hornblende (Hb).

which has undergone autometamorphism.

The hand specimen DT 205 is a fine-grained phaneritic porphyry containing pheocrysts of white feldspar, biotite and quartz, and microphenocrysts of hornblende. The overall colour is mesocratic grey. In thin-section, the plagioclase phenocrysts are zoned oligoclase with poikilitic rims. The groundmass consists of subhedral plagioclase microlites with anhedral grains of quartz and orthoclase. Included in the groundmass are microlites of biotite, apatite, with zircon, monazite, epidote, and chlorite. The quartz grains are partially rimmed by hornblende and biotite. A summary of the mineral abundances appears in Table 10.

Lamprophyre DT 162 (Plate 11)

These rocks are altered and therefore will also be described here. As with the feldspar-porphyry, these are post-porphyry system dykes. Sample DT 162 is a melanocratic grey rock. It is an aphanitic porphyritic rock containing anhedral quartz xenocrysts and hornblende microphenocrysts. In thin section, fluxion is delineated by oligoclase micrlites. Biotite is subordinate to hornblende and partially replaces the latter. Quartz xenocrysts are rimmed by biotite and epidote. Accessories are apatite, monazite, sphene, clinozoicite and orthoclase. Augite appears as relict grains partially altered by biotite
A summary of the mineral abundances appears in Table 10.

Table 10 Modal Percentages of Minerals in Feldspar Porphyry and Lamprophyre

Spec. no.	DT 205(FP)	DT 162(L)	DT 8(QFP)
Mineralogy			
Quartz	14	2	33
Plagioclase (species)	53 (An_{27})	58 (Oligoclase)	38 (An_{37-25})
Orthoclase	5	1	18
Augite		4	
Hornblende	3	18	3
Biotite	9	12	
Apatite	2	trace	
Monazite	trace	trace	trace
Zircon	trace		
Sphene		trace	trace
Opaques	5	5	1
Chlorite	trace		5
Epidote	trace	trace	1

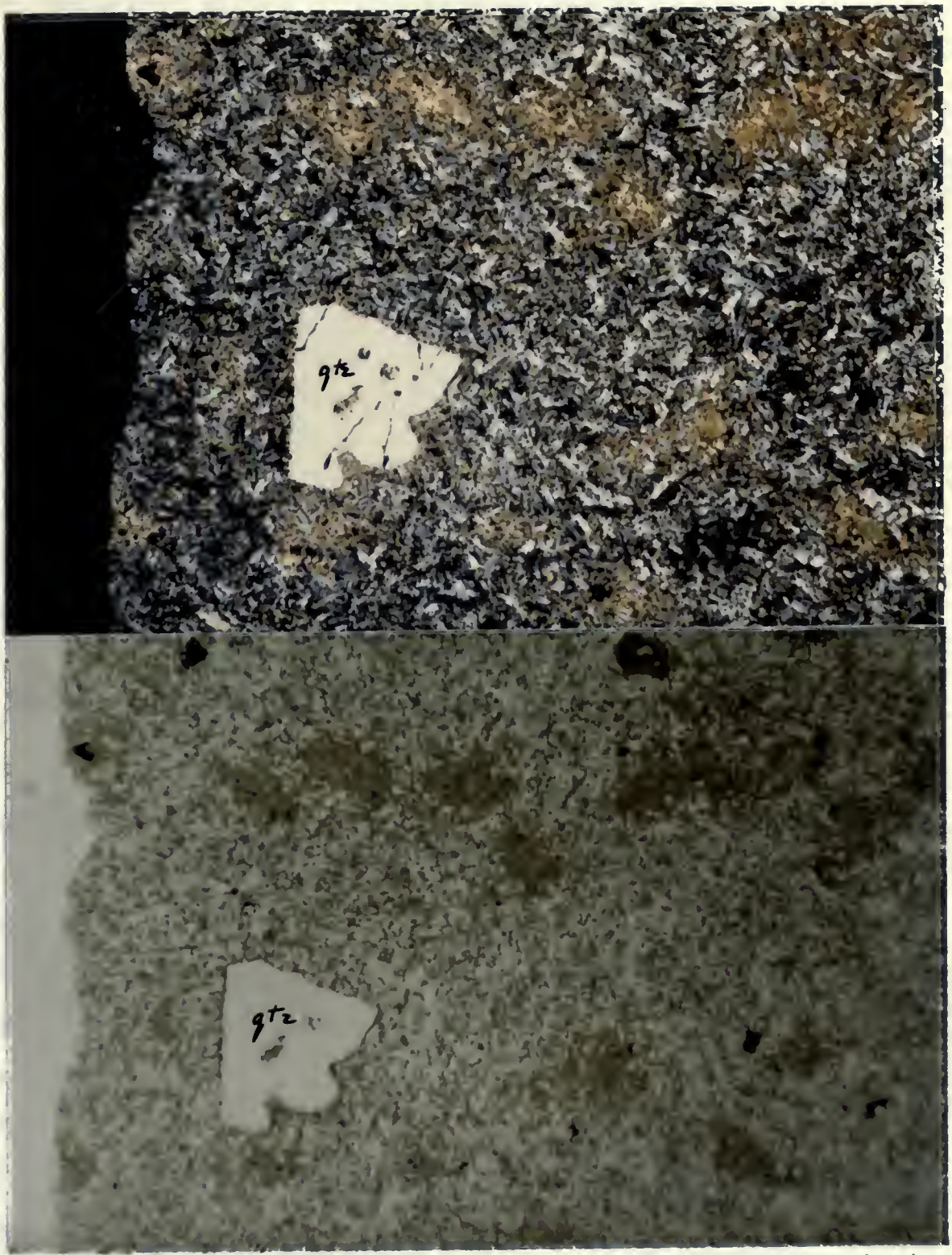

Plate 11 DT162 Lamprophyre containing a rimmed quartz xenocryst (qtz). The reaction rim consists of biotite and epidote, The brown patches in the matrix consist of intergrown biotite and hornblende. Top: crossed polars, Bottom: plane polarized light.

The rimming of quartz in the feldspar porphyry and in the lamprophyre as well as the increase in the abundance of mafic minerals over the quartz-feldspar porphyry (see Table 10) suggests some affinity between these last two rock types. Plots of the data from Tables 5 to 9 (inclusive) appear in Figure 12 which is a quartz-plagioclase + hornblende + kaolin-potash feldspar + biotite + sericite diagram. The figure reveals the trends of alteration in the various rock types. The plot of diorite suite rocks shows a trend of increasing silica and in one case an increase in potash feldspar. In the rocks of andesitic composition there is an increase in silica with a slight increase in potash feldspar. In one case, DT 175 contains secondary biotites which are probably related to autometamorphism rather than later ore mineralizing alteration since it accompanies an increase in silica. Alteration of the coarse porphyritic granodiorite shows a similar path of increasing silica and potash feldspar as in the previous rock types. However, the trend of alteration meets the quartz - kspar join.

Alteration of the quartz-feldspar porphyry is presumed to be autometamorphic. The trend of alteration is dramatically different. It is one of increasing potash feldspar and decreasing silica. The decrease in silica with respect to kspar is unexpected, but compatible with the later formation of later feldspar porphyry dykes and ultimately the formation of the lamprophyre dykes. The process of alteration is desilication.

Figure 11 Mineral Histogram

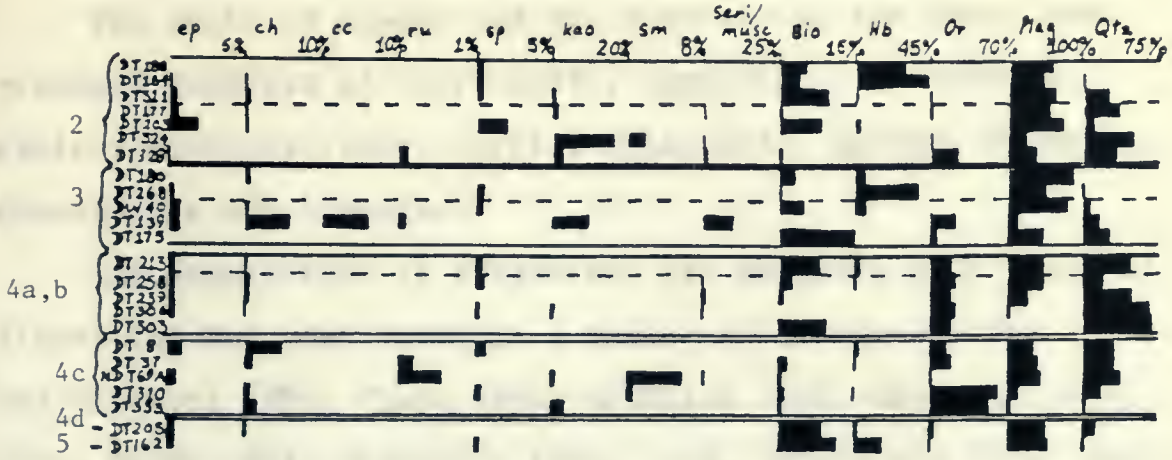

2 - Diorite Suite Rocks

3 - Hornblende-Feldspar Microporphyry, Hornblende/Biotite Porphyry

4a,b- Granodiorite

4c- Quartz-Feldspar Porphyry

4d- Feldspar Porphyry

5 - Lamprophyre

Figure 12 Ternary Plot using Mineralogical Apices for Altered Rocks

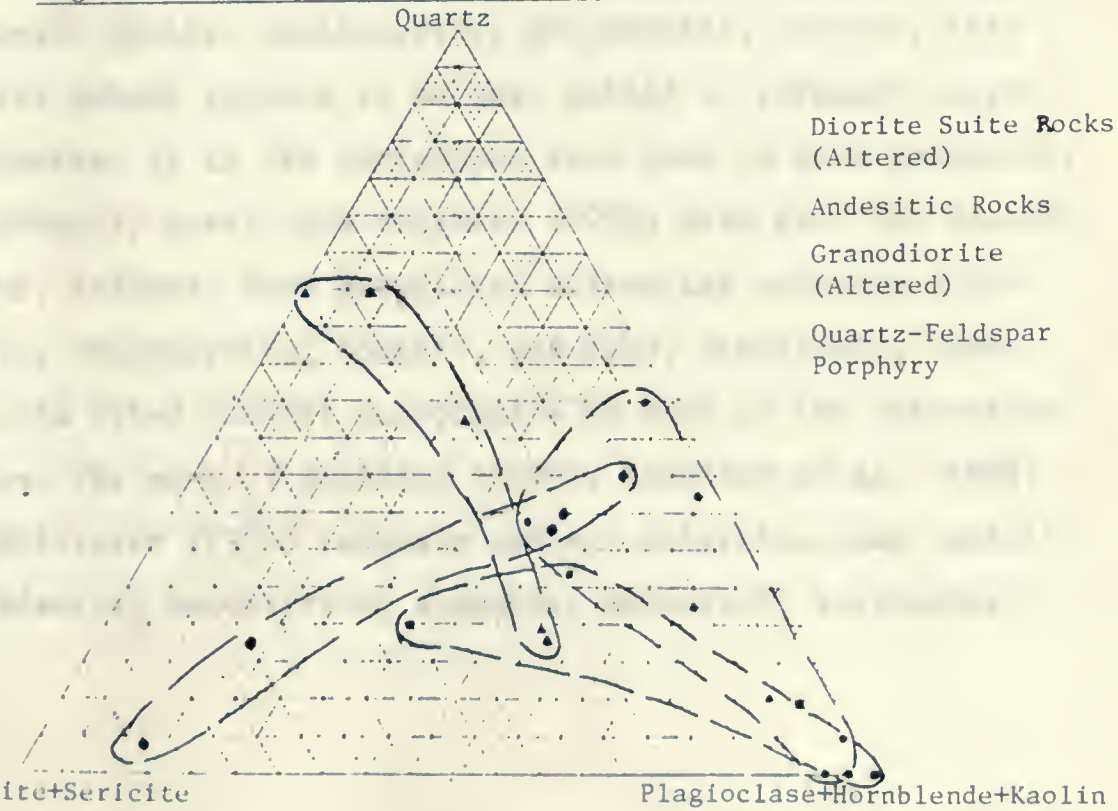

Ore Mineralogy

The suite of opaque and ore minerals in the Sand Creek prospect consists of molybdenite, magnetite, specularite, chalcopyrite,covelline, pyrite, sphalerite, galena, scheelite cassiterite and ilmenite.

The association of opaque and ore minerals with types of alteration has been noted in a number of previous works (Lowell and Guilbert 1970, Clark 1970, Sillitoe 1973, Sillitoe et al 1975, Sharp 1973, Hollister 1974, 1975, Soregaroli 1975, Lowder and Dow 1976, Gorashi-Zadeh 1978, Taylor and Fryer 1980, among others). The diversity of the systems cited however leads to some confusion regarding the type of opaque and ore mineralogy associated with each alteration facies. Lowell and Guilbert lay out a general scheme of propylitic: galena, sphalerite, gold silver minerals, argillic: pyrite, galena and sphalerite, phyllic: pyrite, chalcopyrite and bornite, potassic: pyrite, chalcopyrite, molybdenite, bornite. This general scheme appears to be best suited to porphyry copper occurrences. It is the variations that lead to some confusion. For example, Lowell and Guilbert (1970) also cite the deposit at Ray, Arizona. Here propylitic alteration contains molybdenite, chalcopyrite, bornite, and gold. Similarily, other deposits cited exhibit molybdenite in each of the alteration facies. The work of Sillitoe (1973), Sillitoe et al. (1975) and Hollister (1975) indicate silicic alteration may contain molybdenite, cassiterite, stannite, scheelite, wolframite

as well galena, sphalerite, gold, silver and copper which in the Lowell and Guilbert model are assigned to the propylitic zone. Wolframite also may appear in the potassic zone according to the work of Lowell and Guilbert (1970). Hollister (1975) states that Tungsten is mined from all the alteration zones at the porphyry molybdenum deposits at Compaccha, Peru. Resolution of this may well require not only a general model of vertical zonation of chalcopyrite, molybdenite, bornite grading upward into chalcopyrite, pyrite and finally pyrite as the tables of Lowell and Guilbert (1970) suggest, but a physio-chemical model for porphyry occurrences similar to that which Strong (1981) advances for granophile deposits. Table 11 consists of opaque and ore mineral assemblages and associated alteration for differing rock types.

The sample, DT 272 exhibits zonation on the microscopic scale. In this specimen, the opaque and ore mineralogy grades in a few millimetres from molybdenite smears on a fracture surface to magnetite, chalcopyrite and pyrite disseminations. The associated silicate alteration is potassic at the fracture rim but is propylitic in the rest of the sample. There is no phyllic or argillic assemblage developed. The altering fluids did not infiltrate very far before precipitating the sulphides and the fluids were not caustic enough to form phyllic and argillic alteration.

All of the mineralized samples in Table 11 have undergone potassic or silicic alteration. The silicic alteration

Table 11 Ore Mineralogy, Alteration and Rock Type

Spec. no.	Ore Mineral Assemblage	Alteration	Rock Type
DT 281	py-moly-cp-rare cov-rare sch rare cass	greisen (silicic)	breccia
DT 303	py-moly-cass-sch-rare wolf-rare sphal	silicic/ potassic	granodiorite
DT 117	moly	silicic	greisen quartz vein
DT 294	moly-py-cp-cov	silicic grading to potassic	quartz-feldspar porphyry
DT 65b	moly-py-cp-mt	potassic	quartz vein in schists
DT 57c	moly-py-rare cp-rare mt	potassic strong phyllic strong argillic	diorite?
DT 272	moly-py-cp-mt	potassic prop	granodiorite
DT 223	py-mt-cp-moly-ilm	potassic w weak argillic	quartz-feldspar
DT 30o	py-sphal-cp-cov	potassic weak phyllic weak prop	granodiorite
DT 301	mt-spec-moly-py-	potassic strong prop	granodiorite
DT 278	py-ilm-rare moly	potassic weak arg	granodiorite
DT 128	py-cp-rare galena	potassic	quartz-feldspar porphyry
DT 131	mt	potassic	granodiorite

grades from strong greisen affinities to potassic alteration. The opaque and ore minerals most strongly associated with the silicic assemblage are pyrite and molybdenite with minor cassiterite and scheelite. The opaque and ore minerals associated with potassic alteration appear to be dominantly pyrite, chalcopyrite and molybdenite as well as magnetite and covelline in some cases. The occurrence of sphalerite within the potassic and silicic assemblages may be due to remobilization of pre-existing ores since the specimens DT 303 and DT 306 are close to the contact of the coarse porphyritic granodiorite with the diorite suite rock. It is assumed (1) that the whole porphyry system involves two phases of mineralization and (2) that sphalerite and galena are peripheral as in the Lowell and Guilbert (1970) model.

Summary

The complex of metamorphic and intrusive igneous rocks of the Sand Creek Prospect run the gamut of unaltered to intensely altered rocks. The facies of alteration used here employ the terms 'propylitic' (a) chlorite-epidote-pyrite ± carbonate± rutile± sphene, (b) chlorite- epidote-actinolite- pyrite; 'argillic' (quartz-kaolin-smectite ± chlorite); 'phyllic' (quartz-sericite/muscovite-pyrite); 'potassic' (a) quartz, orthoclase, biotite ± sericite, (b) quartz-biotite-sericite; 'silicic' (quartz, orthoclase,

sericite, cassiterite, wolframite, scheelite).

Unaltered rocks represent schists and gneisses; dioritic rocks, andesitic rocks, and coarse-grained porphyritic granodiorites. Alteration leads to a lightening of colour in all facies except where secondary biotite is introduced. The rock types; hornblende/biotite feldspar porphyry, quartz-feldspar porphyry, feldspar porphyry and lamprophyre are found only in the altered state. The feldspar porphyry appears to have affinities with the lamprophyre. Opaque and ore mineralization is associated with alteration zonation. The strongest associations are pyrite - molybdenite $\pm$ (cassiterite and scheelite) in silicic alteration, and pyrite - chalcopyrite - molybdenite $\pm$ (magnetite and covelline).

The molybdenite mineralization is varied in grain size and texture. It forms: coarse rosettes in quartz veins and disseminations in the quartz - feldspar porphyry; very fine grains in potassic alteration; and smears on joint or fracture surfaces.

Molybdenite smears are mainly found in the west and southern extremities on the map area. Rosettes are found mainly north of the forth branch of Sand Creek. Fine-grained molybdenite is found throughout most of the map area. This textural zonation is evidence that the large set of outcrops in the northeast of the map area is, as Cowan (1970) suggests, a stock. The rosettes are assumed to have formed in an area of sustained high temperatue and H_2O fugacity, whereas the fine-grained and smear molybdenite probably formed in quickly quenched vein systems.

Discussions

Structure

The problem of structural style of emplacement of the molybdenite mineralizing intrusive may be the result of either regional deformation involving a northeast-southwest trending fault system or the emplacement of a large magmatic body on the scale of greater than 20 kilometres diameter. The work of Koide and Bhattacharji (1975) shows that concentric and radial dykes, joints and faults are to be expected from emplacement of magmatic bodies. The scale of the intrusive is not important. A large body underlying an area mainly north of, yet including, the Sand Creek prospect could account for radial dykes with the orientation seen in the map area. The arcuate path of Hell Raving Creek to the north may be a concentric feature. The path of Sand Creek may also fit into this scheme. The distribution of other known mineral occurrences is compatible with this, although not very supportive of this model of emplacement.

On the other hand, the quartz-feldspar porphyry dykes are aligned parallel with the trend of the major valley containing Middle Lake. The distribution trend of previous mineral claims is also roughly parallel to this valley. Thus, it is more likely that the emplacement of the molybdenum mineralizing dykes was within a regime of regional deformation associated ultimately, with formation of the northeast alignment

of the Moseley Creek Valley.

The stereograms (Figure 9a,b,c) exhibit annuli of joint distribution which are marred by maxima, and in Figures 9a,b girdle minima which cross the stereogram. These maxima and minima are considered to be due to deformation later than that associated with the emplacement of the plutons. If, as Koide and Bhattacharji (?) conclude, the emplacement of plutons is associated with radial and concentric fracturing, then an annulus should appear on the stereograms. The sampling bias of the author with respect to late dyke orientation and related joints and especially the occurrence of this later deformation should account for the maxima and the girdle minima.

Petrology

The intrusive complex in the map area has been broken down into four major groups - the diorite suite rocks, andesitic rocks, granodioritic rocks and lamprophyres. The trend of modal composition of the diorite suite rocks suggest that they may represent a single pulse of magma.

The succeeding andesitic rocks, granodioritic rocks and lamprophyres probably represent a second discreet pulse from the same source.

The diorite suite is a family of rocks including diorites, quartz diorites, tonalites and tonalite aplites. This involves a fractionation trend of increasing silica and

a very slight increase in potash feldspar.

The granodiorite suite contains considerably more potassium than the diorite suite as evidenced by primary orthoclase and the abundance of potassic alteration associated with the quartz-feldspar porphyry.

Desilication of the quartz-feldspar porphyry as shown in the preceeding chapter, plus the intrusion of successively more basic and mafic rocks - the feldspar porphyry and lamprophyre - leads to a model of mobilized basic residual magma which accounts for their positions in the intrusive sequence.

Alteration and Overprinting

The pattern of alteration in the map area is due to a succession of intrusive events, involving magmas which contained an increasing abundance of volatiles. Alteration will be divided into two classes, wall rock and deuteric (autometamorphic) alteration. The term 'wall rock' is used here in reference to intruded or invaded rock that is older than the intrusion. These wall rocks are of various ages and some have undergone deuteric alteration prior to the wall rock alteration. 'Deuteric' is used in reference to alteration by late fluids of the intrusive rock being discussed.

The diorite suite rocks have undergone invasion by at least five intrusives; hornblende/biotite-feldspar

porphyry, granodiorite, quartz-feldspar porphyry, feldspar porphyry and lamprophyre. Therefore they are the most complex in terms of alteration. Figure 13 is a diagram of the minerals and dominant alteration facies affecting each rock type. It is important to note the differences between the profiles given for each rock type. The diorite suite rocks fall into discrete facies with little overlap as compared with the other rock types. A notable exception is epidote (a propylitic facies mineral) in the rock dominated by potassic facies alteration. This is the most outstanding example of overprinting within this wall rock.

In the hornblende/biotite feldspar porphyry, orthoclase and biotite both occur in the potassic zone. The orthoclase is considered to be a wall rock alteration partly because of the proximity of the sample to the quartz-feldspar porphyry stock, and dyke system; and partly because samples exhibiting secondary biotite, that were collected away from that porphyry, contain little or no orthoclase. This biotite therefore is deuteric in origin, at least in part, while the orthoclase is considered to be a wall rock alteration mineral associated with the porphyry main stage alteration.

Figure 13 also shows an increase in overlap of the lower grade alteration minerals in the hornblende/biotite feldspar porphyry. This is reflected increasing in the succeeding rocks, the granodiorites and the quartz-feldspar porphyry. It is therefore difficult to assess where deuteric alteration ends and wall rock alteration begins in the

Figure 13 Alteration Facies/Overprinting

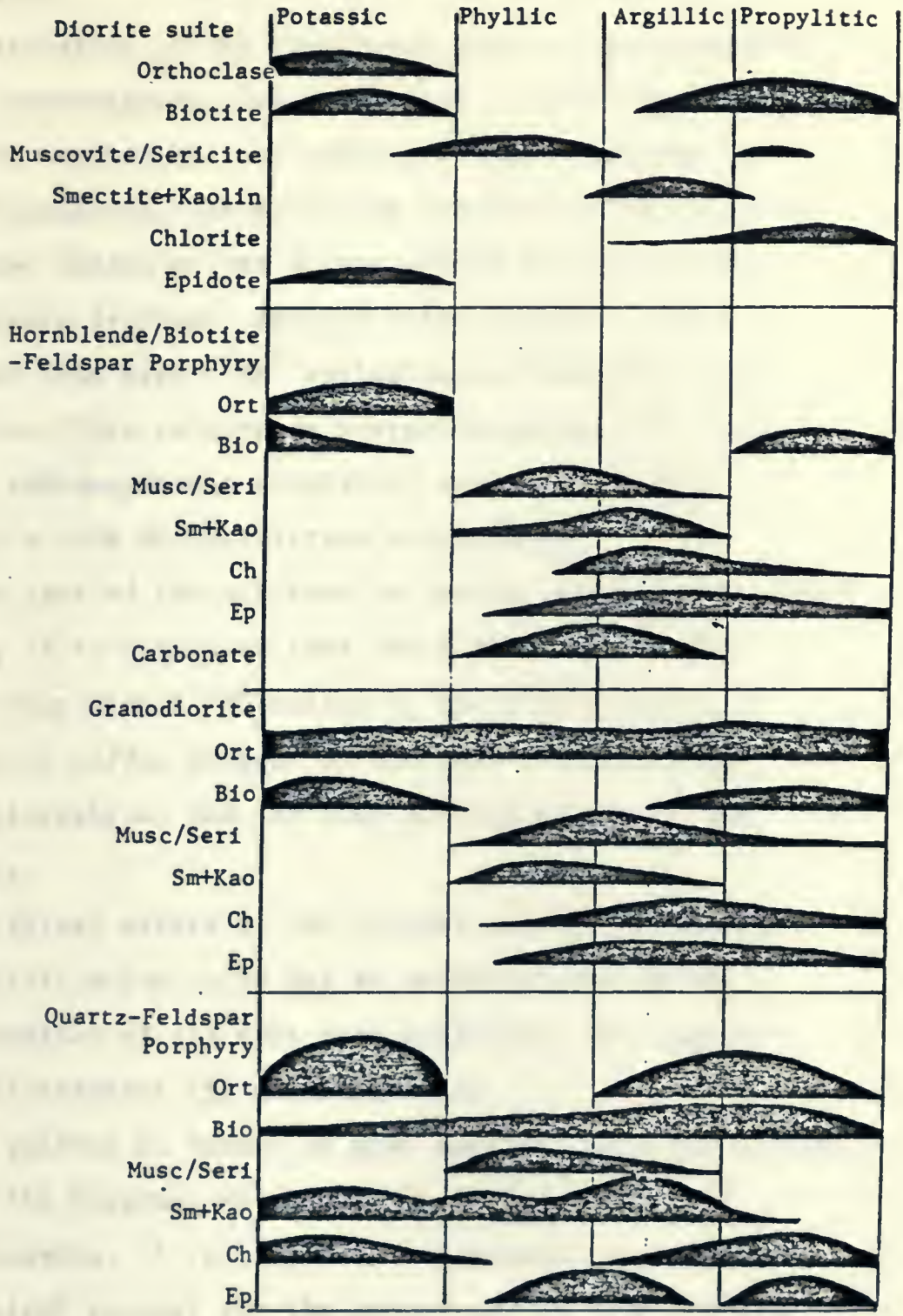

The facies divisions presented here involve domination of one set of alteration minerals over others. Note that the facies become increasingly overprinted lower in the diagram.

granodiorites.

The alteration of the quartz-geldspar porphyry exhibits extensive overprinting. The alteration is considered to be deuteric because the alteration is zoned parallel to the dyke boundaries. The extensive overlap of the minerals of the lower facies on the higher grades is probably due to temperature decrease, coupled with changes in fluid composition from high K^+/H^+ ratios to successively lower K^+/H^+ ratios. This retrograde overprinting was not strong enough to alter the potassic completely and in these cases the minerals form disequilibrium assemblages.

In the case of the molybdenite smears, with thin potassic zone rims. It is suspected that the fluids were quickly quenched, from high K^+/H^+ ratios to low K^+/H^+ ratios, by the wall rock buffer because of the lack of phyllic and argillic alteration, and the fine grained nature of the molybdenite.

The discreet nature of the mineral alteration profile in the diorite suite rocks may be accounted for by any or a combination of (1) wall rock buffering; (2) lack of deuteric alteration; (3) sampling bias.

Since epidote is common in most samples, this may reflect, a bias of the diagram, which was produced from sixteen selected samples. It is possible that Abukuma type metamorphism might account for the appearance of both epidote and chlorite in these rocks. This is hard to disprove. However, if it is considered that greenschist facies

metamorphism of this type is a low pressure phenomenum, it follows that the intrusion of the 'granodiorite pulse' is compatible and/or necessary to Abukuma metamorphism.

Model of Intrusive Sequence

The model used here follows the rationale of the works of Carmichael (1964) and Wright and Fisk (1970). Although their work was based on Thingmuli, Iceland and Kilauea, Hawaii, (both tholeiitic basalt systems) the arguments are applicable to calcalkaline vulcanism and the related plutonic equivalents.

Figure 14 is an inferred reconstruction of the intrusive episode.

It is suggested that two pulses of magma were injected into the upper crust in the area containing the Sand Creek Prospect. 1) the first, the 'diorite' pulse, may have been associated with vulcanism, although this is strictly speculation. The pulse intrudes and rafts preexisting metamorphic rocks. The pluton underwent differentiation to form diorites grading into quartz diorites. 2) These are cut by later tonalite and tonalite aplite dykes.

The second pulse, the ' granodiorite' pulse, involved 3) the injection first, of the andesitic rocks grey-hornblende-feldspar microporphyry and grey-hornblende/biotite-feldspar porphyry. This is assumed to have the composition of the parental magma from which the later differentiates were derived, however it is possible, by invoking the arguments concerning the formation of the feldspar porphyry and lamprophyre, to suggest that the hornblende-feldspar porphyry, and hornblende/biotite feldspar microporphyry

FIGURE 14 Model of Intrusive Sequence (Schematic)

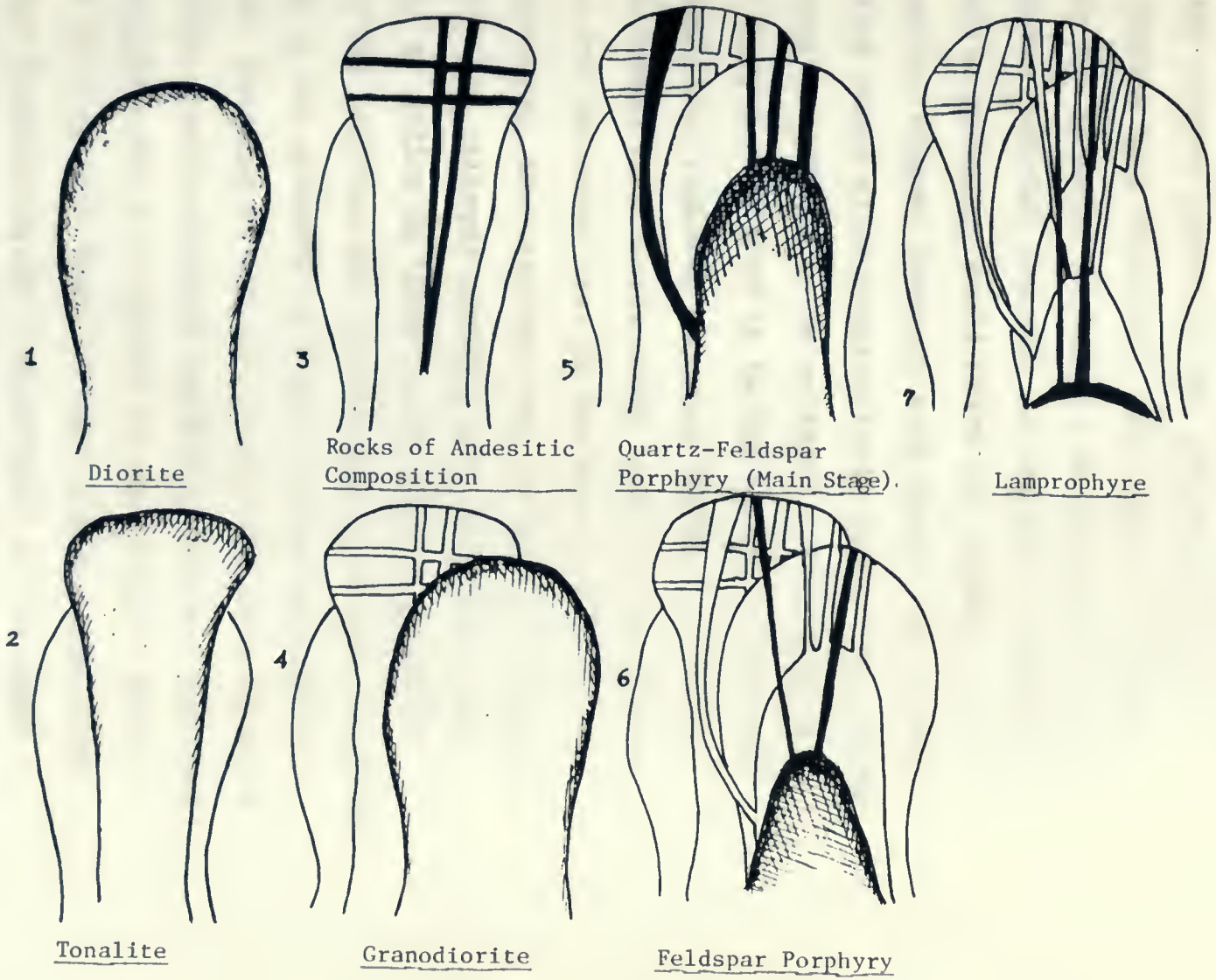

are late fractionated magmas of the 'dioritic pulse'.

4) The coarse granodiorite pluton was emplaced and the coarse porphyritic nature of most of its exposure is indicative of the lowest levels of a subvolcanic environment.

Due to the viscous nature of the granodiorite and peripheral cooling many volatiles would also be trapped deeper within the pluton. 5) Rupture of the pluton nearest the still molten material (as well as regional deformation of a now brittle periphery would allow the formation of a stock and quartz-feldspar porphyry main stage. 6) Further brittle failure would allow progressively more silica undersaturated magma and fluids to be released. Formation of feldspar porphyry is believed to be due to the release of lower differentiated residual magmatic fluids and 7) the lamprophyres formed from levels still lower in the pluton.

Evidence for the model lies in the desilication of the quartz-porphyry, the reaction rims on the quartz xenocrysts in both the feldspar porphyry and lamprophyre and the abundance of mafics in these latter dykes. The mafic character of the residium and remobilization of that residium is indicated by the presence of augite in the lamprophyre sample DT 162. Presence of the rare earth phosphate monazite in granodiorite, quartz-feldspar porphyry, feldspar porphyry and the lamprophyre and its absence in the dioritic rocks may be taken as a genetic trait of this family suite. That rare earth and phosphorous are concentrated in the magma during fractionation is taken as an indication that multi-chamber

fractionation may have occurred.

Formation of the intrusive complex may be from a single batch that underwent differentiation in an intermediate level reservoir-analogous to differentiation in the work of Carmichael (1964), Wright and Fiske (1970), Wright et al (1973) in volcanic environments.

Alternatively, a two-batch melt model must also be considered. Partial melting of descending oceanic lithosphere leads to different magmatic differentiation (Jakes and Gill, 1 70; Gill, 1970) depending upon the depth at which the melting occurs. Cessation of plate movement would allow a steepening of the Benioff Zone underlying the Cordillera and generation of a magma along the trend of calc-alkaline volcanics and shoshonites.

Lamprophyre Origin

The presence of orthoclase with abundant hydrous mafics is indicative of a late stage magma because of the abundance of potassium and hydroxyl ion. The basic nature of the lamprophyre magma can be accounted for by equilibrium being established between the liquid and a mafic residium.

Mineralization and Alteration

Main stage porphyry alteration and mineralization is

presumed to be the result of interaction of the granodiorites and their precusors with halogen and phosphate bearing hydrothermal fluids which first leached then deposited molybdenite and other ore minerals. It is assumed that most of the halogens that left the fluid are in biotites as in the Santa Rita porphyry deposit (Jacobs and Parry, 1979) or with the phosphates in apatite (and monazite?). Main stage alteration is associated with quartz-feldspar porphyry dykes and mineralization is dominantly in the potassic and silicic assemblages.

Alteration by the later feldspar porphyry is weak and alteration by the lamprophyres is unknown.

The main stage alteration exhibits retrograde overprinting. Similar overprinting is described by Ghorashi-Zadeh (1979) in Iran and by Taylor and Fryer (1980) in Turkey. Taylor and Fryer suggest that the two fluid, meteoric-hydrothermal system (Norton and Knight, 1977) collapses inward with decreasing temperature allowing overprinting (particularly phyllic) to occur. They do not account for propyllitic overprinting (which contains no feldspar destruction) of a potassic assemblage in their discussion. It is likely that meteoric water was not very important in the overprinting in the Sand Creek deposit , because the argillic and phyllic zones are very limited in extent. However, oxygen and hydrogen isotopic studies are necessary to verify this.

It is felt that the rocks exposed at the Sand Creek Prospect represent the lower portion of a porphyry mineral

system. This is due to the dominance of plutonic and coarse porphyritic rocks exposed, as well as the absence of a volcanic stratigraphy, the extensive propylitic overprinting of all other alteration facies and the limited amount of argillic-phyllic alteration are considered to be typical of deeper portions of known porphyry copper prospects (eg. Bakircay, Turkey-Taylor and Fryer, 1980). The dominance of molybdenite in the opaque and ore mineralogy may be indicative of the lower portion of a porphyry copper system by the model of Lowell and Guilbert (1970) and the work of Laine (1974). Comparison requires some indication that copper was originally present. Some evidence of this is given by azurite and malachite mineralization in some faults (by supergene processes ?) and sparse chalcopyrite mineralization associated with the molybdenite.

The occurrence is considered to be a plug and dyke porphyry system in accordance with the model used by Kesler (1976). The plug or stock is indicated by the large area of potassic alteration centred on an elliptical set of outcrops of quartz-feldspar porphyry, as well as the textural zonation of the molybdenite.

Conclusions

In conclusion, five major points may be made regarding the intrusive rocks of the Sand Creek Prospect:

1) The intrusive complex is a multiphase porphyry system with one strong and one weak mineralizing event, plus multiphase alteration.

2) The intrusive sequence cutting the iarlier schists and gneisses is a) diorite-quartz diorite, b) tonalite-tonalite aplite, c) hornblende-feldspar microporphyry (andesite) - horblende/biotite-feldspar porphyry (andesite), d) granodiorite - coarse porphyritic granodiorite (plus minor sulphide mineralization), e) quartz-feldspar porphyry (granodiorite-main stage sulphide and oxide mineralization), f) feldspar porphyry, g) lamprophyre.

3) The main stage of alteration and molybdenite mineralization took place in an inhomogenous stress field. Quartz-feldspar porphyry dykes radiate within a restricted range from the stock of the same material. The quartz-feldspar porphyry dykes indicate linear regional deformation.

4) The intrusive rocks of the Sand Creek Prospect probably represent two pulses from a magma reservoir. Differentiation would have occurred both in the lower chamber and in the plutons after emplacement.

5) The granodiorite, quartz-feldspar porphyry, feldspar porphyry, and lamprophyre are considered to represent successive magmatic differentiates tapped from successively

lower residual magma pools.

6) Propylitic overprinting of potassic wall rock alteration and deuteric alteration and the combination of coarse porphyritic and plutonic rocks with little or no volcanic stratigraphy suggests that the Sand Creed prospect represents a lower part of a porphyry system.

Bibliography

Ayres, L.D. and Findlay, D.J.- 1976- Precambrian Porphyry Copper and Molybdenum Deposits in Ontario and Saskatchewan, Geol. Sur. Can. Paper 76-1B, pp 39-41

Burnham, C.W.- 1962- Facies and Types of Hydrothermal Alteration, Econ. Geol. Vol. 57, pp 768-784

Burt, D.M.- 1981- Acidity Salinity Diagrams - Application to Greisen and Porphyry Deposits, Econ. Geol. Vol. 76, pp 832-843

Carmichael, I.S.E., Turner, F.J., and Verhoogen, J.- 1974- Igneous Petrology, McGraw - Hill, U.S.A.

Cathles, L.M.- 1977- An Analysis of the Cooling of Intrusives by Ground Water Convection which Includes Boiling, Econ.Geol., Vol. 72, pp 804-826

Clark, K.F.- 1972- Stockwork Molybdenum Deposits in the Western Cordillera of North America, Econ. Geol., Vol. 67, pp 731-758

Cooper, A.F.- 1979- Petrology of Ocellar Lamprophyres from Western Otago, New Zealand, Jour. of Pet., Vol. 20, pp 139-163

Cowan, W.B.- 1971- Geological Report on the V.B. Mineral Claim Group - Dept. Mines and Petrol., B.C. Assess Report., 2942

Creasey, S.C.- 1959- Some Phase Relations in the Hydrothermally Altered Rocks of Porphyry Cooper Deposits, Econ. Geol., Vol. 54, pp 351-

Currie, J.B. and Reik, G.A.- 1977- A Method of Distingushing Regional Directions of Jointing and of Identifying Joint Sets Associated with Individual Geologic Structures, Can. Jour. Earth Sc., Vol. 14, pp 1211-1228

Feiss, P.G.- 1978- Magmatic Sources of Copper in Porphyry Copper Deposits, Econ. Geol., Vol. 73, pp 397-404

Ghorashi-Zadeh, M.- 1978- Hydrothermal Alteration, Copper Mineralization and Supergene Patterns, Sar Cheshmeh, Iran, M.Sc. Thesis, Brock University, St. Cath., Ont., L2S 3A1

Gill, J.B.- 1970- Geochemistry of Viti Levii, Fiji, and its Evolution as an Island Arc, Contribution Min. Pet., Vol. 27, pp 179

Gilmour, P.- 1976- Mineralized Intrusive Breccias as Guides to Concealed Porphyry Copper Systems, Econ. Geol., Vol. 72, pp 290-303

Godwin, C.I.- 1975- Imbricate Subduction Zones and their Relationship with Upper Cretaceous to Tertiary Porphyry Deposits in the Canadian Cordillera, Can. Jour. of Earth Sc., Vol. 12, pp 1362-1378

Haffty, J. and Noble, D.C.- 1972- Release and Migration of Molbdenum during the Primary Crystallization of Peralkaline Silicic Volcanic Rocks, Econ. Geol., Vol. 67, pp 768-775

Hemley, J.J. and Jones, W.R.- 1964- Chemical Aspects of Hudrothermal Alteration with emphasis on Hydrogen Metasomatism, Econ. Geol., Vol. 59, pp 558-569

Henley, R.W. and McNabb- 1978- Magmatic Vapor Plumes and Ground Water Interaction in Porphyry Copper Emplacement, Econ. Geol., Vol. 73, pp 1-

Hollister, V.F.- 1974a- Porphyry Copper Province of Northern Cordillera

- 1975- The Porphyry Molybdenum Deposit of Compaccha, Peru, and its Geologic Setting, Mineral. Deposita (Berl), Vol. 10, pp 141-151

Hollister, V.F., Potter, R.R. and Barker, A.L.- 1974- Porphyry-Type Deposits of the Appalachian Orogen, Econ. Geol., Vol. 69, pp 618-630

Hunt, J.A. and Kerrick, D.M.- 1977- The Stability of Sphene; Experimental Redetermination and Geologic Implications, Geochim et Cosmochim, Vol. 41, pp 279-288

Hutchinson, C.S.- 1974- Laboratory Handbook of Petrographic Techniques, John Wiley and Sons, U.S.A.

Hyndman, D.W.- 1972- Petrology of Igneous and Metamorphic Rocks, McGraw - Hill, U.S.A.

Jacobs, D.C. and Parry, W.F.- 1979- Geochemistry of Biotite in the Santa Rita Porphyry Copper Deposit, New Mexico, Econ. Geol., Vol. 74, pp 860-887

Jakes, P. and Gill, J.B.- 1970- Rare Earth Elements and the Island Arc Tholeiitic Series, Earth Planet. Sc. Lett., Vol. 9, pp 17-28

Kamb, W.B.- 1959- Appendix to: Ice Petrographic Observations from Blue Glacier, Washington, in relation to Theory and Experiment, Jour. Geophys. Res., Vol. 64, pp 1891-1909

Kesler, S.E.- 1976- Porphyry Copper Deposits - Ore Deposits Workshop Notes, University of Toronto

Kirkham, R.V.- 1971- Intermineral Intrusions and their bearing on the Origin of Porphyry Copper and Molybdenum Deposits, Econ. Geol., Vol. 66, pp 1244-1249

Kirkham, R.V. and Soregaroli, A.E.- 1975- Preliminary Assessment of Porphyry Deposits in the Canadian Appalachians, Geol. Sur. Can., Paper 75-1, Part A

Koide, H. and Bhattacharji, S.- 1975- Formation of Fractures Around Magmatic Intrusions and their Role in Ore Localization, Econ. Geol., Vol. 70, pp 781-799

Laine, R.P.- 1974- Geological - Geochemical Relationships Between Porphyry Copper and Porphyry Molybdenum Ore Deposits, Ph. D. Thesis, U. of Arizona

Lowder, G.G. and Dow, J.A.S.- 1976- Porphyry Copper Mineralization at the Fapadaa Prospect, Northern Sulawesi, Indonesia, Econ. Geol., Vol. 71, pp 701-

Lowell, J.D. and Guilbert, J.M.- 1970- Lateral and Vertical Alteration - Mineralization Zoning in Porphyry Ore Deposits, Econ. Geol., Vol. 65, pp 373-408

McMillan, W.J. and Panteleyev- 1980- Ore Deposit Models - 1., Porphyry Copper Deposits, Geosc. Can., Vol. 7, pp 52-63

Moorhouse, W.W.- 1959- The Study of Rocks in Thin Section, Harper and Row, New York and Evanston, U.S.A.

Murton- 1973- Geochemical Report, A and E Claims, Dept. of Mines and Petrol., B.C. Assess. Rept.

- 1975- Geological and Geochemical Assessment Report 4809, A and E Claims, Dept. Mines and Petrol., B.C. Assess. Rept. 5501

Mutschler, G.E., Wright, E.G., Ludington, S. and Abbot, J.F.- 1981- Granite Molybdenite Systems, Econ. Geol., Vol. 76, pp 874-897

Norton, D.L. and Cathles, L.M.- 1973- Breccia Pipes - Products of Exsolved Vapor from Magmas, Econ. Geol., Vol. 68, pp 540-546

Norton, D.L.- 1978- Sourcelines, Sourceregions, and Pathlines for Fluids in Hydrothermal Systems Related to Cooling Plutons, Econ. Geol., Vol. 73, pp 21-28

Pride D.E. and Robinson, C.S.- 1978- Multiple Intrusion and Hydrothermal Activity, Eastern Breckenridge Mining District, Summit County, Colorado, G.S.A. Bull., Vol. 89, pp 866-874

Rock, N.M.S.- 1977- The Nature and Origin of Lamprophyres: Some Definitions, Distinctions and Derivations, Earth Sc. Rev., Vol 13, pp 123-169

Schuiling, R.D. and Vink, B.W.- 1967- Stability Relations of Some Titamium Minerals (spene, perovskite, rutile, anatase), Geochim. et Cosmochim., Vol. 31, pp 2399-2411

Schwartz, G.M.- 1936- Hydrothermal Alteration in 'Porphyry Copper' Deposits, Am. Min., Vol. 26, pp 209-

Sharp, J.E.- 1978- A Molybdenum Mineralized Breccia Pipe Complex, Redwell Basin, Colorado, Econ. Geol., Vol. 73, pp 369-382

- 1979- Cave Peak, a Molybdenum Mineralized Breccia Pipe Complex in Culberson County, Texas, Econ. Geol., Vol. 74, pp517-

Sinclair, W.D.- 1978- Porphyry Occurrences of Southern Yukon, Current Research, Part A, G.S.C., Paper 78-1A, pp 283-286

Sillitoe, R.H.- 1972- A Plate Tectonic Model for the Origin of Porphyry Copper Deposits, Econ. Geol., Vol. 67, pp 184-197

- 1973- The Tops and Bottoms of Porphyry Copper Deposits, Econ. Geol., Vol. 68, pp 799-815

Sillitoe, R.H., Halls, C. and Grant, J.N.- 1975- Porphyry Tin Deposits in Bolivia, Econ. Geol., Vol. 70, pp 913-927

Soregarcli, A.E.- 1975- Important Characteristics of Some Canadian Cordillera Porphyry Deposits, G.S.C., Paper 75-1, Part B.

Streckeisen, A.- 1973- Classification and Nomenclature of Plutonic Rocks, Geotimes, Vol. 18, pp 26-30

- 1979- Classification and Nomenclature of Volcanic Rocks, Lamprophyres, Carbonatites, and Melilitic Rocks: Recommendations and Suggestions of the I.U.G.S. Subcommission on the Systematics of Igneous Rocks, Geology, Vol. 7, pp 331-335

Taylor, R.P. and Fryer, B.J.- 1980- Multiple Stage Hydrothermal Alteration in Porphyry Copper Systems in Northern Turkey: The Temporal Interplay of Potassic Propylitic and Phyllic Fluids, Can. Jour. Earth Sc., Vol. 17, pp 901-926

Wallace, S.R., MacKenzie, W.B., Blair, R.G. and Muncaster, N.K.- 1978- Geology of the Urad and Henderson Molybdenite Deposits, Clear Creek County, Colorado, with a Section on a Comparison of these Deposits with those at Climax, Colorado, Econ. Geol., Vol. 73, pp 325-

Westra, G. and Keith, S.B.- 1981- Classification and Gneissis of Stockwork Molybdenum Deposits, Econ. Geol., Vol. 76, pp 844-873

Whitney, J.A.- 1977- A Synthetic Model for Vapor Generation in Tonalite Magmas and Its Economic Ramifications, Econ. Geol., Vol. 72, pp 686-690

Winkler, H.G.F.- 1979- Petrogenesis of Metamorphic Rocks, Springer - Verlag, New York, Heidelberg, Berlin

Woodcock, J.R. and Hollister, V.F.- 1978- Porphyry Molybdenite Deposits of the North American Cordillera, Minerals Sc. Engng., Vol 10, pp 3-

Woodworth, G.J., Pearson, D.E. and Sinclair, A.J.- 1977- Metal Distribution Patterns across the Eastern Flank of the Coast Plutonic Complex, South-Central British Columbia, Econ. Geol., Vol. 72, pp 170-183

Wright and Fisk- 1970 Origin of the Differentiated and Hybrid Lavas of Kilauea Volcanoe, Hawaii, Jour. Pet., Vol. 12, pp 1-66

Amendment to the Bibliography

Baadsgaarde, H., Folinsbee, R.E. and Lipson, J.- 1961- Potassium - Argon Dates of Biotites from Cordilleran Granites, G.S.A. Bull., Vol. 72, pp 689-702

Carmichael- 1964- The Petrology of Thingmuli, a Teriary Volcano in Eastern Iceland, Jour. Pet., Vol. 5, pp 435-460

Petrographic Report

spec. no. DW 66
country rock

Hand Spec.

a foliated (phyllitic) dark grey melanocratic very fine grained phaneritic rock containing biotite, feldspar and pyrite and a dark grey green mineral (either chlorite or hornblende). The rock exhibits low competence against hammer blows. The weathered surface exhibits abundant iron staining.

Thin Section

Mineralogy	%	Grain Size	Grain Shape	Texture
Hornblende	30%	120 μ	ragged or emfayed elongate anhedral	in andesine
Biotite	15%	110 μ	euhedral lath-like books	in andesine
Plagioclase An_{48} (Andesine)	50%	60 μ	anhedral equant	porlikitic
Apatite	1%	5 μ to 15 μ	subhedal prisms	in andesine
Hematite	trace	15 μ	anhedral stains	assoc w opaques
Opaques	5%	23 μ	anhedral elongate	assoc mainly w Hb

History

Suspect volcanic ejecta having undergone compression and diagenesis. Andesine not altered to albite, no epidote, or zeolites therefore above assumption is made. Foliated.

Classed As Supracrustal rock indurated volcanic ash compressed

(Oldest rock type) presumable recryetallized and compacted in a volcanic pile.

Petrographic Report

spec. no. DT 188
fine grained diorite

Handspec Desc.

a fine grained phaneritic crystalline melanocratic grey rock, containing grey feldspar and abundant hornblende. The rock has low to moderate competent to hammer blows. The weathered surface has some iron staining. The structure is massive.

Thin Section

Mineral	%	Grain Size	Shape	Texture/Relationship
Plagioclase An44-20 Andesine Olig	60%	120 μ	subhedral - euhedral laths	zoned subophitic some porkilitic An_{20} (apatite inclusions)
Hornblende	30%	80 μ	anhedral ragged laths	exhibit alteration rims of biotite
Biotite	6%	80 μ	subhedral tabular	after Hb
Opaques	2%	23 μ	equant subhedral	random distrib.
Apatite	trace	10 μ	elongate subhedral prisms	random distrib.
Sphene	trace	40 μ	euhedral forming aggregats	assoc w Hb

Petrographic Report

spec. no. DT 184

Diorite suite

Handspec Desc.

a medium grained grey melanocratic rock containing hornblends, pyrite, and a white feldspar. The hornblendes delineate a foliation presumably related to a primary cumulate texture or possibly a flow foliation. The rock has a low to moderate competence to hammer blows. The weathered surface is iron stained. Fracture surfaces contain both chlorite and iron staining.

Thin Section

Mineral	%	Grain Size	Shape	Texture/Relations
Hornblende	44%	1600 μ	anhedral ragged and embayed laths	poilikitic containing small plag grains plus bio laths and alteration patches apatite and pistacite and opaques.
Plagioclase An_{43}	48%	800 μ	ragged embayed laths	grains consist of broken xl's which have subsequently been over grown. Little warping.
Biotite	4%	60 μ	tabular books and anhedral alt patches	altering from Hb and forming tabulae in close assoc w Hb.
Quartz	2%	160 μ	subequant anhedral	strained, interstitial fillings.
Sphene	trace	60 μ	anhedral equant	in Plag.
Apatite	trace	up to 46 μ	subhedral prisms	scatter throughout section.
Hematite	trace	15 μ	equant anhedral grains	is assoc w Hb, bio and plag.
Pistacite	rare	45 μ	subhedral to anhedral elongate	in assoc w Hb and bio and chlorite.

Petrographic Report
Continued

spec. no. DT 184
Diorite suite

Mineral	%	Grain Size	Shape	Texture/Relations
Opaques	1%	23 μ	cubic euhedral	forming large aggregate masses.
Chlorite penninite/ clinochlore	rare			after biotite.
Zircon	rare	40 μ	subhedral prismatic	in assoc w Hb, bio.

History

This rock was emplaced as a crystal mush consisting of plagioclase crystals. Hornblende and plagioclase growth succeeded this overgrowing xl's fragments. Biotite and quartz appeared toward the end of this period and reaction of hornblende with later magmatic fluids formed biotite patches. Later fluids infiltrated via a vein filled fracture at one end of the slide. This is also the cause of the epidote and hematite formation as well as the chlorite.

Petrographic Report

spec. no. DT 311
Diorite suite
Tonalite

Handspecimen Description

a leucocratic coarse grained rock containing white feldspars, quartz and biotite colour is light grey, and the texture is granitic. The specimen is fairly competent with respect to hammer blows.

Thin Section

Mineralogy	%	Grain Size	Shape	Texture/Relationship
Plagioclase An_{37} to 30	66%	800 μ	subhedral to anhedral	broken and overgrown zoned grains contain inclusions of hornblende (porkilitic).
Orthoclase	trace	250 μ	anhedral	perthitic
Quartz	22%	300 μ	anhedral	strained (undulatory extinction).
Biotite	10%	680 μ	subhedral subequant	slightly poikilitic.
Opaques	.5%	230 μ	anhedral equant	in interstices between plag, orthoclase and qlz grains.
Apatite	trace	90 μ	subhedral prismatic	in association with biotite.
Montmorillonite	trace	2 μ	euhedral tabular	altering plagioclase.
Zircon	trace	40 μ	euhedral prismatic	associated with opaques.
Hornblende	trace	100 μ	euhedral prismatic	grain within plagioclase.
Sphene	trace	80 μ	aggregate of subhedral xls	in interstices.
Chlorite	trace		anhedral	after Biotite includes alteration rims and zones.
Epidote	trace		subhedral to euhedral prismatic	in Plagioclase.

Petrographic Report
Continued

spec. no. DT 311

Diorite suite
Tonalite

History

This rock is presumed to have been emplaced as a crystal mush due to the abundance of broken feldspar grains which have been overgrown. The relative abundance of quartz is indicative of a later stage plutonic rock.

Petrographic Report spec. no. DT 180

Handspec Deacription

a fine aphanitic porphyritic rock. Grey mesocratic containing fine phenocryats of hornblende and grey feldspar. There is a dintinct lineation of the hornblende phenos.

The rock has low to moderate tenacity with respect to hammer blows. Fracture surface contains epidote.

Thin Section Description

Minerals	%	Grain Size	Shape	Texture/Relationship
Plagioclase An_{39} (Andesine)	4%	63 μ	euhedral laths	zoned microphenocrysts
Plagioclase An_{35} (Andesine)	86%	15 μ	euhedral laths and fragments	microlites delineating fluxion
Hornblende	6%	300 μ	subhedral to euhedral	microphenocrysts
Biotite	3%	12 μ	tabular	warped grains microphenocrysts, replacement of Hb.
Opaques	trace	3 μ	equant subhedral (cubes?)	disseminated
Limonite	trace	2 μ	irregular anhedral	appears dominately as a stain
Chlorite	trace		anhedral lath-like	
Apatite	trace	1 μ	subhedral prismatic	disseminated

Genetic Implications

The fine grained nature and fluxion suggest that this rock was intruded and chilled quickly. The microphenocrysts of plagioclase and hornblende are older than the finer ground mass. Chlorite is

presumed to be formed from the alteration of biotite. A paragenetic diagram is given below.

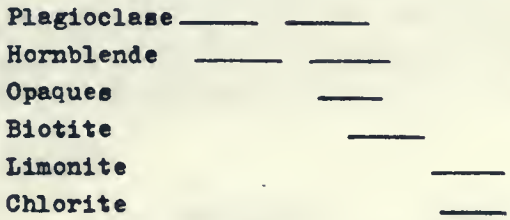

Petrographic Report

spec. no. DT 268

Taken from a subhorizontal sheet in NW terrain

Hand Spec. Desc.

a fine to medium grained mesocratic grey aphanitic porphyritic rock containing phenocrysts of light grey feldspar and more abundant hornblende. The sample exhibits fluxion, alignment of both the hornblendes and feldspars. The sample showed low to moderate competence with respect to hammer blows.

Thin Section

Mineralogy	%	Grain Size	Shape	Texture
Plagioclase An_{31} Andesine	10%	15-7mm	rounded subhedral semi-equant	phenocrysts
Plagioclase An_{29} Oligoclase	45%	45 μ	elongate embayed subhedral laths	zoned nucrolites outlining fluxion
Hornblende	4% 35%	150 μ 13 μ	euhedral laths euhedral embayed to ragged laths	phenocrysts microlites
Opaques py/mt	6%	15 u, 50 μ	equant and subhedral euhedral	scattered randomly in matrix two size modes 50 u py? 15 u?
Apatite	trace	100 u to 23 u	subhedral prisms	in matrix
Quartz	trace	200 μ	equant anhedral rounded	phenocrysts
Epidote	trace	35 μ	rounded elongate subhedral	
Sphene	trace	70 μ	euhedral aggregate	assoc with biotite
Biotite	trace	33 μ	interlocking subhedral subsequent	presumed secondary after plag pheno

History

An intrusive sheet of rounded phenocrysts suggesting emplacement

Petrographic Report spec. no. DT 268

Continued Taken from a subhorizontal sheet in NW terrain

contemporaneous with rapid cooling. Fluxion suggest intrusion continued during growth of microlites. Biotites later replace some feldspar grains.

Classed: Hypabyssal porphyry

Petrographic Report

spec. no. DT 213
qtz monzodiorite
(granodiorite)

Handspec Desc.

a mesocratic leucocratic grey coarse phaneritic crystalline rock containing quartz, white feldspar and grey feldspar and black biotite. This rock is moderately competent to hammer blows. Fracture surfaces contain both chlorite and an iron staining.

Thin Section

Mineralogy	%	Grain Size	Shape	Texture/Relationships
Quartz	17%	900 μ	subequant anhedral	undulatory extinction
Plagioclase An_{39-18}	48%	900 μ	subequant grains	inclusion orthoclase as single xl grains and aggregates, generally show zoning.
Orthoclase	20%	2500 μ	anhedral subelongate	perthitic and poikilitic contains exsolution lamellae and equant grains of plagioclase, bio, Hb.
Biotite	8%	up to 1000 μ	subhedral to anhedral equant	found dominately within orthoclase with apatite opaques sphene, assoc w partial replacement of Hb.
Hornblende	3%	450 μ	ragged to euhedral laths	partially altered to bio.
Opaques	2%	60 μ	equant grains plus irregular aggregates	found dominately in interstices of plag and qtz and within orthoclase xl's.
Epidote	trace	20 μ	subhedral prismatic	distribution throughout the slide but not in plagioclase.

Petrographic Report — spec. no. DT 213

Continued — qtz monzodiorite (granodiorite)

Mineralogy	%	Grain Size	Shape	Texture/Relationships
Sphene	trace	200 μ	euhedral to embayed subhedral	associated dominately with biotite, hornblende and opaques.
Apatite	1%	60 μ	subhedral prisms	associated with other accessories and in rims of plagioclase.
Sericite		6 μ	matted fibres	in plagioclase.
Chlorite	trace			alteration from biotite.

History

possibly emplaced as a fluid saturated crystal mush which under confining pressure formed large crystal grains. Late release of pressure led to zonation of the plagioclase, strain of the quartz and inclusion of mafics and plagioclase in the orthoclase.

Petrographic Report

spec. no. DT 101

metamorphosed country rock

Handspecimen Deacription

a fine grained rock exhibiting phyllitic schistosity and lenticular glomeroporphyroblasts which appear to be dominatly biotite. Colour is melanocratic dark grey. Weathered surfaces are rusty brown. Competence is moderate to low with respect to hammer blows.

Thin Section

Mineralogy	%	Grain Size	Shape	Texture/Relationships
Hornblende	20%	60 μ	elongate subhedral prismatic	forming lenticular aggregates in assoc w bio and distributed throughout the rock defining foliation, some poikiloblastic porphyroblasts.
Biotite	40%	115 μ	elongate tabular euhedral	forming lenticular aggregates in assoc w hb and distributed throughout the rock defining foliation, some poikiloblastic porphyroblasts.
Quartz	1.7%	45 μ	equant anhedral	forming matrix along with plag and porphyroblasts.
Plagioclase	22%	45 μ	equant anhedral	forming with quartz the host.
Epidote	trace	70 μ	anhedral to subhedral prismatic	assoc with biotite and hornblende.
Chlorite	trace	35 μ	anhedral tabular	
Hematite	trace	15 μ	equant anhedral	staining assoc with opaques.
Sphene	1%	100 μ	embayed subhedral	associated intimately with hornblende and biotite interstitial to both.

Petrographic Report spec. no. DT 101

Continued metamorphosed country rock

Mineralogy	%	Grain Size	Shape	Texture/Relationships
Apatite	trace	12 μ	anhedral prismatic	randomly distributed in section.
Opaques (pyrite)	trace	13 μ	ragged anhedral	altered in past to amorphous.

History

Amphibotite facies schist with retrograde affects producing epidote (ie. upper greenschist facies). There is a dramatic increase in grain size with respect to grains in DW 66.

Petrographic Report

spec. no. DT 177
field term: aplite

Handspecimen Description

A leucocratic medium grained rock. Overall colour is cream with grey patches. Contains quartz, white feldspar, chlorite. The rock is moderately competent with respect to hammer blows.

Thin Section

Mineralogy	%	Grain Size	Shape	Texture/Relationship
Quartz	37%	600 μ	anhedral	undulatory extinction in larger grains myrmekitic texture.
Plagioclase An_{27}	58%	1300 μ	anhedral embayed	broken and warped lamellae partial alteration to haolinite.
Microcline	2%	240 μ	anhedral equant	perthitic.
Chlorite	trace	200 μ	anhedral thin tabular	pseudomorphs after biotite.
Epidote (pistacite)	trace	70 μ	anhedral subequant	associated with sericite between plagioclase grains.
Haolinite	1%	2 μ	equant	in all primary phases.
Sericite	trace	12 μ	euhedral tabular	in plagioclase.
Limonite	trace	50 μ	subhedral equant	pseudomorphs after pyrite?
Apatite	trace	40 μ	subhedral prismatic	randomly diatributed.
Biotite	trace	120 μ	subhedral tabular	in plagioclase.

History

intruded as a crystal mush associated with moderate fluid pressures. The presence of microcline suggests slow cooling. The grid iron twinning is not universal and it is therefore suspected that the system was quenched during the transition between orthoclase and microcline.

Classification: Tonalite aplite.

Petrographic Report

spec. no. DT 203
Diorite suite

Handspecimen

Thin Section

Mineralogy	%	Grain Size	Shape	Texture/Relationships
Quartz	9%	800 μ	equant anhedral	undulatory extinction.
Plagioclase An_{41-32}	75%	1800 μ	subhedral to anhedral	zoned, broken, and healed grains warped lamellae common also traces of epidote within.
Hornblende	4%	720 μ	equant subhedral prismatic	interstitial to plag, contains epidote in assoc w bio. and altered partly to bio.
Biotite	7%	360 μ	tabular subhedral	assoc with Hb in interstices also resulting from alteration of hb.
Epidote (pistacite)	2%	200 μ (20 μ)	subhedral prismatic	in assoc with Hb, bio, sphene (and within some plag grains).
Chlorite	trace			from alteration of biotite.
Sphene	2%	140 μ	euhedral wedges	assoc with other accessories.
Opaques (pyrite)	1%	230 μ	euhedral equant	in interatice w other accessories.
Apatite	trace	230 μ	anhedral sub equant	assoc biotites mainly.

Classification: Quartz diorite

Petrographic Report — spec. no. DT 203

Continued — diorite suite

History

After emplacement as a crystal mush metamorphism occurred either as a regional effect which was no complete; plagioclase is not altered to albite or hydrothermal effects altered plagioclase plus biotite and hornblende to plagioclase epidote, sphene, hornblende, biotite and chlorite.

Petrographic Report

spec. no. DT 324
Diorite suite

Handspecimen

This rock is a leucocratic grey-white, the weathered surface is iron stained. It exhibits moderate to low competence with respect to hammer blows. This is a phaneritic medium grained rock containing quartz, whitish (almost opaque) feldspars and muscovite.

Thin Section

Mineralogy	%	Grain Size	Shape	Texture/Relationships
Plagioclase An_{32} Andesine	25%	1600 μ	anhedral equant to subequant	cataclastic texture, abundant haolinigation and alteration to smectite and sercite.
Quartz	50%	1200 μ	anhedral subequant	strained
Orthoclase	trace	1300 μ	anhedral	perthitic interstitial to quartz and plag
Muscovite	1%	970 μ	tabular subhedral	warped (curved cleavage traces) interstitial after biotite?
Smectite	2%	100 μ	anhedral elongate	in plagioclase
Kaolinite	17%	1 μ		in plagioclase and orthoclase
Limonite	1%	45 μ	anhedral	after pyrite?
Opaques	3%	5 μ	anhedral	in veins of quartz.
Apatite	trace	10 μ	subhedral prismatic	in plagioclase

Classed: Altered diorite suite rock
Phyllic facies over printed by argillic facies.

Petrographic Report spec. no. DT 328

Hand Specimen Description

Thin Section

Mineralogy	%	Grain Size	Shape	Texture/Relationship
Quartz	33%	450 μ	anhedral equant to irregular	free grain and in granophyric texture with orthoclase
Plagioclase An_{32} Andesine	38%	450 μ	anhedral subequant	exhibiting broken and warped lamellae
Orthoclase	24%	1000 μ	anhedral irregular	secondary and perthitic
Biotite	trace	25 μ	anhedral irregular	relict
Muscovite	1%	350 μ	anhedral tabular	after biotite and hornblende
Kaolinite	3%			inclusions in plagioclase
Apatite	trace	20 μ	subhedral prismatic	randomly distributed
Opaques leucoxene and pyrite	trace	30 μ	anhedral subequant	random distribution
Rutile	rare	60 μ	euhedral prismatic	assoc with quartz and epidote after sphene?
Epidote Clincozoicite	rare	60 μ	anhedral	

Comments

epidote mainly associated with rutile is thought to be products of the break down of primary sphene (with increasing P Co_2? and decreasing T)

Petrographic Report spec. no. DW 40

H/BFP

Handspecimen Desc.

a mesocratic to melanocratic fine grained porphyritic rock containing white phenocrysts of feldspar and dark green microphenocrysts of hornblende. The specimen exhibited moderate competence with respect to hammer blows.

Thin Section

Mineralogy	%	Grain Size	Shape	Texture/Relationships
Plagioclase An_{44} Andesine	78%	1840 μ 28 μ	subhedral laths anhedral subequant	interlocking laths containing healed fractures. Also warped laths exhibit slight zonation (phenos and glomerophenos)
Biotite	5%	80 μ	anhedral subequant	after hornblende, partial and complete alteration of hb grains
Hornblende	7%	280 μ	anhedral to subhedral prismatic	partially altered to biotite
Quartz	8%	2 μ	anhedral irregular elongate	wormy grains forming myrmekitic texture in plagioclase
Opaques	1%	90 μ	anhedral to subhedral equant	randomly disseminated
Chlorite (blue-green)	trace		anhedral scaley aggregates	pseudomorphs after biotite
Epidote (pistacite)	trace	180 μ	subhedral prismatic	in association with chlorite
Apatite	trace	80 μ	anhedral prismatic	associated with biotite
Sphene	0.5%	140 μ	subhedral to euhedral aggregate	
Monazite	trace	140 μ	anhedral aggregate	associated with hornblende

Petrographic Report
Continued

spec. no. DW 40

H/b FP

History

Emplaced as a crystal saturated magma which crystallized in part during transport. Warped and broken plagioclase phenocrysts are taken as evidence of movement succeeding partial consolidation of the magma. The myrmekitic texture is generally held to involve the presence of a potash feldspar, however none was seen in thin section and sodium cobaltinitrite staining piled to indicate the presence of the K-spar.

Classification

IUGS tholeiitic basalt

unsatisfactory since low mafic content equivalent to plag. is andesine, quartz, leuco. and diorite mafics are hb, bio, and chlorite. Prefer andesite.

Petrographic Report spec. no. DT 139

Hand specimen description

Thin Section description

Mineralogy	%	Grain Size	Shape	Texture/Relationships
Quartz	14%	80 μ	anhedral irregular	as bleb and as graphic intergrowths with orthoclase
Orthoclase	24%	15 μ	anhedral elongate to irregular	granophyric texture
Epidote	trace	15 μ		
Chlorite	6%	220 μ	subhedral tabular	after biotite
Carbonate	6%	70 μ	anhedral	partially and completely replacing plag phenos
Kaolinite	10%	2 μ		
Muscovite	10%	35 μ	anhedral plates	partially replacing plagioclase and biotite
Plagioclase An_{34}	15%	1900 μ	subhedral to anhedral	relict phenocryats no zonation
Opaques (leucoxene)	trace	120 μ		after sphene
Opaques (ph?)	4%	115 μ		assoc with chlorite
Rutile	rare	28 μ	acicular	in apatite
Apatite	trace	140 μ	euhedral prismatic	

Petrographic Report spec. no. DT 179

H/BFP

Handspec desc.

a mesocratic grey fine grained porphyritic rock exhibiting fine flow structure and phenocrysts of white feldspar and black biotite. Fractures appear to contain chlorite. The rock is moderately competent to hammer blows.

Thin Section

Mineralogy	%	Grain Size	Shape	Texture/Relationships
Plagioclase An_{36-21}	18%	460 μ	subhedral to euhedral	strongly zoned phenocrysts with slight ragged overgrowth (poikilitic?)
An_{20}	30%	10 μ	anhedral elongate	microlites in groundmass
Quartz	trace	80 μ	anhedral	phenocrysts
Quartz	27%	10 μ	anhedral equant	microlites in groundmass
Biotite I	9%	110 μ	thin tabular subhedral	poikilitic-containing apatite and warped
Biotite II	6%	25 μ	tabular xls forming aggre-	after Hb? assoc w quartz grains and as microlites in groundmass
Orthoclase	1%	450 μ	anhedral ragged	poikilitic rims containing qtz and plag.
Orthoclase	8%	10 μ	anhedral	replacing microlites in groundmass
Apatite	2%	23 μ	subhedral prismatic	in assoc with biotite also randomly distributed in groundmass
Monazite	trace	60 μ	anhedral aggregates	in assoc with opaques and biotite
Chlorite (penninite)	trace	25 μ	tabular anhedral	after bio?

Petrographic Report

Continued

epec. no. DT 179

H/B FP

Mineralogy	%	Grain Size	Shape	Texture/Relationships
Hematite	trace	1 μ	equant grains and aggregates	rims on opaques
Opaques	1%	55 μ	equant subhedral	randomly distributed generally in assoc with biotite, zircon and monozite
Zircon	trace		subhedral prismatic	

Petrographic Report

spec. no. DT 258

granodiorite suite

Handspecimen description

Thin Section

Mineralogy	%	Grain Size	Shape	Texture/Relationships
Plagioclase An_{38-6} Andesine albite	49%	2400 μ	subequant anhedral	zoned with poikilitic rims containing Hb, qtz. sericitic alteration near grain cores
Orthoclase	26%	24000 μ	anhedral subelongate prismatic	megacryste, poikilitic contsining all primary and perthitic texture phases.
Quartz	19%	1740 μ	equant anhedral	poikilitic rims containing small grains of plag and orthoclase
Biotite	3%	900 μ	equant tabular	altering to chlorite poikilitic containing apatite
Hornblende	trace	160 μ	subhedral	found only within plag and othoclase grains
Epidote (piatacite)	trace	36 μ	anhedral subequant	small grains in plag
		450 μ	subhedral prismatic	larger in biotite
Chlorite	trace			altering from biotite
Sphene	trace	700 μ	subhedral to euhedral	porphyroblastic in assoc with opaques, hematite and epidote
Opaques	1%	230 μ	euhedral elongate and equant anhedral	in aggregates essoc with sphene, ep., biotite and chlorite

Petrographic Report
Continued

spec. no. DT 258

granodiorite suite

Mineralogy	%	Grain Size	Shape	Texture/Relationships
Apatite	trace	50 μ	anhedral prismatic	closely assoc. w biotite
Smectite	trace	4 μ	anhedral tabular	primarily in plagioclase
Hemstite	trace	2 μ	anhedral	rimming opaques and discreet patches in close assoc. with opaques

Petrographic Report spec. no. DT 239

Handspec desc.

Thin Section

Mineralogy	%	Grain Size	Shape	Texture/Relationships
Quartz	47%	1200 μ	anhedral sub-equant	
Plagioclase digoclase	28%	1300 μ	anhedral sub-equant	slightly zoned exhibiting warped lamellae
Orthoclase	22%	1900 μ	anhedral irregular	perthitic with poikilitic rims
Biotite	1%	800 μ	anhedral tabular	partially replaced by musc and ch
Monazite	rare	240 μ	anhedral irregular	associated with chlorite in orthoclase
Muscovite	1%	770 μ	euhedral tabular	associated with biotite which it replaces and chlorite
Chlorite	trace	300 μ	anhedral	partially replacing bio
Opaques	trace	250 μ	anhedral irregular	
Epidote	trace	200 μ	anhedral irregular	in plagioclase
Apatite	rare	230 μ	subhedral prismatic	associated with biotite
Garnet	rare	550 μ	anhedral equant	poikiloblastic contains ep. and chlorite

Petrographic Report

spec. no. DT 306

Polished Section

Mineralogy	%	Grain Size	Shape	Texture/Relationship
Pyrite	6%	900 μ	euhedral to subhedral	some grains broken includes subequant cpy bleb
Molybdenite	trace	110 μ	anhedral	generally free some grains assoc. with cpy
Chalcopyrite	0.2%	95 μ	anhedral subequant	free grains as well as exsolved blebs in sphal and pyrite. Also commonly assoc. with covelline
Sphalerite	2%	250 μ	anhedral irregular to vermiculate	occurs as free grains and in assoc. with pyrite. Cpy commonly included as exsolution blebs
Covelline	trace	70 μ	anhedral subequant to irregular	associated with cpy

Thin Section

Mineralogy	%	Grain Size	Shape	Texture/Relationship
Quartz	67%	225 μ	anhedral subequant	also mutually embayed with orthoclase forms veins
Orthoclase	25%	70 μ	anhedral to irregular elongate	exhibits ragged overgrowths and mutual embayments with qtz and partial replacement of plagioclase
Muscovite/ Sericite	trace	55 μ	ragged sheafs	in plagioclase
Plagioclase An_{33} Andesine	5%	1150 μ	ragged embayed subequant	relict primary grains exhibiting embayed edges and replacement by orthoclase

Petrographic Report apec. no. DT 306

Thin Section
Continued

Mineralogy	%	Grain Size	Shape	Texture/Relationship
Kaolinite	1%	1 μ		in Orthoclase
Beryl?	trace	140 μ	subhedral	associated mainly with
Zircon	trace	55 μ	euhedral to subhedral	closely assoc. with beryl
Limonite	trace	1 μ	anhedral	aggregate masses
Chlorite	rare	60 μ	radiating scales	in groundmass after secondary biotite
Sphene	rare	55 μ	euhedral	in groundmass
Clinozoicite	trace	100 μ	anhedral irregular	in groundmass
Apatite	1%	500 μ	subhedral prismatic	assoc. with pyrite often in broken grains

Petrographic Report

spec. no. DT 303

granodiorite suite

Polished Section

Mineralogy	%	Grain Size	Shape	Texture/Relstionships
Pyrite	5%	800 μ	anhedral equant	large broken grains
Molybdenite	.1%	110 μ 1 μ	subhedral tabular	large warped grains assoc. with py. Also fine dissemination in gangue.
Chalcopyrite	trace	50 μ	anhedral equant	grains within pyrite
Cassiterite	trace	30 μ	subequant anhedral	grains associated with cpy in py and in gangue
Scheelite	trace	200 μ	anhedral irregular	mainly associated with gangue
Wolframite	rare	10 u x 1 μ	euhedral prismatic	eassociated with cpy in pyrite
Sphalerite	rare	40 μ	subequant anhedral	in pyrite and gangue

Thin Section

Mineralogy	%	Grain Size	Shape	Texture/Relationships
Quartz	62%	900 μ	equant to subequant	replacing feldspars also in fine grained veins
Orthoclase	22%	200 μ	euhedral to anhedral	grains within quartz grains
Phlogopite	11%	10 μ	euhedral tabular	matted aggregates running roughly parallel to length of the section

This rock has apparently undergone one potassic alteration but verges on silicic alteration. The latter suggestion is based upon the notion that the silicic assemblage grages into greisen of which cassiterite, scheelite and wolframite are considered to be members and there appears to be only a slight increase in orthoclase from the previously observed granodiorite suite rocks.

Note: Scheelite was identified by fluorescence and white internal reflections as well as a dark grey colour.

Cassiterite was identified on the basis of yellow-brown internal reflections and brown-grey colour.

Petrographic Report

spec. no. DT 8
QFP

Handspec

a leucocratic aphanitic porphritic rock. Matrix is a grey-vary colour and contains phenocrysts of plagioclase, orthoclase, biotite and hornblende.

The rock has low to medium competence with respect to hammer blows.

Thin Section

Mineralogy	%	Grain Size	Shape	Texture/Relationships
Plagioclase An_{39-25}	22%	5020 u	anhedral prismatic	zoned poikilitic phenocrysts containing
An_{25}	16%	24 μ	equant anhedral	microlites in groundmass
Quartz	14%	1800 μ	irregular anhedral	phenocrysts
	19%	24 μ	equant anhedral	microlites
Orthoclase	9%	4400 μ	euhedral prismatic	phenocrysts some perthitic
	9%	24 μ	anhedral subequant	microlites in groundmass
Hornblende	3%	860 μ	euhedral prismatic	microphenocrysts some partially chloritized
Chlorite	5%	1400 μ	warped equant tabular	pseudomorphs after biotite phenocrysts poikiloblastic containing epidote
Epidote (pistacite)	1%	300 μ to 40 μ	subhedral prismatic	large xls assoc. with chlorite small grains assoc with plag
Opaques (py?)	1%	50 μ	equant subhedral	randomly distributed
Sphene	trace	340 μ	euhedral	assoc. with chlorite, as well as the rest of the felsic matrix and the feldspars

Petrographic Report — spec. no. DT 8

Continued — QFP

Mineralogy	%	Grain Size	Shape	Texture/Relationship
Monazite	trace	450 μ	anhedral irregular	assoc. with chloritized biotite

History

This rock was emplaced as a crystal undersaturated liquid and underwent alteration (as an autometamorphic process?). This is a hypabyssal rock which probably formed at higher levels in a volcanic system.

It may be classed as porphyritic rhyolite but equivalent to granodiorite rather than granite.

Petrographic Report

spec. no. DT 37
Qtz. feldspar porp.

Handspec Desc.

An aphanitic mesocratic grey porphyry contain abundant phenocrysts of white feldspar, black biotite, green amphibole and quartz. Pyrite is also present. The rock exhibits an alteration rim assumed to be caused by weathering. The rim contains brown quartz and feldspars. The weathered surface is earthy and iron stained.

Thin Section

Mineral	%	Grain Size	Shape	Texture/Relationship
Plagioclase Olig An_{14}	33%	450 μ	rounded sub-hedral stubby laths	phenocrysts and glomero-phenocrysts locally poikilitic texture (qtz inclusion and Hb and ap)
	9%			
Quartz	22%	450 μ	equant anhedral rounded to sub-hedral	containing fractures with
	10%			
Orthoclase	trace			
	21%			
Biotite	2%	110 μ	subhedral ragged tabular	slightly poikilitic some grains chloritized sagenitic texture (rutile)
Hornblende	1%	80 μ	ragged embayed subhedral laths	poikilitic containing fine grained fspar and partly replaced by sphene
Monazite	rare	100 μ	subhedral aggregates	largely assoc. with Hb and appears free in matrix
Rutile	rare	1 μ	acicular	also as fine xls in bio.
Apatite	trace	10 μ	rounded sub-hedral prisms	

Petrographic Report — spec. no. DT 37

Continued — Qtz feldspar porp

Mineral	%	Grain Size	Shape	Texture/Relationship
Opaque (py)	1%	110 μ	broken euhedral crystals	
Chlorite	trace	25 μ	pseudomorphs after biotite and alteration rims	

History

Petrographic Report

spec. no. DT N69A

QFP

Handspec description

A leucocratic beige coloured rock. Fine grained porphyritic contains quartz, feldspar phenocrysts, and pyrite.

Thin Section

Mineralogy	%	Grain Size	Shape	Texture/Relationship
Plagioclase An_6	38%	4000 μ	anhedral laths	phenocrysts, glomero-phenocrysts often embayed by quartz breakage of phenos seen little or no zonation
Albite	9%	230 μ	equant	microlites
Quartz	17%	2530 μ	anhedral irregular	phenocrysts
	23%	160 μ		microlites
Orthoclase	2%	720 μ	anhedral	phenocrysts-perthitic texture
		120 μ	prismatic	partially altered to sericite
Sericite	1%	115 μ	anhedral tabular	in plagioclase and orthoclase
Muscovite		240 μ	anhedral tabular	after biotite
Montmorillonite	6%	40 μ	anhedral tabular	in plag and rimming some opaques
Kaolinite	1%			altering feldspars
Apatite	trace	115 μ	subhedral prismatic	randomly distributed
Epidote Clinozoilite	trace	55 μ	anhedral aggregates	
Opaques	1%	450 μ	broken otherwise euhedral	rimmed by sericite and mon.

Petrographic Report — spec. no. DT N69A

Continued — QFP

Mineralogy	%	Grain Size	Shape	Texture/Relationship
Biotite	trace	300 μ	embayed euhedral	found within quartz partially altered exhibiting sagenitic texture
Rutile	trace	12 μ	euhedral	in biotite relicts assoc. with apatite

Classed

Rhyolite - equivalent to granodiorite porphyry

exhibits a retrograde assemblage: Biotite muscovite
Plagioclase albite and sericite
monmorillonite
kaolinite, epidote

albitized, kaolinized, propyllitized

Petrographic Report spec. no. DT 310

Handspec

a light grey (leucocratic) aphanitic rock containing phenocrysts of white feldspar, quartz, biotite and hornblende. Staining indicates the groundmass is dominated by orthoclase.

Thin Section

Mineralogy	%	Grain Size	Shape	Texture/Relationship
Quartz	2%	1600 μ	subhedral	phenocrysts
	15%		bipyramindal	
Plagioclase An_{31-22}	12%	2200 μ	subhedral	zoned glomerophenocrysts
Andesine-Olig	5%		prismatic	
Orthoclase	64%	24 μ	anhedral laths	microlites in groundmass
Biotite	1%	1100 μ	subhedral prismatic	slightly altered phenocrysts some microlites
Hornblende	trace	450 μ	euhedral tabular	slightly embayed contains sphene
Sphene	rare	180 μ	subhedral wedge	in hornblende
Smectite	trace	7 μ	anhedral tabular	in plagioclase
Chlorite	1%	100 μ	ragged patches	partial replacement of biotite
Monazite	rare	200 μ	anhedral irregular	in biotite and groundmass
Opaques	1%	8 μ	anhedral equant	

Petrographic Report Spec. no. DT 333

Handspec desc.

An aphanitic, greenish leucocratic porphyritic rock containing phenocrysts of white feldspar, quartz, biotite, Staining indicates groundmass is dominated by K-spar.

Thin Section

Mineralogy	%	Grain Size	Shape	Texture/Relationship
Quartz	3%	950 μ	anhedral irregular	rounded phenocryst relicts
Plagioclase An_{32}	8%	1300 μ		highly altered relicts
Orthoclase	57%	230 μ	anhedral intergrowth	replacing plagioclase microlites
Biotite	trace	900 μ		highly altered to chlorite
Chlorite	2%	60 μ	euhedral tabular	after biotite microlites
Kaolinite	4%	2-4 μ		in orthoclase and plag
Carbonate	1%	180 μ	anhedral subequant	replacing plagioclase
Sericite/ Muscovite	23%	150 μ	anhedral to euhedral	in plag and groundmass after biotite
Apatite	rare	46 μ	subhedral	assoc. with muscovite
Opaques	2%	85 μ	euhedral cubic	

Petrographic Report spec. no. DT 205

Handspecimen desc.

a fine grained phaneritic porphyritic rock containing phenocrysts of white feldspar, biotite, quartz and microphenocrysts of amphibole. The rock exhibits a low to moderate competence with respect to hammer blows.

Thin Section

Mineral	%	Grain Size	Shape	Texture/Relationships
Plagioclase An_{27} Oligo	7%	680 μ	subhedral subequant	zoned phenocryst with poikilitic rims also glomerophenos
Plagioclase An_{26}	63%	60 μ	subhedral equant to elongate	microlites in matrix
Quartz	trace	450 μ	anhedral sub-equant	enocrysts
Quartz	trace	60 μ	anhedral equant	microlites
Orthoclase	5%	60 μ	anhedral equant	microlites in matrix
Biotite	1%	460 μ	anhedral prismatic	poikilitic containing apatite and sphene
Hornblende	3%	80 μ	subhedral ragged prisms	microphenocrysts and microlites
Apatite	2%	10 μ	subhedral prismatic	random distribution
Chlorite(penn)	trace	230 μ	tabular	after biotite
Epidote	trace		subhedral prismatic	in plag phenos
Monazite	trace	175 μ	anhedral aggregate	
Biotite	8%	25 μ	subhedral tabular	assoc. with opaques, quartz and hb
Opaques(pyrite)	5%	15 μ	subhedral equant	seriate size distribution
Zircon	trace		subhedral prismatic	in bio with pleiochroic halo

Petrographic Report

spec. no. DT 162
lamprophyre

Handspec desc.

a melanocratic dark grey aphanitic porphritic rock containing quartz phenocrysts, dark green pyroboles and a few white feldspars. It has moderate to low competence with respect to hammer blows.

Thin Section

Mineralogy	%	Grain Size	Shape	Texture/Relationship
Plagioclase	58%	230 u	anhedral laths	microlites outlining fluxion often warped
Oligioclase				
Hornblende	18%	230 u	microlites phenocrysts	evenly distributed assoc. with abundance biotite
Biotite	12%	20 u to 70 u	fine matted needles and tabular grains	assoc. with phenocrysts of hornblende partially replacing hornblende
Clinozoicite	trace	25 u	anhedral	randomly disseminated
Orthoclase	1%	20 u	anhedral	randomly disseminated
Quartz	2%	2000 u	anhedral rounded embayed	xenocrysts rimmed by bio and epidote
Augite	4%	40 u	subhedral	ragged in assoc with bio
Monazite	trace	90 u	subhedral	poorly formed in assoc with mafics
Opaques	5%	45 u	subhedral equant	randomly disseminated
Apatite	trace	2 u	subhedral prismatic	randomly disseminated larger grains mainly assoc. with biotite
Sphene	trace	90 u	subhedral wedges	in assoc. with mafics

History emplaced as a late phase. The rock has picked up quartz xenocrysts which exhibit embeyed reaction rims covered by biotite and epidote. This type of reaction rim is described by Moorhouse (1959) as involving pyroxenes.

Classed: Kersantite (IUGS)

HE SAND CREEK
T

ve

b

porphyry (andesite)

rphyry (andesite)

ite aplite

orite

dykes, rafts